AD_____

Award Number: W81XWH-08-1-0380

TITLE: Elucidating the Tumor-Suppressive Role of SLITs in Maintaining the Basal Cell Niche

PRINCIPAL INVESTIGATOR: Lindsay Hinck

CONTRACTING ORGANIZATION: University of California, Santa Cruz
Santa Cruz, CA 95064

REPORT DATE: October 2011

TYPE OF REPORT: Final

PREPARED FOR: U.S. Army Medical Research and Materiel Command
Fort Detrick, Maryland 21702-5012

REPORT DOCUMENTATION PAGE

Form Approved
OMB No. 0704-0188

1. REPORT DATE *(DD-MM-YYYY)*	2. REPORT TYPE	3. DATES COVERED *(From - To)*
01-10-2011	Final	1 JUL 2008 - 31 Sep 2011

4. TITLE AND SUBTITLE

Elucidating the Tumor-Suppressive Role of SLITs in Maintaining the Basal Cell Niche

5a. CONTRACT NUMBER

5b. GRANT NUMBER

W81XWH-08-1-0380

5c. PROGRAM ELEMENT NUMBER

6. AUTHOR(S)

Lindsay Hinck

E-Mail: lhinck@ucsc.edu

5d. PROJECT NUMBER

5e. TASK NUMBER

5f. WORK UNIT NUMBER

7. PERFORMING ORGANIZATION NAME(S) AND ADDRESS(ES)

University of California, Santa Cruz
Santa Cruz, CA 95064

8. PERFORMING ORGANIZATION REPORT NUMBER

9. SPONSORING / MONITORING AGENCY NAME(S) AND ADDRESS(ES)

U.S. Army Medical Research and Materiel Command
Fort Detrick, Maryland 21702-5012

10. SPONSOR/MONITOR'S ACRONYM(S)

11. SPONSOR/MONITOR'S REPORT NUMBER(S)

12. DISTRIBUTION / AVAILABILITY STATEMENT

Approved for Public Release; Distribution Unlimited

13. SUPPLEMENTARY NOTES

14. ABSTRACT

The research performed over the last thirty-nine months is based on the hypothesis that SLIT/ROBO1 signaling regulates interactions between myoepithelial and luminal epithelial cells, and that loss of this activity results in the destabilization of the basal cell niche. Over the past 12 months, we have extended our analysis on the excess population of stem and progenitor cells discovered in Slit2-/-;Slit3-/- and Robo1-/- mammary glands. We identified Robo1 as a target of TGF-β1, whose actions increase the levels of ROBO1 specifically in the basal compartment. This upregulation of SLIT/ROBO1 signaling, in turn, inhibits canonical WNT signaling in the basal layer by regulating the subcellular localization of β-catenin, reducing the proliferation of progenitor cells and ultimately reducing the number of myoepithelial cells. Since myoepithelial cells produce growth factors that stimulate branching, we show that the overall consequence of enhanced SLIT/ROBO1 signaling is reduced branch formation. These studies identify a novel developmental role for SLITs in regulating cell proliferation and, as such, they provide a gratifying developmental correlate for the role of SLITs during tumorigenesis when they function to suppress tumor cell proliferation.

15. SUBJECT TERMS

breast, Slit2, Robo1, basal cell

16. SECURITY CLASSIFICATION OF:			17. LIMITATION OF ABSTRACT	18. NUMBER OF PAGES	19a. NAME OF RESPONSIBLE PERSON
a. REPORT	b. ABSTRACT	c. THIS PAGE			USAMRMC
U	U	U	UU	52	19b. TELEPHONE NUMBER *(include area code)*

Table of Contents

INTRODUCTION:

There is a growing appreciation that myoepithelial cells function as "epithelial gatekeepers" to organize tissue structure, including cells in the breast stem cell niche, and to generate the barrier between epithelium and stroma by secreting the basal lamina. SLITs are a family of secreted proteins originally identified in the nervous system where they repel and attract axons, and promote their branching. SLITs are expressed throughout the epithelial compartment, whereas the SLIT receptor, ROBO1 (DUTT1), is expressed exclusively on basal cells during mammary gland development, switching to a subpopulation of luminal cells in the adult gland{. Numerous studies have found that the expression of *Slits* and *Robo1* is downregulated during human breast tumor progression, especially in basal-like subtypes. The research we performed over the past 39 months under the auspices of an IDEA Award is based on the hypothesis that SLIT/ROBO1 signaling regulates interactions between myoepithelial and luminal epithelial cells, and that loss of this activity results in the destabilization of the basal cell niche and subsequent formation of ductal lesions with basal characteristics. Over the past 12 months, we extended our analysis as outlined in last year's report and characterized the basal cell compartment in *Slit2-/-;Slit3-/-* and *Robo1-/-* mammary glands. To perform these studies, we adopted new techniques (FACS analysis, serial transplantation and mammosphere cultures) that were not described in our funded application but, because the field has moved rapidly, these techniques are now considered standard for stem cell analysis in the mammary gland.

BODY:

The research we performed under the auspices of an IDEA Award was based on the hypothesis that SLIT/ROBO1 signaling regulates interactions between myoepithelial and luminal epithelial cells, and that loss of this activity results in the destabilization of the basal cell niche and subsequent formation of ductal lesions with basal characteristics. Three aims were proposed in the original application:

I. Characterize the hyperplastic lesions observed in *Slit2-/-;Slit3-/-* and *Robo1-/-* mammary glands.

II. Evaluate whether loss of *Slit* in human breast tumors corresponds with basal tumor characteristics.

III. Identify the signaling effectors in myoepithelial cells that mediate SLIT/ROBO1 adhesion.

We accomplished each of these Aims, publishing 3 articles and 1 review with acknowledged support of the Congressionally Directed Medical Research Program. In the first paper published in *Cancer Research* (Marlow et al., 2008) we characterized *Slit2-/-;Slit3-/-* and *Robo1-/-* lesions and showed that either loss of *Slits* or their *Robo1* receptor in murine mammary gland or human breast resulted in the co-ordinate upregulation of the SDF1/CXCR4 signaling axis. We further demonstrated using a xenograft model that *Slit* overexpression downregulates *Cxcr4* and suppresses tumor growth. In a second paper published in *Developmental Cell* (Macias et al., 2011), we identified the molecular basis for the adhesive and hyperplastic phenotype observed in knock-out lesions by showing that b-catenin controls the proliferation and adhesion of basal cells downstream of SLIT/ROBO1 signaling. A third paper, published in *PNAS* (Marlow et al., 2010), demonstrated increased mammary angiogenesis due to loss of *Robo4* in the vasculature, combined with the release of pro-angiogenic factors, such as SDF1 and VEGF, from hyperplastic mammary lesions. Finally, a review paper that discusses current progress in targeting the SLIT/ROBO pathway in cancer therapies has also been recently published in *The Journal of Mammary Gland Biology and Neoplasia* (Harburg and Hinck, 2011).

Below, I detail the accomplishments under each Aim of the original award.

Specific Aim I: Characterize the hyperplastic lesions observed in *Slit2-/-;Slit3-/-* and *Robo1-/-* mammary glands.

We molecularly characterized *Slit2-/-;Slit3-/-* and *Robo1-/-* lesions using a battery of immunohistochemical markers. Much of this work has been published (Macias et al., 2011; Marlow et al., 2008). In brief, we discovered that knock-out lesions have elevated proliferation and defective adhesion. By studying these defects during early post-natal mammary gland development, we discovered that cell proliferation increases early in development in cap cells of end buds due to deregulation of b-catenin signaling. This loss of growth control generates an overabundance of myoepithelial cells, which produce an excess of growth factors, such as FGF2, that spurs cell growth. These surplus myoepithelial cells eventually invade the luminal population, disrupting cell adhesion. Moreover, over time these excess growth factors, along with other changes that occur such as upregulation of CXCR4 and SDF1, spur the development of hyperplastic lesions with basal characteristics.

We also identified the effects of losing *Slit* expression on the mammary vasculature (Marlow et al., 2010). We identified a stromal source of SLIT, mural cells encircling blood vessels, and showed that either loss of *Slit* expression in the stroma or loss of *Robo4* expression in the endothelium leads to elevated blood vessel density and complexity by activating VEGFR2 signaling through the Src and focal adhesion kinases. However, loss of SLIT/ROBO4 signaling, alone, was insufficient for the effect. Instead, it has to be combined with an angiogenic stimulus such as preneoplasia or pregnancy. Taken together, our results indicate a guardianship role for *Robo4* in development and disease processes during which it restricts VEGF/VEGFR2 signaling.

Specific Aim II: Evaluate whether loss of *Slit* expression in human breast tumors corresponds with basal tumor characteristics.

We surveyed *Slit2, Slit3, Robo1* and basal marker expression in human breast tumors by RT-qPCR and immunohistochemistry and published our findings (Marlow et al., 2008). We also observed that loss of SLIT/ROBO1 signaling corresponds with breast cancers of the basal subtype. Recently, however, it has been shown that some basal-like breast cancers arise from luminal progenitor cells, which are normally incapable of generating outgrowths, but that acquire self-renewal properties in patients carrying the BRCA1 mutation. Remarkably, these luminal progenitor cells form cancers with basal-like histological characteristics. Mice carrying *Slit2-/-;Slit3-/-* mammary tissue also develop hyperplasias with basal characteristics, suggesting that the SLIT/ROBO1 pathway, like BRCA, controls some aspect of luminal progenitor generation and/or proliferation. We have pursued this observation, generating preliminary data supporting the idea that SLIT/ROBO1 signaling regulates spindle orientation and, consequently, asymmetric versus symmetric cell division. These data were included in an application for a two year extension of this IDEA award that was submitted in August, 2011. Positive results from this proposed investigation would provide an explanation for the defects in MaSC/progenitor differentiation observed in breast tumors with aberrant SLIT/ROBO1 signaling.

Specific Aim III: Identify the signaling effectors in myoepithelial cells that mediate SLIT/ROBO1 adhesion.

We identified b-catenin signaling downstream of SLIT/ROBO1 in cap cells of end buds; these cells differentiate into myoepithelial cells (Macias et al., 2011). In research that is still unpublished, we also identified rac, paxillin, actin and focal adhesion kinase as downstream effectors in myoepithelial cells of SLIT/ROBO1 adhesion and they may be regulated by the Abl tyrosince kinase. Our current data suggest that SLIT/ROBO1 signaling regulates the formation of the myoepithelial cell layer and may be pivotal in establishing and maintaining the gate-keeping function of this cell layer. Below are two figures from a manuscript we are working that show the phenotype of myoepithelial cells (MECs) in *Robo1* glands. The actin cytoskeleton is severely compromised in Robo1-/- glands as evidenced by the single “braid” of actin present in knock-out myoepithelial cells, compared to the meshwork of actin present in knockout (Figure 1). We have documented that SLIT2 activates Rac and that this activation remodels the actin cytoskeleton. Figure 2 shows pull-down assays on lysates from primary cultures of mammary cells using a GST fusion protein of the PAK1 binding

domain (GST-PBD) that binds activated Rac1. A comparison of wildtype and knockout cells reveals an approximately 66% decrease in activated Rac1 in *Robo1-/-* animals. Conversely, when we assessed the effects of adding recombinant SLIT2 to wildtype cells, we observed an approximately 2.5-fold increase in Rac1 activity. To determine whether the increase in Rac1 activity occurs in myoepithelial cells that express ROBO1, we purified them, added recombinant SLIT2 and performed pull-down assays. Again, we observed a significant increase in Rac1 activity in response to SLIT2 treatment. We are finishing up these and other studies in order to submit a manuscript describing our result.

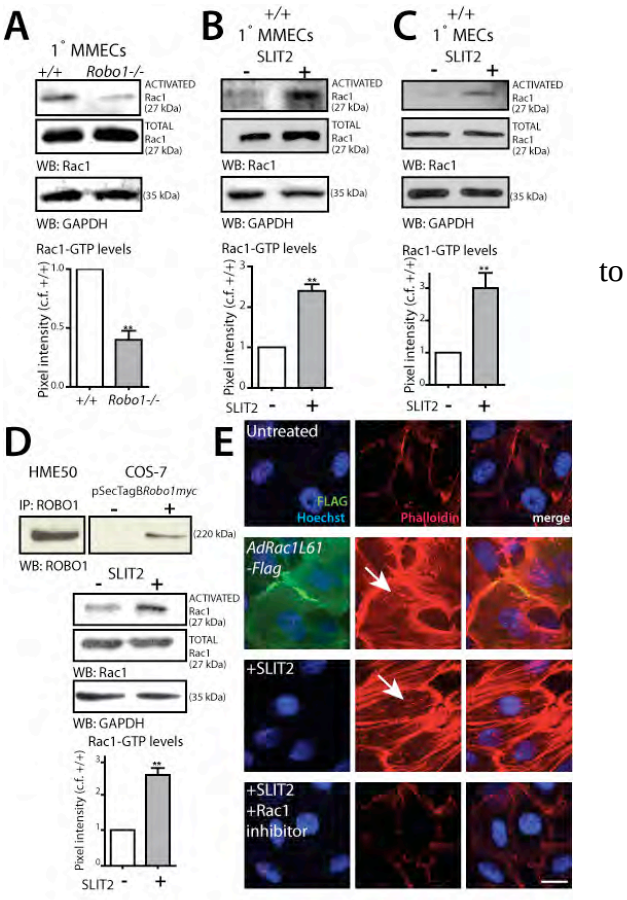

Figure 2: Slit/Robo1 signaling activate Rac to organize the actin cytoskeleton. (A-C) Primary MMECs, either total myoepithelial and luminal epithelial cells (A, B) or myoepithelial-enriched cultures (C) were lysed and assayed for activated Rac1 using p21-activated kinase binding domain (PAK1-PBD). (A) Decreased levels of activated Rac1 in the absence of *Robo1* and, conversely, (B, C) increased levels upon SLIT2 treatment *Top*: representative immunoblots for GTP-Rac1, total Rac1, and loading control GAPDH. *Bottom*: quantitative analysis of Rac1 activation. (*n*=3 experiments; ** *P*<0.001; *t* test). (D) ROBO1 expression in human MEC cell line HME50 as revealed by immunoprecipitation/immunoblotting of HME50 and control COS-7 cells transfected with pSecTagB*Robo1myc*. HME50 lysates display increased actived Rac1 levels after SLIT2 treatment (*n*=3 experiments; ** *P*<0.001; *t* test.) (E) Similar morphological changes in cells infected with activated Rac1 (Rac1-N19-Flag) or treated with SLIT2. Individual channel images showing FLAG staining to detect activated Rac1 (green), phalloidin (red) and DAPI nuclei (blue). Merged images reveal increased stress fibers in HME50 cells either infected with activated Rac1 or treated with SLIT2. Scale bars: 10µm (E).

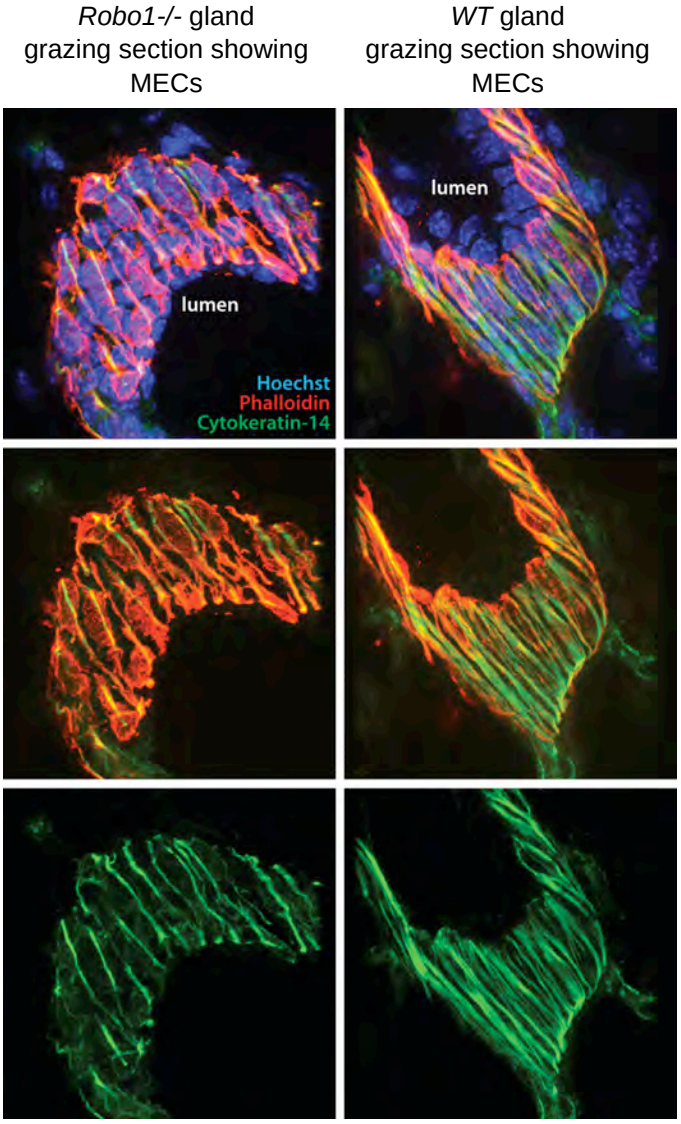

Figure 2: Loss of Slit/Robo1 signaling disrupts the actin cytoskeleton. Grazing section of Robo1-/- (left) and wildtype (right) ducts showing the myoepithelial cell (MEC) layer.

KEY RESEARCH ACCOMPLISHMENTS:

- Identified the tumor suppressive function of *Slits* in breast/mammary gland (Marlow et al., *Cancer Research*, 2008)
- Identified the effects of losing SLIT/ROBO1 expression on mammary vasculature (Marlow et al., *PNAS*, 2010).
- Showed that loss of SLIT/ROBO1 signaling disrupts basal cell proliferation by interfering with b-catenin signaling (Macias et al., *Dev Cell* 2011)
- Discovered Rac as a downstream effector of SLIT/ROBO1 signaling and potential link to Abl signaling in the gland (Macias et al., in preparation, 2011).
- Identified a stem cell signature in *Slit2-/-;Slit3-/-* glands (Ballard et al., current studies)

REPORTABLE OUTCOMES:

Papers:

Harburg GC, Hinck L. 2011. Navigating breast cancer: axon guidance molecules as breast cancer tumor suppressors and oncogenes. *Journal Mammary Gland Biol Neoplasia*. Sep;16(3):257-70.

Macias H, Moran A, Samara Y, Moreno M, Compton JE, Harburg G, Strickland P, Hinck L. 2011. SLIT/ROBO1 signaling suppresses mammary branching morphogenesis by limiting basal cell number. *Developmental Cell*, Jun 14;20(6):827-40.

Marlow R., Binnewies M., Sorensen L.K., Monica S. D., Strickland P., Forsberg E.C., Li D.Y., Hinck L. 2010. Vascular Robo4 restricts pro-angiogenic VEGF signaling in breast, *Proc Natl Acad Sci U S A*. Jun 8;107(23):10520-5. PMID: 20498081

Marlow R., Strickland, P., Lee J.S.. Wu X., PeBenito M., Binnewies M., Le E., Moran A., Macias H., Cardiff R.D., Sukumar S., Hinck. 2008. SLITs suppress tumor growth and microenvironment by silencing *Sdf1/Cxcr4* within breast epithelium. *Cancer Research*, Oct 1;68(19):7819-27.

Abstracts:

Mimmi Ballard, Naomi Iwai and Lindsay Hinck. The Role of SLIT/ROBO signaling in asymmetric self-renewal of mammary stem cells. *Mammary Gland Biology Gordon Conference.* June 12-17, 2011.

Gwyn Harburg and Lindsay Hinck. The role of SLIT/ROBO signaling in mammary stem cell self-renewal and progenitor cell fate. *Mammary Gland Biology Gordon Conference.* June 6-11, 2010.

Rebecca Marlow, Mikhail Binnewies, Phyllis Strickland, Camilla Forsberg, Dean Li and Lindsay Hinck. Loss of *Slit* expression within the epithelium promotes angiogenesis and neoplastic transformation in breast. *Keystone Symposia: Extrinsic Control of Tumor Genesis and Progression.* March 15-20, 2009.

Rebecca Marlow, Jennifer Compton, Phyllis Strickland, Lindsay Hinck. SLIT/ROBO signalling regulates mammary gland longevity by regulating progenitor cell fate. *Mammary Gland Biology Gordon Conference.* June 14-19, 2009.

Rebecca Marlow, Mikhail Binnewies, Phyllis Strickland, Camilla Forsberg, Dean Li and Lindsay Hinck. Loss of *Slit* expression within the epithelium promotes angiogenesis and neoplastic transformation in breast. *Mammary Gland Biology Gordon Conference.* June 14-19, 2009.

LIST OF PERSONNEL:

Mimmi Ballard
Hector Macias
Angel Moran
Jen Compton
Melissa Moreno
Gwyndolyn Harburg
Rebecca Marlow
Lindsay Hinck

CONCLUSIONS:

Evidence is growing that myoepithelial cells function as "natural tumor suppressors" because they organize tissue structure, including cells in the breast stem cell niche, and generate the barrier between epithelium and stroma by secreting the basal lamina. In the last three years under the auspices of this Idea award, we identified SLITs as breast tumor suppressors, a function that has since been identified in other tumor types. We also identified one mechanism underlying this tumor suppressive role, the negative regulation of β-catenin signaling by SLIT in the basal cell compartment. In addition, we made the unanticipated discovery that loss of *Slit* in pericytes surrounding the vasculature contributes to sprouting angiogenesis during pregnancy and tumor progression by upregulating VEGF/VEGFR signaling.

In the past year, we have continued our characterization of SLIT/ROBO1 signaling, focusing on the regulation on the cytoskeleton by the Abl tyrosine kinase which, in turn, we believe may regulate Rac and β–catenin. Other pathways (e.g. PI-3 kinase/Akt signaling) may be in involved as well. These studies are delineating a novel pathway by which SLIT/ROBO1 signaling modulates mammary basal cell adhesion and cell proliferation. In addition, we have been pursuing studies to further characterize the effects of SLIT/ROBO1 signaling on mammary stem cells, based on serial transplantation assays that showed loss of *Slits* resulting in delayed senescence of MaSC/progenitor cells. These studies suggest that SLITs may function in the stem cell niche to control MaSC and progenitor cell division.

In sum, the stem cell hypothesis for breast tumors posits that cancer stem cells, a small population of self-renewing cells within a tumor, are responsible for breast cancer progression and recurrence. This suggests that the targets of malignant transformation are normal stem/progenitor cells. Many laboratories are attempting to identify and characterize cancer stem cells. These efforts will be greatly aided by a better understanding of normal stem cells, their identification *in situ*, and elucidation of their regulation during normal development. Our data suggest that SLITs regulate proliferation and adhesion of cell in the basal compartment, including at least one population of stem cells. We have applied for an extension of this award with the aim of characterizing the *Slit2-/-;Slit3-/-* longevity phenotype. This research promises to provide insight into mechanisms by which normal stem/progenitor cells are regulated, leading to potential insights into how they may be deregulated upon cancerous transformation.

APPENDICES:

- pdf of our paper in the *Journal of Mammary Gland Biology and Neoplasia*
- pdf of our paper in *Developmental Cell*
- pdf of our paper in the *Proceedings of the National Academy of Sciences*
- pdf of our paper in *Cancer Research*

J Mammary Gland Biol Neoplasia (2011) 16:257–270
DOI 10.1007/s10911-011-9225-1

Navigating Breast Cancer: Axon Guidance Molecules as Breast Cancer Tumor Suppressors and Oncogenes

Gwyndolen C. Harburg · Lindsay Hinck

Received: 7 June 2011 / Accepted: 19 July 2011 / Published online: 5 August 2011

Abstract Slit, Netrin, Ephrin, and Semaphorin's roles in development have expanded greatly in the past decade from their original characterization as axon guidance molecules (AGMs) to include roles as regulators of tissue morphogenesis and development in diverse organs. In the mammary gland, AGMs are important for maintaining normal cell proliferation and adhesion during development. The frequent dysregulation of AGM expression during tumorigenesis and tumor progression suggests that AGMs also play a crucial role as tumor suppressors and oncogenes in breast cancer. Moreover, these findings suggest that AGMs may be excellent targets for new breast cancer prognostic tests and more effective therapeutic strategies.

Keywords Axon guidance molecules · Netrin · Semaphorin · Ephrin · Slit · Robo

Abbreviations

AGM	Axon Guidance Molecule
CUB	Complement-Homology Domain
EGF	Epidermal Growth Factor
ER	Estrogen Receptor
Ig	Immunoglobulin
MAM	Meptin/A5/Mu-Phosphatase Homology Domain
TEB	Terminal End Bud

The Slit, Netrin, Eph/ephrin, and Semaphorin families were originally characterized as axon guidance molecules (AGMs) in the developing nervous system, where they act as repulsive or attractive factors to guide axonal growth and migration [1]. Over the past decade they have also been shown to play roles in other mammalian organs, including the mammary gland, as mediators of tissue morphogenesis, cell adhesion, and proliferation [2]. Dysregulation of AGMs in the mammary gland has been linked to breast cancer initiation and progression, both through autocrine effects on tumor cells as well as paracrine effects on endothelial cells that promote angiogenesis. As the angiogenic role of AGMs has been well reviewed elsewhere, here we focus on the autocrine effects as they pertain to breast cancer [3–5]. In this review, we explore the dual nature of AGMs in breast cancer tumorigenesis and progression and consider their potential in development of new diagnostic markers and therapeutics.

G. C. Harburg · L. Hinck (✉)
Department of Molecular, Cell and Developmental Biology,
University of California,
Santa Cruz, CA 95064, USA
e-mail: hinck@biology.ucsc.edu

AGMs in the Mammary Gland

It is only in the past fifteen years that researchers have begun exploring the role of AGMs in organs outside the nervous system. AGMs, belonging to each of the four families, are expressed in the mammary gland (Table 1), but for the most part their function is unknown. Many AGMs are upregulated during puberty, and are often enriched in the terminal end buds (TEBs), a developmental structure distinctive for its high proliferation levels and invasive behavior. Other AGMs, such as SLIT3 and ROBO2 are only expressed in the mature mammary epithelia, where they may regulate the basal level of proliferation during normal epithelial cell turnover [6]. Taken together, these expression patterns in both normal and diseased mammary gland suggest that AGMs are important for gland morphogenesis, epithelial homeostasis, and breast cancer development or progression.

Table 1 Expression of Slit/Robo, Netrins, Eph/Ephrins, and Semaphorins in the mammary gland

	Time of Expression		Cellular Localization
	Puberty	Adult	
Slit/Robo			
Slit2	+	+	epithelia [6]
Slit3	−	+	epithelia [6]
Robo1	+	+	puberty: cap cells of the TEB and myoepithelial cells, adult: some luminal cells, stroma [6]
Robo2	−	+	subset of myoepithelial cells [6]
Netrins			
Netrin-1	+	?	prelumenal epithelial cells during development and stroma [11]
Netrin-4	?	+	epithelia and basal lamina [30]
DCC	−	+	epithelia [11, 69]
Un5H	+	+	only expressed in fibroblasts during puberty [11, 25]
Neogenin	+	+	cap cells and subset of prelumenal cells during development [11]
Ephrins			
EphrinA1	?	+	luminal cells, stroma, and fat [70]
EphrinB1	+	?	enriched in TEB, but also expressed at low levels in ducts [71]
EphrinB2	+	+	ducts and end buds, luminal, absent during lactation [8, 46]
EphrinB3	?	?	[72]
EphA2	+	+	enriched in TEBs during puberty [71], expressed in luminal cells in adult [70]
EphA7	?	+	upregulated in the mammary gland during early pregnancy [72]
EphB3	?	?	[72]
EphB4	+	+	myoepithelia of ducts and alveoli [46]
EphB6	?	+	[73]
Semaphorins			
Sema3A	−	−	[74]
Sema3B	+	+	in TEB, but not ducts during development [74]
Sema3C	+	+	fat and stroma [74]
Sema3E	−	−	[74]
Sema3F	−	+/−	detected in human mammary gland, but not mouse [74, 75]
Sema4A	+	+	fat stroma, epithelia [72], upregulated during lactation and involution [76]
Sema4B	−	+	upregulated during involution [76]
Sema4D	+	+	expressed in TEB, ducts, and stroma during development in mouse. [74] upregulated during lactation [76]
Sema4F	+	+	epithelia, fat, and stromal expression [74]
Sema6B	−	?	[74]
Sema6C	−	+	[77]
Sema6D	−	+	[77]
Sema7A	−	+	Upregulated during involution [76]
Neuropilin1	+	+	epithelia, fat, and stromal expression [74]
Neuropilin2	−	+	expressed in adult epithelia, but absent during development [74]
PlexinA1	?	?	expressed in tumors, but normal expression unknown [78]
PlexinA2	+	?	expressed in epithelia [74]
PlexinA3	+	?	expressed in epithelia [74]
PlexinB1	?	+	[79]
PlexinB2	+	?	expressed in epithelia; enriched in TEB [74]
PlexinD1	+	?	epithelia, fat, and stromal expression [74]

Although few AGMs have available knockout mouse models, those that exist often have mammary gland phenotypes supporting a role for AGMs in normal gland development. These models indicate that there are three major roles for AGMs in gland development: proliferation, adhesion, and migration. Alterations in proliferation of mammary epithelial cells have been seen in mice with disrupted Eph/ephrin and Slit signaling. For example, *Epha2* deficiency leads to deficient mammogenesis, in which there is a failure of the mammary gland to fill the fat pad, while overexpression of *Ephb4* or *Efnnb2* in a transgenic mouse model leads to growth retardation of the mammary gland, and altered proliferation and apoptosis in mammary epithelial cells [7–9]. Conversely, loss of Slit signaling in *Slit2*;*Slit3* or *Robo1* knockout mice results in increased epithelial proliferation and development of ductal hyperplasias [10]. Mice with disrupted Slit, Netrin, or Eph/ephrin signaling also have altered cell adhesion that results in aberrant mammary gland morphology. Both *Slit/Robo* and *Netrin/Neogenin* knockout mice display disrupted cell adhesion in the TEB [6, 11]. *Ephb4* overexpressing mice have irregular alveolar morphology in which epithelial cells partly lose cell-cell contacts with their neighbors [8]. Thus, AGMs are important factors in normal mammary gland development.

Are AGMs Tumor Suppressors in the Breast?

The link between AGMs and highly proliferative regions of the mammary gland suggest that AGMs may be important in regulating normal epithelial proliferation. This brings up the question of whether AGMs also regulate proliferation during breast tumorigenesis. Although neither loss nor overexpression of AGMs, alone, has been linked to development of mammary tumors in mouse models, perturbation of their expression in a cancer-prone genetic environment has been shown to alter time to tumor development and aggressiveness of resulting tumors. Here, we present evidence supporting a role for AGMs as tumor suppressors in the breast that act by inhibiting proliferation and metastasis.

AGMs in Breast Cancer

Slit/Robo

Slit/Robo signaling acts as both a tumor suppressor and anti-metastatic factor in breast cancer. There are three Slits expressed in mammals—Slit1, Slit2, and Slit3. They act as ligands for Robo receptors, of which there are 4 in mammals, Robo 1–4 (Fig. 1). Slits are not freely diffusible

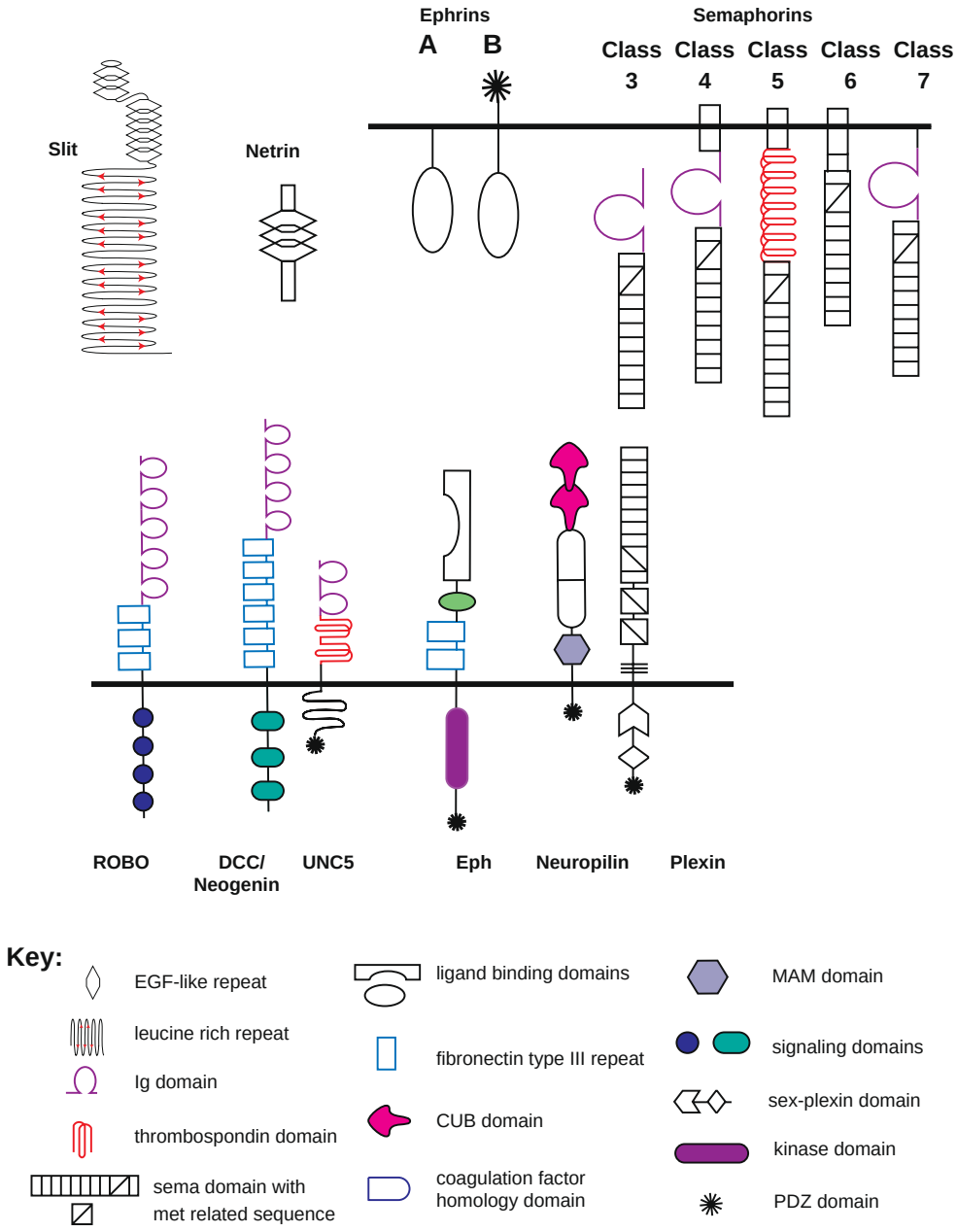

Figure 1 Axon Guidance Molecule Ligands and Receptors. Top: AGM ligands Slits, Netrins, and Class 3 Semaphorins are all secreted proteins, whereas Class 4–7 semaphorins and ephrins-A and B are tethered to the membrane via GPI or transmembrane linkages. Bottom: AGM receptors are all single-pass transmembrane proteins. Domain structures are schematically represented

due to their association with heparin sulfate proteoglycans, such as glypican and syndecan [3]. *Slit2*, which is broadly expressed in the mammary gland during development and adulthood, is lost in 43–63% of sampled breast cancers, while *Slit3*, expressed only in the adult mammary gland, is lost in 16% (Table 2) [12, 13]. The Slit receptor, *Robo1*, is also lost in 2–19% of sampled breast tumors and ~5% of breast cancer cell lines (Table 2) [14], whereas potential roles for *Robo2* or *Robo3* in regulating mammary development and tumorigenesis have not been explored. The primary mechanism for loss of *Slit/Robo* expression in breast cancer is hypermethylation, rather than chromosomal arrangements or deletions [12–14]. Of particular note, both *Slit2* and *Robo1* show hypermethylation and gene silencing at early stages of breast cancer development, with *Slit2* hypermethylation even detected in 8–14% of histologically normal breast tissues [12, 14]. This suggests that loss of SLIT/ROBO signaling is an early event in tumor progression.

Slits may act through the Robo1 receptor to prevent tumor formation. In support of this, *Slit2;Slit3* knockout mouse mammary glands display an identical phenotype to *Robo1* knockout mice in which the glands develop ductal hyperplasias [6, 10]. The ductal hyperplasias are a result of increased proliferation in the ductal epithelia, indicating that SLIT/ROBO1 signaling regulates cell proliferation [10, 15]. In support, breast cancer cell lines MCF-7 or MDA-MB-231 that overexpress SLIT2 or SLIT3, or that are treated with SLIT2 conditioned medium have reduced proliferation and reduced ability to form colonies in Matrigel as indicated by fewer colonies and smaller colony size [10, 12]. In vivo, MDA-MB-231 or MCF7 cells overexpressing *Slit2* also give rise to tumors that are significantly smaller than those generated from control cells [10, 12]. Concordantly, knockdown of *Robo1* in MCF7 cells leads to increased proliferation, while knockdown of *Robo1* in MCF7 cells overexpressing *Slit2* returns proliferation to near control levels [16]. These studies support a role for SLIT2/ROBO1 signaling in regulating cancer cell proliferation.

SLIT/ROBO signaling is not only important in regulating cell proliferation, but also plays an important role in maintaining proper cell-cell adhesion and preventing tumor metastasis. SLIT2 has been proposed to act as an adhesive factor by binding to ROBO1-expressing myoepithelial cells and mediating their adhesion to luminal cells, perhaps through indirect binding of heparin sulfate proteoglycans [6]. The localization of ROBO1 to the plasma membrane

Table 2 AGM expression in breast cancer and breast cancer cell lines

Slit/Robo	
Slit2	Lost in 43–63% of breast cancers (methylation) [10, 12, 66]; reduced expression in breast cancer cell lines [12, 80]
Slit3	Lost in 16% of breast cancers (methylation) [10, 13]; reduced expression in breast cancer cell lines [13]
Robo1	Lost in 2–19% of breast cancers (methylation) [14]; Rarely lost in breast cancer cell lines (exon 2 deletion) [14, 80, 81]
Netrins	
Netrin-1	Increased in metastatic breast cancer [23]; Highly expressed in many breast cancer cell lines [23]
Netrin-4	Lost in breast cancer, particularly in ER− tumors [27, 30]; Not expressed in breast cancer cell lines [27]
DCC	Lost in breast cancer (LOH); Expression also lost in breast cancer cell lines [23, 69, 82–85]
Unc5H	Lost in ~50% of breast cancers [25]
Neogenin	Lost in ~95% of invasive ductal carcinomas; No loss seen in breast cancer cell lines [26]
Ephrins	
EphrinA1	No correlation between expression and breast cancer malignancy [86]
EphrinB2	Expression is lost in breast cancer cell lines [45]
EphA2	Increased in 40% of breast cancers [34]; Overexpressed in ER− breast cancer cell lines [36, 42]
EphB4	Increased in 23–65% of breast cancers (amplification of 7q.22 in 29% of cases) [44, 47, 48, 87]; Increased expression in breast cancer cell lines (amplification) [44, 47]
EphB6	Lost in metastatic breast cancer [73, 88]; Lost in invasive breast cancer cell lines (methylation) [73, 88, 89]
Semaphorins	
Sema3A	Expressed in breast cancer and breast cancer cell lines [78]
Sema3B	Unknown, but Sema3B is located at 3p21.3, a site of frequent allele loss and methylation in breast cancer [57]
Sema3E	Increased in 69% of breast cancers [90]; Increased expression in breast cancer cell lines [90]
Sema3F	Unknown, but Sema3F is located at 3p21.3, a site of frequent allele loss and methylation in breast cancer [57]
Sema4D	Increased in breast cancers [63]
PlexinA1	Is expressed in cancers, although whether there are changes in expression is unknown [78]
PlexinB1	Increased expression in ER+ breast cancer [91] Lost in ER− breast cancers [79]

where it could act adhesively is regulated by USP33, a deubiquitinating enzyme of the USP family, which stimulates the redistribution of ROBO1 to the plasma membrane in response to SLIT2 [17]. *Slit2;Slit3* and *Robo1* knockout mice both exhibit defects in cell adhesion between luminal and myoepithelial cells leading to disruptions in ductal architecture [6, 10]. In tumors, SLIT2 may also act adhesively to prevent metastasis by inhibiting detachment of tumor cells. Overexpression of SLIT2 in MCF7 cells has been shown to reduce the amount of beta-catenin in the nucleus and enhance its co-localization with E-cadherin at the plasma membrane, potentially strengthening cell contacts [16] (Fig. 2). In contrast, MCF7 cells in which *Robo1* is knocked down form large disorganized colonies, in comparison to the smooth, well-organized colonies that arise from control cells [10]. These results suggest that SLIT2/ROBO1 signaling is important in the mammary gland for maintaining appropriate cell-cell contacts.

The effect of SLIT2 on subcellular localization of beta-catenin may not only enhance cell adhesion, but can also inhibit cell proliferation by blocking canonical Wnt signaling (Fig. 2). During mammary gland development, SLIT2 limits the proliferation of cap cells in the terminal end bud by increasing the cytoplasmic and membrane pools of beta-catenin at the expense of its nuclear pool, suggesting that subcellular redistribution of beta-catenin is sufficient to inhibit cell proliferation. In vitro studies show that SLIT2 antagonizes downstream signaling of pro-proliferative factors, such as EGF, by blocking activation of AKT [16] (Fig. 2). This inhibition of AKT, in turn, results in activation of GSK-beta, which inhibits beta-

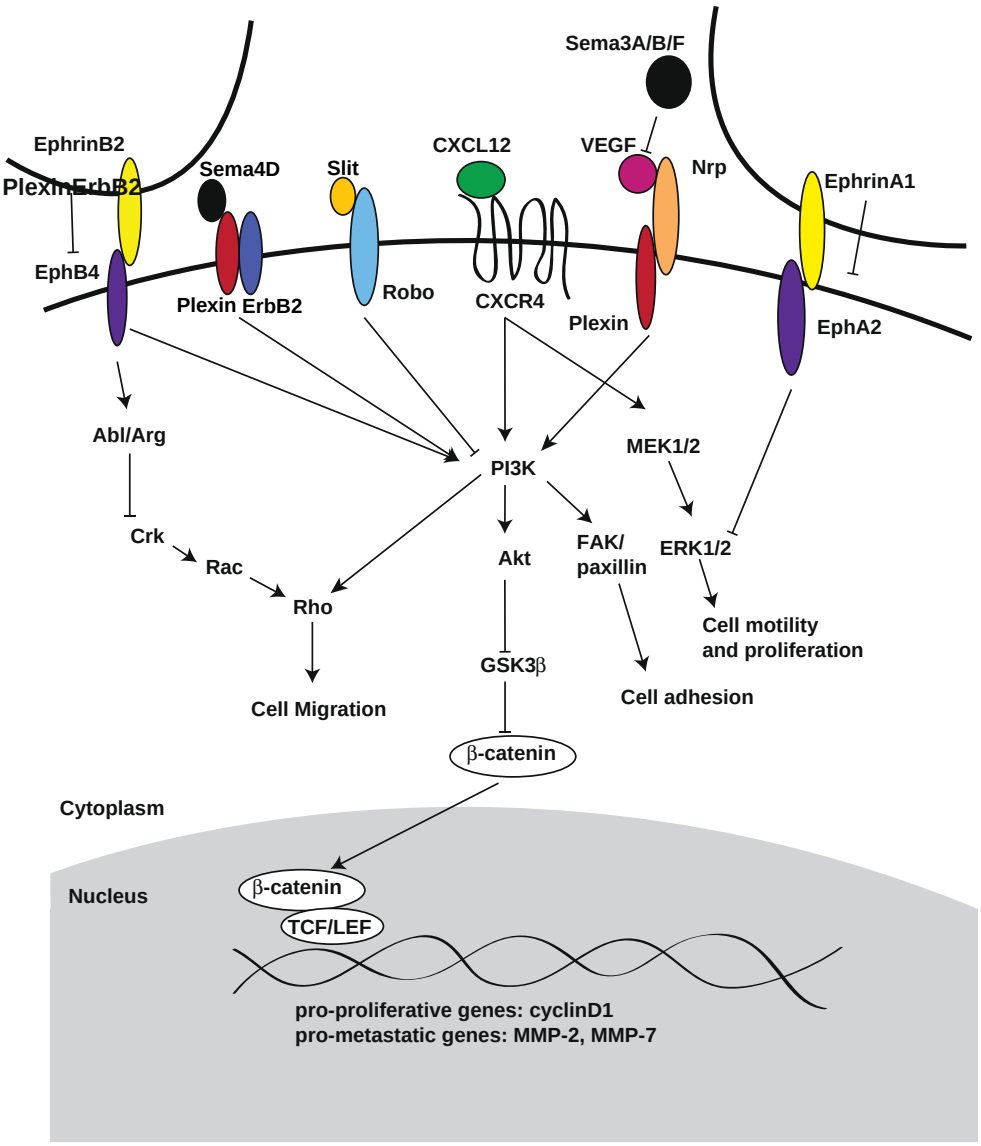

Figure 2 Axon Guidance Molecules Regulate Key Pathways involved in Cell Proliferation and Migration. Many AGMs regulate cell proliferation and migration through activation or inhibition of PI3K signaling. EPHB4 and SEMA4D are both positive regulators of PI3K signaling, leading to enhanced proliferation and migration, while EFNB2, SLITs, and SEMA3A, B, and F all inhibit PI3K signaling, by inhibiting EPHB4 kinase-independent signaling, CXCL12/CXCR4 signaling, and VEGF signaling respectively

catenin translocation to the nucleus. SLIT2-induced exclusion of beta-catenin from the nucleus results in decreased expression of beta-catenin downstream transcriptional targets, such as *cyclin D1*, which may account for the observed decreases in cell proliferation. *Slit2*-overexpressing cancer cells also show decreased levels of MMP-2 and MMP-9, extracellular matrix proteases implicated in tumor progression and metastasis [16] (Fig. 2). Thus, *Slit2* expression results in a change in the subcellular localization of beta-catenin, reducing its nuclear localization and decreasing transcription of pro-proliferative genes while increasing its membrane-association and enhancing cell adhesion.

SLIT/ROBO signaling also regulates cell-cell adhesion and metastasis indirectly by mediating CXCL12/CXCR4 signaling (Fig. 2). The CXCL12 receptor, CXCR4, is not expressed in the normal mammary gland, but can be detected in tumor cells during early stages of tumor development [10, 18, 19]. CXCR4 expression is responsible for homing of breast cancer cells to common sites of metastasis, such as bone, lung, and brain, where the CXCL12 ligand is highly expressed [18]. CXCR4 expression is regulated by SLIT2, since *Slit2*-overexpressing cells show reduced levels of *Cxcr4*, while *Slit2;Slit3* knockout tissue shows increased levels of *Cxcr4* [10]. There is also an inverse correlation between *Slit2* and *Cxcr4* levels in breast tumors, suggesting that loss of SLITs plays an important role in tumor progression [10]. One possibility arising from these studies is that SLITs could function therapeutically to inhibit the CXCL12/CXCR4 chemokine axis. Indeed, SLIT has been shown to function as a non-competitive antagonist to block CXCL12-induced chemotaxis and invasion [20, 21]. SLIT also inhibits CXCL12-induced tyrosine phosphorylation of RAFTK, FAK, and paxillin, which maintain focal adhesions and preserve cell-cell contacts [17, 20], while inhibiting Src kinase, phosphatidylinositol 3-kinase (PI3-kinase), and ERK1/2 activation, all signaling mechanisms implicated in regulating cell motility [20]. Together these results show that the regulation of Wnt and CXCL12/CXCR4 pathways by SLIT2 is important for maintaining cell adhesion and preventing tumor cell metastasis.

Netrin

Netrin (*Ntn1*) signaling may also play a role in regulating tumor cell proliferation and metastasis; however, rather than the presence or absence of ligand mediating tumorigenesis, it is primarily the concentration of ligand that determines the outcome of ligand/receptor signaling [3]. The netrin receptors DCC and UNC5H are immunoglobulin superfamily members (Fig. 1), and have been identified as "dependence receptors," because in the absence of netrin-1 ligand these receptors are postulated to induce apoptosis [22]. In breast cancer cell lines, *Ntn1* is often highly expressed, as would be expected if its expression were essential for survival (Table 2) [23]. Furthermore, it was shown that reduction of *Ntn1* expression in these high expressing breast cancer cell lines results in increased apoptosis [23]. These findings support the hypothesis that NTN1 acts as a pro-survival factor in the breast, although the in vivo translation of this concept is controversial. *Ntn1* knockout mice exhibit a small increase in apoptosis, but this only occurs in a select population of cells in the TEB during development and seems to be due to anoikis-induced apoptosis [11]. This suggests that in the mouse mammary gland, NTN1 is not an essential survival factor. Conversely, loss of *Dcc* receptor expression in a knockout model, which would presumably allow a cell to escape from NTN1 regulation, does not result in tumorigenesis [24]. This may be due to the fact that, as with other genes discussed in this review, loss of *Dcc* may increase tumor susceptibility, but is not sufficient to initiate tumorigenesis.

Studies performed using human breast cancer cell lines suggest the alternate possibility that NTN1 exerts its pro-survival effect via UNC5H, rather than DCC receptors [23]. In line with this idea, one study reported that *Unc5h* expression is lost in about 50% of breast tumors (Table 2) [25]. These tumors would presumably gain a survival advantage because they would no longer be dependent on NTN1, which is required to prevent receptor-mediated apoptosis. In this circumstance, the remaining 50% of tumors, which still express *Unc5h*, are expected to upregulate *Ntn1*, which would protect the cells from unliganded receptor. Currently, it is unclear when during tumor progression *Ntn1* expression becomes upregulated. A different study has shown that *Ntn1* is rarely upregulated in primary tumors, but does show massive upregulation during tumor progression [23]. This finding suggests that NTN1 pro-survival signaling is important for promotion of more aggressive, metastatic breast cancers, but may not play an important role in the primary tumor during its initiation. The importance of NTN1 in regulating tumor progression is highlighted by the findings that breast cancer cell lines, expressing high levels of *Ntn1*, also tend to be highly aggressive and form metastases in mice, while knockdown of *Ntn1* by injection of *Ntn1* siRNA into mice reduces the formation of lung metastases by 4T1 cells [23]. Taken together, these studies suggest that in metastases that retain UNC5H expression, high levels of NTN1 promote further tumor progression and metastasis by conferring survival advantage; however, more studies will be required to confirm this hypothesis.

The consequences of NTN1 signaling through the neogenin (*Neo1*) receptor are not well described in breast cancer, but indicate that NEO1 may play a tumor

suppressor role. *Neo1* expression is lost in almost 95% of invasive ductal carcinomas (Table 2) [26]. Although loss of expression is not commonly seen in breast cancer cell lines, one study found that expression was lost in a breast cancer cell model where progressive environmental insults result in incremental increases in tumorigenicity and corresponding progressive decreases in *Neo1* expression [26]. Knockout mouse studies have shown that NTN1/NEO1 interaction is necessary for the appropriate adhesion and stabilization of the highly proliferative cap cells of the TEB, and that loss of *Ntn1* and *Neo1* leads to breaks in the basal lamina, a phenomenon necessary for tumor progression [11]. These findings suggest that NTN1/NEO1 signaling may be an important in preventing tumor metastases, but warrants further exploration.

Netrin-4 (*Ntn4*) may also act as a ligand for NEO1 and UNC5H, but there is little indication that it is necessary to prevent dependence-mediated apoptosis like NTN1 [27–29]. In fact, while *Ntn4* is normally expressed by epithelial cells of the breast, its expression is often suppressed by hypermethylation during tumorigenesis [27, 30, 31]. In matched normal and tumor samples from breast cancer patients, *Ntn4* is expressed at lower levels or lost entirely in tumors, and expression is often lost in breast cancer cell lines (Table 2) [27, 31]. Interestingly, NTN4 has a biphasic effect on cell proliferation, where low levels stimulate cell growth, and high concentrations inhibit cell growth [27]. The downstream pathways regulating this biphasic effect have not been explored, but work done in pancreatic cells shows that NTN4 can inhibit the Jnk pathway leading to decreased phosphorylation of JNK2, AKT, and JUN, and presumably decreased tumor cell proliferation and survival [27]. Thus, loss of *Ntn4* during tumor progression would be presumed to confer survival advantage on tumor cells. Much research still needs to be done to determine the role of NTN4 in breast cancer development.

Eph/Ephrin

Unlike the other AGMs, that have clear ligand and receptor categories, Ephs and ephrins can signal bidirectionally, with the potential to behave as both ligand and receptor. Forward signaling, which we will address in this review, is dependent on Eph tyrosine kinase activity and propagates in the Eph-expressing cell. Reverse signaling, which may play a role in breast cancer angiogenesis, depends on Src-family kinases and propagates in the ephrin-expressing cell [5, 32]. Ephs, the tyrosine kinase receptors for ephrins, are classified into EphA and EphB subtypes, which generally correspond to their ligand preference (Fig. 1). The Ephrin ligands are classified as members of the ephrin-A or ephrin-B families based on their plasma membrane association, which is either GPI-anchored or transmembrane, respectively (Fig. 1). Although a number of Ephs and ephrins are expressed in the mammary gland, the majority of breast cancer research has focused on ephrin-A1 (EFNA1)/EPHA2 and ephrin-B2 (EFNB2)/EPHB4. In both of these Eph/ephrin pairs, the ephrins play a tumor suppressor role by regulating the expression and activity of the Eph receptors. In the absence of EFNA1 or EFNB2, the activity of EPHA2 and EPHB4 is oncogenic and promotes both cell proliferation and metastasis.

EFNA1 acts as a tumor suppressor by initiating EPHA2 forward signaling, as well as by triggering the ligand-dependent phosphorylation, internalization, and degradation of EPHA2, which can otherwise act oncogenically [33]. EPHA2 is normally expressed at low levels in the mammary gland, but its expression is significantly increased in 40% of breast cancers (Table 2) [34]. Overexpression of *EphA2* in MCF10A cells, a non-tumorigenic epithelial cell line, confers the ability to give rise to colonies in vitro, as well as tumors in vivo [7, 34]. In contrast, high expression levels of the EFNA1 ligand correlate with a more "normal" epithelial-like phenotype in breast cancer cells and can inhibit colony formation in MDA-MB-231 and MCF10A cells that overexpress EPHA2 [34, 35]. EFNA1 initiation of EPHA2 forward signaling in breast cancer cells results in increased caspase-3 activity, reduced ERK activation and attenuated Ras/MAPK pathway activation in response to EGF (Fig. 2) [35, 36]. Thus, EFNA1 signaling normally prevents tumor formation by inhibiting proliferation and promoting apoptosis of EPHA2-expressing cells. When the ratio of EFNA1:EPHA2 becomes unbalanced during tumorigenesis, EFNA1 no longer regulates EPHA2-expressing cells, and EPHA2 ligand-independent signaling is able to promote tumor progression.

EFNA1 can also inhibit EPHA2-mediated breast cancer metastasis. In non-metastatic cells, EPHA2 co-localizes with E-cadherin at the cell membrane at points of cell-cell contact where contact with EFNA1 maintains forward signaling and promotes cell adhesion [37]. In metastatic cells, EPHA2 expression decreases at points of cell-cell contact, instead becoming diffuse or enriched within membrane ruffles at the leading edge of migrating metastatic cells, where it colocalizes with F-actin. EFNA1-mediated tyrosine phosphorylation of EPHA2 is also decreased in metastatic cells, however EPHA2 remains active through gain of ligand-independent oncogenic signaling [37]. If overexpression of EPHA2 occurs in "normal" MCF10A cells, it leads to their malignant transformation, allowing them to rapidly form tumors that show invasive characteristics, including loss of cell-cell contact and decreased cell-ECM adhesion [34]. This transformation can be reversed by treatment with EFNA1, which impairs cell migration and anchorage-dependent

growth in breast cancer cells [38]. Concordantly, loss of *EphA2* expression in *MMTV-Neu*;*EphA2*-/- mice or knockdown of its expression in 4T1 cells results in impaired lung metastasis and decreased motility in transwell migration assays [7, 39]. These data suggest that in *Efna1*-expressing tumors, EFNA1-mediated degradation of EPHA2 prevents metastasis. The loss of *Efna1* expression during tumor progression leads to overexpression of EPHA2 and, consequently, a more invasive, metastatic phenotype.

Several mechanisms may be involved in mediating EPHA2-induced migration. First, RhoA activation appears to play a role. Loss of *EphA2* in *MMTV-Neu*;*EphA2*-/- mice, decreases levels of both total and active-GTP-bound RHOA, and inhibits cell migration. Overexpression of activated RHOA restores cell motility, supporting the notion that RHOA activation contributes to EPHA2-mediated migration [7]. Second, EPHA2 may also promote migration through activation of the non-canonical Wnt pathway. Overexpression of *EphA2* in breast cancer cells results in upregulation of genes associated with the non-canonical Wnt pathway—four and a half LIM domains 2 (*Fhl2*) and *Wnt6*, both associated with the promotion of tumor invasiveness [40]. Third, *EphA2* overexpression increases FAK phosphorylation at tyrosine 925, which is associated with integrin adhesion and E-cadherin down-regulation [40]. Lastly, EPHA2 also interacts with Ephexin4, a Dbl family GEF, leading to local activation of Rac by DOCK4, formation of cortactin-rich protrusions, and promotion of ligand-independent cell polarization and migration [41]. Thus, *EphA2* overexpression in breast cancer results in the activation of a number of pathways involved in promoting migration and invasiveness.

Estrogen appears to play a significant role in mediating EPHA2 signaling. An inverse correlation between estrogen receptor (ER) status and EPHA2 expression exists in which ER-overexpressing tumors show little or no EPHA2 expression, and ER-negative tumors show high levels of EPHA2 expression [42]. Furthermore, estradiol treatment of non-transformed mammary epithelial cells decreases EPHA2 expression in a dose-dependent manner, an effect that is reversible by tamoxifen. This suggests that one of the consequences of losing normal ER signaling during cancer progression is increased EPHA2 expression, which contributes to an increasing aggressive phenotype. It also appears that EPHA2 desensitizes breast cancer cells to the effects of estrogen because tumors derived from *EphA2*-overexpressing ER+MCF-7 cells increase in size in response to estrogen, but retain their tumorigenic potential in the absence of supplemental estrogen and are less sensitive to tamoxifen [43]. Further studies have shown that a monoclonal antibody, which mimics the binding of EFNA1 to EPHA2, reverses this effect of *EphA2* overexpression and restores tamoxifen sensitivity [40]. Thus a potentially promising therapeutic strategy could involve dual targeting of EPHA2 and ER, with the goal of re-sensitizing breast cancer cells to tamoxifen by restoring the normal regulation of EPHA2 in breast tumors overexpressing this AGM.

The relationship of EFNB2 to EPHB4 is similar to that just described for EFNA1/EPHA2 in which binding of EFNB2 to EPHB4 leads to tumor suppression through ligand-activation of forward signaling, involving EPHB4 phosphorylation and degradation [44]. Like EPHA2, ligand-stimulated EPHB4 forward signaling results in tumor suppression [44], and when EFNB2/EPHB4 forward signaling becomes perturbed, due to changes in expression levels during tumorigenesis, kinase-independent EPHB4 signaling can promote tumor progression [32].

An imbalance in EFNB2 and EPHB4 expression occurs during tumorigenesis, which may promote ligand-independent EPHB4 signaling. EFNB2, like EFNA1, is also lost during cancer progression, with only weak expression of EFNB2 observed in some invasive ductal carcinoma cells and with weak-to-absent EFNB2 expression in 75% of sampled breast cancer cell lines, while non-transformed cells show high EFNB2 expression (Table 2) [44, 45]. EFNB2 expression is also absent in two cancer models, Wap-*ras* and Wap-*myc* tumors [46]. The loss of EFNB2 in breast tumors correlates with increased EPHB4 expression, affirming the ligand/receptor relationship whereby EFNB2 ligand keeps EPHB4 receptor expression in check in normal tissue. EPHB4 expression, similar to EPHA2, is increased in a large proportion of breast cancers, with one study showing that 65% of breast cancers had moderate to strong straining of EPHB4, usually with cytoplasmic localization (Table 2) [44, 47, 48]. Moreover, expression of EPHB4 is increased with clinical stage and histological grade of the tumor and positively correlates with DNA aneuploidy and S-phase fraction; however, there is no association with patient survival [48]. These studies suggest that in the absence of EFNB2, EPHB4 may provide a survival advantage, and in fact, overexpression of EPHB4, alone, may be sufficient for its activation [44]. Short-term activation of EPHB4 forward signaling in breast cancer cells using clustered EFNB2, which allows for EPHB4 activation but not its internalization and degradation, results in increased phosphorylated-AKT [44]. This suggests that in the absence of EFNB2, which terminates EPHB4 forward signaling, EPHB4 may promote constitutive pro-survival AKT signaling (Fig. 2). Furthermore, this PI3K-AKT pathway may also regulate EPHB4 expression in a feed-forward loop as treatment with PI3K or AKT inhibitors leads to complete loss of EPHB4 expression in SK-BR-3 cells. Thus, one way EFN2B inhibits the oncogenic activity of EPHB4 is by preventing its constitutive, pro-survival signaling, which can occur upon its overexpression.

A second way that EFNB2 appears to function as a tumor suppressor is by signaling through EPHB4 to actively inhibit proliferation. This has been demonstrated in breast cancer cell lines by treating them with EFNB2-Fc that mimics ligand binding and inhibits spheroid growth of MCF-7, MDA-MB-231, and MDA-MB-453 cells by reducing proliferation and enhancing apoptosis [45]. Other studies have shown that this EFNB2/EPHB4 forward signaling is through the Abl-Arg tyrosine kinase family and ultimately acts to inhibit Rac (Fig. 2) [45]. Rac has been implicated in breast cancer cell proliferation and may also promote metastasis by upregulating MMP expression. The notion that Abl/Arg is downstream of EFNB2 is supported by studies in which the Abl-inhibitor, Gleevec, blocks the effects of EFNB2 on cell growth and survival, and also abolishes the inhibition of tumor growth that can be achieved in vivo using EFNB2-Fc [45]. Taken together, these studies show that EFNB2 functions as a tumor suppressor by both actively engaging EPHB4 in anti-proliferative signaling through Ras and by promoting the degradation of EPHB4, which, as a result, prevents its constitutive oncogenic signaling.

EFNB2 also inhibits breast cancer cell migration, probably through bi-directional signaling. In MCF10A cells, EFNB2/EPHB4 is concentrated at cell-cell junctions. Blocking the ligand/receptor association using an antagonist peptide is sufficient to disturb the integrity of the junctions [45]. Studies show that activation of EPHB4 forward signaling with EFNB2-Fc reduces cell migration, decreases Crk activation and inhibits MMP-2 expression and these effects in turn restrict cell motility and invasion. Conversely, knockdown of *EphB4* in breast cancer cells, in which EPHB4 has presumably gained ligand-independent activity, leads to similar decreases in MMP-9 and MMP-2 activity as well as uPA levels, and reduced breast cancer cell migration and invasion [44]. In vivo, there is evidence that bi-directional or reverse signaling is important for metastasis prevention. Overexpression of either a mutant *Efnb2* that is unable to reverse signal or *EphB4* under an MMTV-NeuT background increases incidence of metastasis [8, 9, 49]. The mechanism by which EFNB2 reverse signaling controls metastasis is unknown, but one possibility is that as demonstrated with EFNB1 in *Xenopus*, tyrosine phosphorylation of EFNB2 may disrupt its association with the Par polarity complex member, PAR6, allowing PAR6 to interact with CDC42-GTP, inducing aPKC, and establishing tight junctions [50, 51]. Loss of EFNB2 or loss of reverse signaling would thus lead to disruption of tight junctions, which might account for the increased incidence of metastasis. Together these studies provide further evidence that EFNB2 ligand binding of EPHB4 is necessary to maintain normal cellular adhesion and inhibit inappropriate cell migration [45].

Semaphorins

Semaphorins are unique among the AGMs both in their expression and the manner in which they act as tumor suppressors. There are 21 semaphorins expressed in vertebrates that are divided into 8 classes, with only classes 3–7 expressed in vertebrates. The primary focus of this review is Class 3 semaphorins and they are secreted proteins, whereas class 4–7 semaphorins are membrane-anchored (Fig. 1). Semaphorin receptors are plexins, which consists of 4 subfamilies (types A–D), and neuropilins 1 (NP1) and 2 (NP2) (Fig. 1). Class 4–7 semaphorins and SEMA3E bind directly to specific plexins and activate plexin-mediated signal transduction, while the remainder of Class 3 semaphorins bind to neuropilins, which act as the binding receptor, and then associate with type A plexins or plexinD1 (PLXND1) to mediate signal transduction [4]. A number of semaphorins are upregulated in tumors, suggesting that they are important players in tumorigenesis (Table 2).

The ratio of VEGF to SEMA3 expression may be a key determinant in tumor progression. Several studies show that $VEGF_{165}$ and a subset of Class-3 semaphorins, SEMA3A, 3B, and 3F, both bind to the b1 domain of neuropilins, and thus may act as competitive inhibitors to each other [52, 53], while an alternative view is that both ligands can bind to neuropilins at independent binding sites to initiate antagonistic signaling pathways [54]. When $VEGF_{165}$ levels are higher than SEMA3A, 3B, and 3F, VEGF165 binding to NP1 enhances breast cancer cell survival by maintaining constitutive elevation of PI3K activity [55, 56]. This effect is independent of VEGFR signaling, as $VEGF_{165}$ acts as a pro-survival factor in breast cancer cells, such as MDA-MB-231, which express NP1 and NP2, but not VEGFR1 or VEGFR2 [55, 57]. High levels of SEMA3A, 3B, or 3F block $VEGF_{165}$ binding to NP1, resulting in the inhibition of the PI3K/AKT pathway and promotion of apoptosis (Fig. 2) [55]. Reducing the activity of the PI3/AKT pathway can also have consequences for cell migration through downstream stimulation of GSK-3beta activity and inhibition of pro-proliferative beta-catenin signaling. SEMA3A induction of GSK-3beta activity in a breast cancer cell line has been linked to increased expression of alpha2beta1 integrin, leading to increased adhesion, and decreased migration and invasion [58]. Thus, some members of the SEMA3 family function to inhibit breast cancer cell migration and promote their apoptosis, by inhibiting the binding of $VEGF_{165}$ to neuropilin, thereby blocking PI3/AKT activation in the mammary gland.

In contrast to the clear pro-apoptotic role of the previously described subset of class-3 semaphorins, the effect of other semaphorins on cell migration and metastasis is less well defined. SEMA3F repulses cell migration in NP2-expressing breast cancer cells, but does not alter motility in cells that only express NP1 [59, 60]. Instead, in NP1-expressing cells,

SEMA3F reduces the levels of membrane-associated E-cadherin and beta-catenin, leading to a corresponding decrease in cell adhesion and eventual cell detachment from the tissue culture plate [59, 60]. These findings suggest that SEMA3F may play a pro-metastatic role by promoting tumor cell detachment, however the authors interpreted the results differently, proposing that SEMA3F may be upregulated in normal tumor-adjacent mammary epithelia during early tumorigenesis in an attempt to prevent tumor cells from spreading and attaching to stroma during extravasation [60]. Clearly, the in vivo implications of these in vitro studies merits attention to determine how SEMA3F affects breast cancer metastasis. In contrast, SEMA3B, previously described as a pro-apoptotic factor, promotes migration in breast cancer cells, suggesting that its expression may be beneficial during early tumorigenesis by inhibiting tumor growth, but could promote metastasis during later stages of cancer progression [61]. SEMA3C, another class-3 semaphorin has no reported effects on cell proliferation, but acts as a pro-metastatic AGM. Studies show that overexpression of SEMA3C in breast cancer cell lines results in increased migration, but whether this corresponds to increased metastasis in vivo has not been explored [62]. Instead, in vitro studies have shown that SEMA3C activity is regulated by ADAMTS1 cleavage, increasing its availability to tumor cells. ADAMTS1 is acutely upregulated in metastatic breast cancer cells, suggesting that co-expression of ADAMTS1 and SEMA3C in tumors may drive metastasis [62]. These studies demonstrate that, while class-3 semaphorins often act as tumor suppressors by suppressing cell proliferation during early tumorigenesis, they may switch to an oncogenic role during tumor progression by promoting tumor metastasis.

In contrast to class-3 semaphorins, SEMA4D regulates cell migration by mediating plexin binding to tyrosine kinases. SEMA4D is highly expressed in invading tumor epithelial cells, where it is can be diffusely detected in the cytoplasm or robustly on the cell-surface [63]. As described earlier, class-4 semaphorins bind directly to plexins to initiate plexin-mediated signaling. In breast cancer cells, SEMA4D activates PlexinB1 (PLXNB1) to promote or inhibit metastasis in a context dependent manner. Binding of SEMA4D to PLXNB1 can lead to stable association of PLXNB1 and activation of receptor tyrosine kinases MET or ERBB2, resulting in tyrosine phosphorylation of both receptors. Again, this appears to be a situation where the relative expression of receptors determines the activity of a Semaphorin [64]. In the presence of ERBB2, SEMA4D increases migration by activating the PI3K/AKT pathway, resulting in pro-migratory RHOA-mediated signaling (Fig. 2). In contrast, in the presence of MET, SEMA4D inhibits migration through inhibition of integrin function, a process that involves R-RasGAP activity or P190RhoGAP-dependent RHO inhibition [64]. Thus, SEMA4D has opposing effects on RHO activity and cell migration, mediated by PLXNB1 interaction with either MET or ERBB2.

Putting AGMs into Context

SEMA4D's ability to act as both a pro-migratory and anti-migratory factor depending on expression of ERBB2 and MET underscores the importance of cellular context in ascribing tumor suppressor or oncogene labels to some AGMs [64]. EPHA2 also exhibits a context dependent oncogenic effect in which its loss only inhibits tumorigenesis under an *MMTV-Neu* background, which overexpresses ERBB2, but not in *MMTV-PyV-mT* transgenic mice, which expresses only moderate levels of ERBB2 [7]. This study also shows that EPHA2 physically interacts with and is phosphorylated by activated ERBB2 to promote tumor progression [7]. It is interesting that SEMA4D and EPHA2 both acquire oncogenic activity only in the context of ERBB2 overexpression. This suggest that blockade of ERBB2 overexpression during cancer treatment may have a secondary effect on these AGMs by "deactivating" their oncogenic activity.

Another principle that is repeated in most of the AGM families is the importance of relative ratios of ligands and receptors in determining oncogenic or tumor suppressor activities. This is the basic concept of NTN1 function, where in the presence of DCC or UNC5H, high levels of NTN1 are thought to be pro-survival, and thus oncogenic, while loss of NTN1 expression leads to induction of apoptotic signaling. In contrast, NTN4 appears to act in a converse manner where low levels of NTN4 promote proliferation, while high levels inhibit cell growth—reinforcing the concept that relative ligand/receptor levels determine function. This same concept has been echoed in Eph/ephrin signaling, wherein ephrins act to suppress Eph forward signaling, thus acquiring a role as tumor suppressors. When the balance of Eph/ephrin signaling is perturbed, either by loss of ephrin expression or Eph overexpression, EPHA4 and EPHB2 signaling is no longer suppressed, and they become oncogenic. Thus, changes in the relative expression of these ligand/receptor pairs during tumorigenesis can have a profound outcome on the role of these signaling pathways in promoting or inhibiting tumor progression.

Use of AGMs in Cancer Diagnosis and as Therapeutic Targets

AGMs show promise as breast cancer diagnostic/prognostic markers as well as potential therapeutic targets. We have

already discussed the prognostic value of AGM expression in tumor samples. What is of even greater interest is that these changes can often be detected in patient blood plasma samples. Recent studies have shown that plasma NTN1 is increased in breast cancer patients [65]. *Slit2* methylation is also increased in breast cancer patients, with a complete concordance between tumor and paired sera [66]. These findings may form the foundation for the development of quick, non-invasive breast cancer prognostic tests, and in the case of *Slit2*, which appears to be methylated early during cancer progression, may lead to more effective early diagnostic tests. Targeting of pro-oncogenic or pro-metastatic AGMs using siRNA or cytotoxin-conjugated ligands, may also be an effective strategy for treating breast cancer. For example, injection of antisense-EphB4 oligo (siRNA) into mice that had been inoculated with tumor cells led to a reduction in tumor growth and smaller tumor size, with a corresponding decrease in proliferation and increase in apoptosis [44]. Similarly, injection of a cancer xenograft model with EFNB2-Fc, which like the antisense-EPHB4 oligo inhibits EphB4 forward signaling, results in decreased tumor growth [45]. As mentioned previously, treatment with a monoclonal antibody that mimics the binding of EFNA1 to EPHA2, inhibits EPHA2 oncogenic activity and restores tamoxifen sensitivity in breast cancer cells [40]. Likewise, treatment of EPHA2-overexpressing breast cancer cells with cytotoxin-conjugated EFNA1 induced apoptosis [67]. Targeting of NTN1 using siRNA or inducing its multimerization using a recombinant soluble fifth fibronectin domain of DCC also may be a potential therapy for inhibition of metastasis [23, 68]. These studies may pave the way for development of more effective breast cancer therapeutics in the future.

Acknowledgments This work was supported by funds from the NIH RO1 (CA-128902, L.H.), Congressionally Directed Medical Research Program (W81XWH-08-1-0380, L.H.), Santa Cruz Cancer Benefit Group (L.H.) and the California Institute of Regenerative Medicine (TG2-01157, G.H.).

References

1. Dickson BJ. Molecular mechanisms of axon guidance. Science. 2002;298(5600):1959–64. doi:10.1126/science.1072165.
2. Hinck L. The versatile roles of "axon guidance" cues in tissue morphogenesis. Dev Cell. 2004;7(6):783–93. doi:10.1016/j.devcel.2004.11.002.
3. Mehlen P, Delloye-Bourgeois C, Chedotal A. Novel roles for Slits and netrins: axon guidance cues as anticancer targets? Nat Rev Cancer. 2011;11(3):188–97. doi:10.1038/nrc3005.
4. Neufeld G, Kessler O. The semaphorins: versatile regulators of tumour progression and tumour angiogenesis. Nat Rev Cancer. 2008;8(8):632–45. doi:10.1038/nrc2404.
5. Pasquale EB. Eph receptors and ephrins in cancer: bidirectional signalling and beyond. Nat Rev Cancer. 2010;10(3):165–80. doi:10.1038/nrc2806.
6. Strickland P, Shin GC, Plump A, Tessier-Lavigne M, Hinck L. Slit2 and netrin 1 act synergistically as adhesive cues to generate tubular bi-layers during ductal morphogenesis. Development. 2006;133(5):823–32. doi:10.1242/dev.02261.
7. Brantley-Sieders DM, Zhuang G, Hicks D, Fang WB, Hwang Y, Cates JM, et al. The receptor tyrosine kinase EphA2 promotes mammary adenocarcinoma tumorigenesis and metastatic progression in mice by amplifying ErbB2 signaling. J Clin Invest. 2008;118(1):64–78. doi:10.1172/JCI33154.
8. Munarini N, Jager R, Abderhalden S, Zuercher G, Rohrbach V, Loercher S, et al. Altered mammary epithelial development, pattern formation and involution in transgenic mice expressing the EphB4 receptor tyrosine kinase. J Cell Sci. 2002;115(Pt 1):25–37.
9. Haldimann M, Custer D, Munarini N, Stirnimann C, Zurcher G, Rohrbach V, et al. Deregulated ephrin-B2 expression in the mammary gland interferes with the development of both the glandular epithelium and vasculature and promotes metastasis formation. Int J Oncol. 2009;35(3):525–36.
10. Marlow R, Strickland P, Lee JS, Wu X, Pebenito M, Binnewies M, et al. SLITs suppress tumor growth in vivo by silencing Sdf1/Cxcr4 within breast epithelium. Cancer Res. 2008;68(19):7819–27. doi:10.1158/0008-5472.CAN-08-1357.
11. Srinivasan K, Strickland P, Valdes A, Shin GC, Hinck L. Netrin-1/neogenin interaction stabilizes multipotent progenitor cap cells during mammary gland morphogenesis. Dev Cell. 2003;4(3):371–82.
12. Dallol A, Da Silva NF, Viacava P, Minna JD, Bieche I, Maher ER, et al. SLIT2, a human homologue of the Drosophila Slit2 gene, has tumor suppressor activity and is frequently inactivated in lung and breast cancers. Cancer Res. 2002;62(20):5874–80.
13. Dickinson RE, Dallol A, Bieche I, Krex D, Morton D, Maher ER, et al. Epigenetic inactivation of SLIT3 and SLIT1 genes in human cancers. Br J Cancer. 2004;91(12):2071–8. doi:10.1038/sj.bjc.6602222.
14. Dallol A, Forgacs E, Martinez A, Sekido Y, Walker R, Kishida T, et al. Tumour specific promoter region methylation of the human homologue of the Drosophila Roundabout gene DUTT1 (ROBO1) in human cancers. Oncogene. 2002;21(19):3020–8. doi:10.1038/sj.onc.1205421.
15. Macias H, Moran A, Samara Y, Moreno M, Compton JE, Harburg G, et al. SLIT/ROBO1 signaling suppresses mammary branching morphogenesis by limiting basal cell number. Dev Cell. 2011;20(6):827–40. doi:10.1016/j.devcel.2011.05.012.
16. Prasad A, Paruchuri V, Preet A, Latif F, Ganju RK. Slit-2 induces a tumor-suppressive effect by regulating beta-catenin in breast cancer cells. J Biol Chem. 2008;283(39):26624–33. doi:10.1074/jbc.M800679200.
17. Yuasa-Kawada J, Kinoshita-Kawada M, Rao Y, Wu JY. Deubiquitinating enzyme USP33/VDU1 is required for Slit signaling in inhibiting breast cancer cell migration. Proc Natl Acad Sci USA. 2009;106(34):14530–5. doi:10.1073/pnas.0801262106.
18. Muller A, Homey B, Soto H, Ge N, Catron D, Buchanan ME, et al. Involvement of chemokine receptors in breast cancer metastasis. Nature. 2001;410(6824):50–6. doi:10.1038/35065016.
19. Schmid BC, Rudas M, Rezniczek GA, Leodolter S, Zeillinger R. CXCR4 is expressed in ductal carcinoma in situ of the breast and in atypical ductal hyperplasia. Breast Cancer Res Treat. 2004;84(3):247–50. doi:10.1023/B:BREA.0000019962.18922.87.
20. Prasad A, Fernandis AZ, Rao Y, Ganju RK. Slit protein-mediated inhibition of CXCR4-induced chemotactic and chemoinvasive signaling pathways in breast cancer cells. J Biol Chem. 2004;279(10):9115–24. doi:10.1074/jbc.M308083200.
21. Wu JY, Feng L, Park HT, Havlioglu N, Wen L, Tang H, et al. The neuronal repellent Slit inhibits leukocyte chemotaxis induced by

chemotactic factors. Nature. 2001;410(6831):948–52. doi:10.1038/35073616.
22. Llambi F, Causeret F, Bloch-Gallego E, Mehlen P. Netrin-1 acts as a survival factor via its receptors UNC5H and DCC. EMBO J. 2001;20(11):2715–22. doi:10.1093/emboj/20.11.2715.
23. Fitamant J, Guenebeaud C, Coissieux MM, Guix C, Treilleux I, Scoazec JY, et al. Netrin-1 expression confers a selective advantage for tumor cell survival in metastatic breast cancer. Proc Natl Acad Sci USA. 2008;105(12):4850–5. doi:10.1073/pnas.0709810105.
24. Fazeli A, Dickinson SL, Hermiston ML, Tighe RV, Steen RG, Small CG, et al. Phenotype of mice lacking functional Deleted in colorectal cancer (Dcc) gene. Nature. 1997;386(6627):796–804. doi:10.1038/386796a0.
25. Thiebault K, Mazelin L, Pays L, Llambi F, Joly MO, Scoazec JY, et al. The netrin-1 receptors UNC5H are putative tumor suppressors controlling cell death commitment. Proc Natl Acad Sci USA. 2003;100(7):4173–8. doi:10.1073/pnas.0738063100.
26. Lee JE, Kim HJ, Bae JY, Kim SW, Park JS, Shin HJ, et al. Neogenin expression may be inversely correlated to the tumorigenicity of human breast cancer. BMC Cancer. 2005;5:154. doi:10.1186/1471-2407-5-154.
27. Nacht M, St Martin TB, Byrne A, Klinger KW, Teicher BA, Madden SL, et al. Netrin-4 regulates angiogenic responses and tumor cell growth. Exp Cell Res. 2009;315(5):784–94. doi:10.1016/j.yexcr.2008.11.018.
28. Qin S, Yu L, Gao Y, Zhou R, Zhang C. Characterization of the receptors for axon guidance factor netrin-4 and identification of the binding domains. Mol Cell Neurosci. 2007;34(2):243–50. doi:10.1016/j.mcn.2006.11.002.
29. Lejmi E, Leconte L, Pedron-Mazoyer S, Ropert S, Raoul W, Lavalette S, et al. Netrin-4 inhibits angiogenesis via binding to neogenin and recruitment of Unc5B. Proc Natl Acad Sci USA. 2008;105(34):12491–6. doi:10.1073/pnas.0804008105.
30. Esseghir S, Kennedy A, Seedhar P, Nerurkar A, Poulsom R, Reis-Filho JS, et al. Identification of NTN4, TRA1, and STC2 as prognostic markers in breast cancer in a screen for signal sequence encoding proteins. Clin Cancer Res. 2007;13(11):3164–73. doi:10.1158/1078-0432.CCR-07-0224.
31. Fujikane T, Nishikawa N, Toyota M, Suzuki H, Nojima M, Maruyama R, et al. Genomic screening for genes upregulated by demethylation revealed novel targets of epigenetic silencing in breast cancer. Breast Cancer Res Treat. 2010;122(3):699–710. doi:10.1007/s10549-009-0600-1.
32. Noren NK, Lu M, Freeman AL, Koolpe M, Pasquale EB. Interplay between EphB4 on tumor cells and vascular ephrin-B2 regulates tumor growth. Proc Natl Acad Sci USA. 2004;101(15):5583–8. doi:10.1073/pnas.0401381101.
33. Walker-Daniels J, Riese 2nd DJ, Kinch MS. c-Cbl-dependent EphA2 protein degradation is induced by ligand binding. Mol Cancer Res. 2002;1(1):79–87.
34. Zelinski DP, Zantek ND, Stewart JC, Irizarry AR, Kinch MS. EphA2 overexpression causes tumorigenesis of mammary epithelial cells. Cancer Res. 2001;61(5):2301–6.
35. Noblitt LW, Bangari DS, Shukla S, Knapp DW, Mohammed S, Kinch MS, et al. Decreased tumorigenic potential of EphA2-overexpressing breast cancer cells following treatment with adenoviral vectors that express EphrinA1. Cancer Gene Ther. 2004;11(11):757–66. doi:10.1038/sj.cgt.7700761.
36. Macrae M, Neve RM, Rodriguez-Viciana P, Haqq C, Yeh J, Chen C, et al. A conditional feedback loop regulates Ras activity through EphA2. Cancer Cell. 2005;8(2):111–8. doi:10.1016/j.ccr.2005.07.005.
37. Zantek ND, Azimi M, Fedor-Chaiken M, Wang B, Brackenbury R, Kinch MS. E-cadherin regulates the function of the EphA2 receptor tyrosine kinase. Cell Growth Differ. 1999;10(9):629–38.
38. Wykosky J, Palma E, Gibo DM, Ringler S, Turner CP, Debinski W. Soluble monomeric EphrinA1 is released from tumor cells and is a functional ligand for the EphA2 receptor. Oncogene. 2008;27(58):7260–73. doi:10.1038/onc.2008.328.
39. Brantley-Sieders DM, Fang WB, Hicks DJ, Zhuang G, Shyr Y, Chen J. Impaired tumor microenvironment in EphA2-deficient mice inhibits tumor angiogenesis and metastatic progression. FASEB J. 2005;19(13):1884–6. doi:10.1096/fj.05-4038fje.
40. Gokmen-Polar Y, Toroni RA, Hocevar BA, Badve S, Zhao Q, Shen C et al. Dual targeting of EphA2 and ER restores tamoxifen sensitivity in ER/EphA2-positive breast cancer. Breast Cancer Res Treat. 2010. doi:10.1007/s10549-010-1004-y.
41. Hiramoto-Yamaki N, Takeuchi S, Ueda S, Harada K, Fujimoto S, Negishi M, et al. Ephexin4 and EphA2 mediate cell migration through a RhoG-dependent mechanism. J Cell Biol. 2010;190(3):461–77. doi:10.1083/jcb.201005141.
42. Zelinski DP, Zantek ND, Walker-Daniels J, Peters MA, Taparowsky EJ, Kinch MS. Estrogen and Myc negatively regulate expression of the EphA2 tyrosine kinase. J Cell Biochem. 2002;85(4):714–20. doi:10.1002/jcb.10186.
43. Lu M, Miller KD, Gokmen-Polar Y, Jeng MH, Kinch MS. EphA2 overexpression decreases estrogen dependence and tamoxifen sensitivity. Cancer Res. 2003;63(12):3425–9.
44. Kumar SR, Singh J, Xia G, Krasnoperov V, Hassanieh L, Ley EJ, et al. Receptor tyrosine kinase EphB4 is a survival factor in breast cancer. Am J Pathol. 2006;169(1):279–93. doi:10.2353/ajpath.2006.050889.
45. Noren NK, Foos G, Hauser CA, Pasquale EB. The EphB4 receptor suppresses breast cancer cell tumorigenicity through an Abl-Crk pathway. Nat Cell Biol. 2006;8(8):815–25. doi:10.1038/ncb1438.
46. Nikolova Z, Djonov V, Zuercher G, Andres AC, Ziemiecki A. Cell-type specific and estrogen dependent expression of the receptor tyrosine kinase EphB4 and its ligand ephrin-B2 during mammary gland morphogenesis. J Cell Sci. 1998;111(Pt 18):2741–51.
47. Berclaz G, Andres AC, Albrecht D, Dreher E, Ziemiecki A, Gusterson BA, et al. Expression of the receptor protein tyrosine kinase myk-1/htk in normal and malignant mammary epithelium. Biochem Biophys Res Commun. 1996;226(3):869–75. doi:10.1006/bbrc.1996.1442.
48. Wu Q, Suo Z, Risberg B, Karlsson MG, Villman K, Nesland JM. Expression of Ephb2 and Ephb4 in breast carcinoma. Pathol Oncol Res. 2004;10(1):26–33. doi:PAOR.2004.10.1.0026.
49. Kaenel P, Schwab C, Mulchi K, Wotzkow C, Andres AC. Preponderance of cells with stem cell characteristics in metastasising mouse mammary tumours induced by deregulated EphB4 and ephrin-B2 expression. Int J Oncol. 2011;38(1):151–60.
50. Lee HS, Nishanian TG, Mood K, Bong YS, Daar IO. EphrinB1 controls cell-cell junctions through the Par polarity complex. Nat Cell Biol. 2008;10(8):979–86. doi:10.1038/ncb1758.
51. Lee HS, Daar IO. EphrinB reverse signaling in cell-cell adhesion: is it just par for the course? Cell Adh Migr. 2009;3(3):250–5.
52. Gu C, Limberg BJ, Whitaker GB, Perman B, Leahy DJ, Rosenbaum JS, et al. Characterization of neuropilin-1 structural features that confer binding to semaphorin 3A and vascular endothelial growth factor 165. J Biol Chem. 2002;277(20):18069–76. doi:10.1074/jbc.M201681200.
53. Vander Kooi CW, Jusino MA, Perman B, Neau DB, Bellamy HD, Leahy DJ. Structural basis for ligand and heparin binding to neuropilin B domains. Proc Natl Acad Sci USA. 2007;104(15):6152–7. doi:10.1073/pnas.0700043104.
54. Appleton BA, Wu P, Maloney J, Yin J, Liang WC, Stawicki S, et al. Structural studies of neuropilin/antibody complexes provide insights into semaphorin and VEGF binding. EMBO J. 2007;26(23):4902–12. doi:10.1038/sj.emboj.7601906.

55. Bachelder RE, Crago A, Chung J, Wendt MA, Shaw LM, Robinson G, et al. Vascular endothelial growth factor is an autocrine survival factor for neuropilin-expressing breast carcinoma cells. Cancer Res. 2001;61(15):5736–40.
56. Castro-Rivera E, Ran S, Brekken RA, Minna JD. Semaphorin 3B inhibits the phosphatidylinositol 3-kinase/Akt pathway through neuropilin-1 in lung and breast cancer cells. Cancer Res. 2008;68 (20):8295–303. doi:10.1158/0008-5472.CAN-07-6601.
57. Castro-Rivera E, Ran S, Thorpe P, Minna JD. Semaphorin 3B (SEMA3B) induces apoptosis in lung and breast cancer, whereas VEGF165 antagonizes this effect. Proc Natl Acad Sci USA. 2004;101(31):11432–7. doi:10.1073/pnas.0403969101.
58. Pan H, Wanami LS, Dissanayake TR, Bachelder RE. Autocrine semaphorin3A stimulates alpha2 beta1 integrin expression/function in breast tumor cells. Breast Cancer Res Treat. 2009;118 (1):197–205. doi:10.1007/s10549-008-0179-y.
59. Nasarre P, Constantin B, Rouhaud L, Harnois T, Raymond G, Drabkin HA, et al. Semaphorin SEMA3F and VEGF have opposing effects on cell attachment and spreading. Neoplasia. 2003;5(1):83–92.
60. Nasarre P, Kusy S, Constantin B, Castellani V, Drabkin HA, Bagnard D, et al. Semaphorin SEMA3F has a repulsing activity on breast cancer cells and inhibits E-cadherin-mediated cell adhesion. Neoplasia. 2005;7(2):180–9. doi:10.1593/neo.04481.
61. Rolny C, Capparuccia L, Casazza A, Mazzone M, Vallario A, Cignetti A, et al. The tumor suppressor semaphorin 3B triggers a prometastatic program mediated by interleukin 8 and the tumor microenvironment. J Exp Med. 2008;205(5):1155–71. doi:10.1084/jem.20072509.
62. Esselens C, Malapeira J, Colome N, Casal C, Rodriguez-Manzaneque JC, Canals F, et al. The cleavage of semaphorin 3C induced by ADAMTS1 promotes cell migration. J Biol Chem. 2010;285(4):2463–73. doi:10.1074/jbc.M109.055129.
63. Basile JR, Castilho RM, Williams VP, Gutkind JS. Semaphorin 4D provides a link between axon guidance processes and tumor-induced angiogenesis. Proc Natl Acad Sci USA. 2006;103 (24):9017–22. doi:10.1073/pnas.0508825103.
64. Swiercz JM, Worzfeld T, Offermanns S. ErbB-2 and met reciprocally regulate cellular signaling via plexin-B1. J Biol Chem. 2008;283(4):1893–901. doi:10.1074/jbc.M706822200.
65. Ramesh G, Berg A, Jayakumar C. Plasma netrin-1 is a diagnostic biomarker of human cancers. Biomarkers. 2011;16(2):172–80. doi:10.3109/1354750X.2010.541564.
66. Sharma G, Mirza S, Prasad CP, Srivastava A, Gupta SD, Ralhan R. Promoter hypermethylation of p16INK4A, p14ARF, CyclinD2 and Slit2 in serum and tumor DNA from breast cancer patients. Life Sci. 2007;80(20):1873–81. doi:10.1016/j.lfs.2007.02.026.
67. Wykosky J, Gibo DM, Debinski W. A novel, potent, and specific ephrinA1-based cytotoxin against EphA2 receptor expressing tumor cells. Mol Cancer Ther. 2007;6(12 Pt 1):3208–18. doi:10.1158/1535-7163.MCT-07-0200.
68. Mille F, Llambi F, Guix C, Delloye-Bourgeois C, Guenebeaud C, Castro-Obregon S, et al. Interfering with multimerization of netrin-1 receptors triggers tumor cell death. Cell Death Differ. 2009;16(10):1344–51. doi:10.1038/cdd.2009.75.
69. Ho KY, Kalle WH, Lo TH, Lam WY, Tang CM. Reduced expression of APC and DCC gene protein in breast cancer. Histopathology. 1999;35(3):249–56.
70. Vaught D, Chen J, Brantley-Sieders DM. Regulation of mammary gland branching morphogenesis by EphA2 receptor tyrosine kinase. Mol Biol Cell. 2009;20(10):2572–81. doi:10.1091/mbc.E08-04-0378.
71. Kouros-Mehr H, Werb Z. Candidate regulators of mammary branching morphogenesis identified by genome-wide transcript analysis. Dev Dyn. 2006;235(12):3404–12. doi:10.1002/dvdy.20978.
72. Chodosh LA, Gardner HP, Rajan JV, Stairs DB, Marquis ST, Leder PA. Protein kinase expression during murine mammary development. Dev Biol. 2000;219(2):259–76. doi:10.1006/dbio.2000.9614.
73. Fox BP, Kandpal RP. EphB6 receptor significantly alters invasiveness and other phenotypic characteristics of human breast carcinoma cells. Oncogene. 2009;28(14):1706–13. doi:10.1038/onc.2009.18.
74. Morris JS, Stein T, Pringle MA, Davies CR, Weber-Hall S, Ferrier RK, et al. Involvement of axonal guidance proteins and their signaling partners in the developing mouse mammary gland. J Cell Physiol. 2006;206(1):16–24. doi:10.1002/jcp.20427.
75. Xiang RH, Hensel CH, Garcia DK, Carlson HC, Kok K, Daly MC, et al. Isolation of the human semaphorin III/F gene (SEMA3F) at chromosome 3p21, a region deleted in lung cancer. Genomics. 1996;32(1):39–48. doi:10.1006/geno.1996.0074.
76. Clarkson RW, Wayland MT, Lee J, Freeman T, Watson CJ. Gene expression profiling of mammary gland development reveals putative roles for death receptors and immune mediators in post-lactational regression. Breast Cancer Res. 2004;6(2):R92–R109. doi:10.1186/bcr754.
77. Qu X, Wei H, Zhai Y, Que H, Chen Q, Tang F, et al. Identification, characterization, and functional study of the two novel human members of the semaphorin gene family. J Biol Chem. 2002;277 (38):35574–85. doi:10.1074/jbc.M206451200.
78. Bachelder RE, Lipscomb EA, Lin X, Wendt MA, Chadborn NH, Eickholt BJ, et al. Competing autocrine pathways involving alternative neuropilin-1 ligands regulate chemotaxis of carcinoma cells. Cancer Res. 2003;63(17):5230–3.
79. Rody A, Holtrich U, Gaetje R, Gehrmann M, Engels K, von Minckwitz G, et al. Poor outcome in estrogen receptor-positive breast cancers predicted by loss of plexin B1. Clin Cancer Res. 2007;13(4):1115–22. doi:10.1158/1078-0432.CCR-06-2433.
80. Schmid BC, Rezniczek GA, Fabjani G, Yoneda T, Leodolter S, Zeillinger R. The neuronal guidance cue Slit2 induces targeted migration and may play a role in brain metastasis of breast cancer cells. Breast Cancer Res Treat. 2007;106(3):333–42. doi:10.1007/s10549-007-9504-0.
81. Sundaresan V, Chung G, Heppell-Parton A, Xiong J, Grundy C, Roberts I, et al. Homozygous deletions at 3p12 in breast and lung cancer. Oncogene. 1998;17(13):1723–9. doi:10.1038/sj.onc.1202103.
82. Kashiwaba M, Tamura G, Ishida M. Frequent loss of heterozygosity at the deleted in colorectal carcinoma gene locus and its association with histologic phenotypes in breast carcinoma. Virchows Arch. 1995;426(5):441–6.
83. Reale MA, Hu G, Zafar AI, Getzenberg RH, Levine SM, Fearon ER. Expression and alternative splicing of the deleted in colorectal cancer (DCC) gene in normal and malignant tissues. Cancer Res. 1994;54(16):4493–501.
84. Thompson AM, Morris RG, Wallace M, Wyllie AH, Steel CM, Carter DC. Allele loss from 5q21 (APC/MCC) and 18q21 (DCC) and DCC mRNA expression in breast cancer. Br J Cancer. 1993;68(1):64–8.
85. Wakita K, Kohno N, Sakoda Y, Ishikawa Y, Sakaue M. Decreased expression of the DCC gene in human breast carcinoma. Surg Today. 1996;26(11):900–3.
86. Ogawa K, Pasqualini R, Lindberg RA, Kain R, Freeman AL, Pasquale EB. The ephrin-A1 ligand and its receptor, EphA2, are expressed during tumor neovascularization. Oncogene. 2000;19 (52):6043–52. doi:10.1038/sj.onc.1204004.
87. Somiari SB, Shriver CD, He J, Parikh K, Jordan R, Hooke J, et al. Global search for chromosomal abnormalities in infiltrating ductal carcinoma of the breast using array-comparative genomic hybridization. Cancer Genet Cytogenet. 2004;155(2):108–18. doi:10.1016/j.cancergencyto.2004.02.023.

88. Fox BP, Kandpal RP. DNA-based assay for EPHB6 expression in breast carcinoma cells as a potential diagnostic test for detecting tumor cells in circulation. Cancer Genomics Proteomics. 2010;7(1):9–16.
89. Fox BP, Kandpal RP. Transcriptional silencing of EphB6 receptor tyrosine kinase in invasive breast carcinoma cells and detection of methylated promoter by methylation specific PCR. Biochem Biophys Res Commun. 2006;340(1):268–76. doi:10.1016/j.bbrc.2005.11.174.
90. Christensen C, Ambartsumian N, Gilestro G, Thomsen B, Comoglio P, Tamagnone L, et al. Proteolytic processing converts the repelling signal Sema3E into an inducer of invasive growth and lung metastasis. Cancer Res. 2005;65(14):6167–77. doi:10.1158/0008-5472.CAN-04-4309.
91. Rody A, Karn T, Ruckhaberle E, Hanker L, Metzler D, Muller V, et al. Loss of Plexin B1 is highly prognostic in low proliferating ER positive breast cancers–results of a large scale microarray analysis. Eur J Cancer. 2009;45(3):405–13. doi:10.1016/j.ejca.2008.10.016.

Developmental Cell
Article

SLIT/ROBO1 Signaling Suppresses Mammary Branching Morphogenesis by Limiting Basal Cell Number

Hector Macias,[1] Angel Moran,[1] Yazeed Samara,[1] Melissa Moreno,[1] Jennifer E. Compton,[1] Gwyndolen Harburg,[1] Phyllis Strickland,[1] and Lindsay Hinck[1,*]
[1]Department of Molecular, Cell and Developmental Biology, University of California, Santa Cruz, CA 95064, USA
*Correspondence: hinck@biology.ucsc.edu
DOI 10.1016/j.devcel.2011.05.012

SUMMARY

In the field of breast biology, there is a growing appreciation for the "gatekeeping function" of basal cells during development and disease processes yet mechanisms regulating the generation of these cells are poorly understood. Here, we report that the proliferation of basal cells is controlled by SLIT/ROBO1 signaling and that production of these cells regulates outgrowth of mammary branches. We identify the negative regulator TGF-β1 upstream of *Robo1* and show that it induces *Robo1* expression specifically in the basal layer, functioning together with SLIT2 to restrict branch formation. Loss of SLIT/ROBO1 signaling in this layer alone results in precocious branching due to a surplus of basal cells. SLIT2 limits basal cell proliferation by inhibiting canonical WNT signaling, increasing the cytoplasmic and membrane pools of β-catenin at the expense of its nuclear pool. Together, our studies provide mechanistic insight into how specification of basal cell number influences branching morphogenesis.

INTRODUCTION

Like other glandular organs, the mammary gland (breast) contains a bilayered epithelial structure consisting of an outer layer of basal myoepithelial cells (MECs) encircling an inner layer of luminal epithelial cells (LECs) (Silberstein, 2001). Historically, the basal layer has been largely overlooked by researchers, who focused instead on LECs, considered the origin of most carcinomas. Recently, however, appreciation has grown for the importance of this basal layer as an "epithelial gatekeeper," generating the boundary between epithelial and stromal compartments, organizing tissue structure, maintaining stem cells, and suppressing cancerous growth (Barsky and Karlin, 2006; Gudjonsson et al., 2005). Nevertheless, the mechanisms regulating the generation and proliferation of these cells are poorly understood.

During postnatal mammary morphogenesis, highly mitotic structures at the tips of growing ducts called "end buds" invade the fatty stroma and establish the mammary tree. Cap cells, composing the basal layer of the end bud, differentiate into MECs that fully ensheath the ducts (Williams and Daniel, 1983). During pregnancy, however, the LEC population greatly expands as alveoli develop, resulting in sparse MEC coverage as basal cells stretch to accommodate the increased volume. This discontinuous coverage of an expanding LEC population also occurs during tumorigenesis when uncontrolled growth of LECs breaks through the myoepithelial barrier, resulting in the transition from ductal carcinoma in situ to infiltrating ductal carcinoma. Thus, understanding the mechanisms that regulate basal cell proliferation promises insight into basic developmental processes such as tissue morphogenesis and disease processes such as tumor metastasis.

Branching morphogenesis is a developmental program that imparts functional complexity to many biological systems (Andrew and Ewald, 2010). End bud bifurcation generates the primary ductal architecture, but lateral outgrowth of secondary and tertiary ducts is required to achieve full arborization of the mammary tree (Silberstein, 2001). The branching pattern of the mammary gland is stochastic, with the major requirement being an open ductal architecture that allows pregnancy-induced alveolar infilling. Consequently, inhibitory signals are critical and TGF-β1 is a key negative regulator of this process (Ewan et al., 2002; Ingman and Robertson, 2008; Nelson et al., 2006). It functions by inhibiting cellular proliferation, but how it restricts cell growth, especially in a cell type-specific manner, is not well defined. In LECs, noncanonical WNT5A acts downstream of TGF-β1 (Pavlovich et al., 2011; Roarty and Serra, 2007) and inhibits cell growth by antagonizing canonical WNT signaling (Roarty et al., 2009). In cap cells or MECs, no downstream mediators of TGF-β1 have been identified to date.

SLITs are a conserved family of secreted proteins that were originally discovered in the nervous system, where they signal through ROBO receptors to mediate axonal guidance and branching (Brose et al., 1999; Wang et al., 1999). Their guidance function is well conserved and involved in directing migration of many cell types, including neural crest, immune, and tumor cells (Ypsilanti et al., 2010). In contrast, the branching function of SLITs has been chiefly described in the vascular system (Jones et al., 2008; Marlow et al., 2010) and seldom in epithelial organs of vertebrate animals (Grieshammer et al., 2004), where instead a distinct role for SLITs and ROBOs as tumor suppressors has been identified (Dallol et al., 2005; Marlow et al., 2008; Prasad et al., 2008; Yang et al., 2010). Thus, SLIT/ROBO signaling is emerging as an important regulator of cellular interactions.

In the mammary gland during branching morphogenesis, SLITs are expressed by both LECs and MECs, whereas expression of ROBO1 is restricted to just basal cap cells and MECs (Strickland et al., 2006). In the current study, we investigate the mechanism by which loss of *Slit*s or *Robo1* results in a precocious branching phenotype characterized by an excess of disorganized MECs. We identify the negative regulator, TGF-β1, upstream of ROBO1 and show that it induces *Robo1* specifically in the basal layer, functioning together with SLIT2 to control branch formation. We determine that basal cell number alone influences branch number and demonstrate that SLIT/ROBO1 signaling limits branch formation by antagonizing canonical WNT signaling and restricting basal cell proliferation.

RESULTS

ROBO1 Inhibits Branching Morphogenesis of Mammary Epithelium

To investigate a role for SLIT/ROBO1 signaling in epithelial branching morphogenesis, we examined the *Robo1* loss-of-function phenotype by transplanting *Robo1*$^{-/-}$ and wild-type (WT) littermate epithelium into contralateral fat pads of immunocompromised (*Foxn1*^{nu}) mice that were precleared of their endogenous mammary epithelial buds prior to puberty (Strickland et al., 2006). For this initial analysis, we used transplanted epithelium to assess the outgrowth and branching of epithelia without potential secondary effects of the *Robo1*$^{-/-}$ mutation and to ensure that both *Robo1*$^{-/-}$ and WT tissues were subject to the same hormonal environment. We observed that *Robo1*$^{-/-}$ and WT ducts grew to similar lengths, but that *Robo1*$^{-/-}$ transplants displayed excessive side branching (Figure 1A). We quantified the phenotype and found a >2-fold increase in secondary branches and tertiary buds in *Robo1*$^{-/-}$ transplants (Figure 1B) but no significant difference in primary branch number (Figure 1C), indicating that increased lateral bud formation, rather than excessive end bud bifurcation, is responsible for the phenotype. We previously observed that transplanted knockout tissue contains a hyperplastic phenotype (Marlow et al., 2008; Strickland et al., 2006), and therefore we quantified branching in intact, unmanipulated *Robo1*$^{-/-}$ glands. Intact glands are similarly hyperbranched (H.M., unpublished data), but during this early stage of development they do not display the hyperplastic changes associated with transplanted tissue (see Figure S1A available online).

We also examined branching morphogenesis in an organotypic culture model generated from intact *Robo1*$^{-/-}$ glands in which aggregated cells (Figure 1D) or ductal fragments (Figure S1B) were grown in growth factor-reduced Matrigel (Ewald et al., 2008; Holliday et al., 2009). *Robo1*$^{-/-}$ organoids were devoid of hyperplastic changes, such as luminal infilling, and contained a bilayered epithelium (Figure 1D; Figure S1C). The majority of *Robo1*$^{-/-}$ organoids were branched, whereas WT organoids were unbranched hollow structures (Figure 1E). The few WT organoids containing branches had an average of three branches, whereas *Robo1*$^{-/-}$ organoids had twice as many branches (Figure 1F). Fragment organoids generated from *Robo1*$^{-/-}$ tissue also recapitulated the hyperbranched phenotype (Figures S1B and S1D). Together, these data demonstrate that under the same conditions, *Robo1*$^{-/-}$ epithelium generates more branches than WT epithelium.

SLIT2 Is the ROBO1 Ligand that Inhibits Mammary Branching

SLITs are ligands for ROBO1, and previous studies have shown that *Slit2* and *Slit3*, but not *Slit1*, are expressed in the mammary gland (Strickland et al., 2006). To evaluate whether combined loss of *Slit2* and *Slit3* phenocopies the *Robo1*$^{-/-}$ hyperbranching defect, we transplanted *Slit2*$^{-/-}$;*Slit3*$^{-/-}$ epithelium into precleared fat pads of *Foxn1*^{nu} mice. Loss of *Slit*s, similar to loss of *Robo1*, led to a significant increase in secondary branches and tertiary buds but no difference in primary duct number (Figures 2A and 2B).

Next, we examined whether exogenous SLIT inhibits branch formation. We implanted, at the forefront of WT mammary trees, Elvax slow-release pellets containing either recombinant SLIT2, observed by immunohistochemistry in a 5 mm radius around the pellet (H.M., unpublished data), or control BSA (Figure 2C). Elvax is a biologically compatible polymer that is used to deliver molecules, including functionally inert BSA (Silberstein and Daniel, 1987). SLIT2, rather than SLIT3, was implanted because it is highly expressed during branching morphogenesis (Strickland et al., 2006). After 7 days, secondary branching was suppressed in regions near SLIT2 pellets (Figure 2C, right, box), with the few branches in proximity containing small lateral buds, which frequently turned away from SLIT2 (Figure 2C, arrow). The distance between secondary branches, located within 5 mm of the pellets, was significantly longer in regions surrounding SLIT2 pellets (Figure 2D). There was also a preference for growth away from SLIT2, and this was quantified by counting the secondary branches extending toward (ipsilateral) or away from (contralateral) the pellets (Figure 2E). These data show that SLIT2 inhibits lateral branch formation but not the growth of primary ducts past the pellet.

We also examined the effects of SLIT2 on organoid branching. Because WT organoids are largely unbranched in the absence of growth factors (Figures 1D–1F), we induced branching by adding hepatocyte growth factor (HGF), and then challenged the cultures with SLIT2. There was an 80% reduction in the number of WT branched organoids, a reduction that did not occur with *Robo1*$^{-/-}$ organoids (Figures 2F–2H). Together, these studies strongly support the idea that SLIT2 and ROBO1 function in a ligand/receptor relationship to regulate lateral branching during mammary morphogenesis.

ROBO1 Is a Downstream Effector of TGF-β1 in Myoepithelial Cells

TGF-β1 is a key negative regulator of mammary ductal development and branching morphogenesis. One explanation for our data is that SLIT/ROBO1 signaling is downstream of TGF-β1 and, indeed, transcriptional profiling experiments identified *Robo1* as a TGF-β1-upregulated transcript in mammary cell lines (Labbe et al., 2007). To investigate the biological significance of this result, we cultured primary mammary epithelial cells (ECs) with TGF-β1 along with inhibitors of both protein synthesis (cycloheximide) and the TGF-β1 receptor type 1 (SB431542). We found a TGF-β1-induced, ~2-fold increase in *Robo1* mRNA and protein, with the change in mRNA prevented by the presence of either inhibitor (Figures 3A and 3B), suggesting that TGF-β1 signaling upregulates ROBO1 via a noncanonical

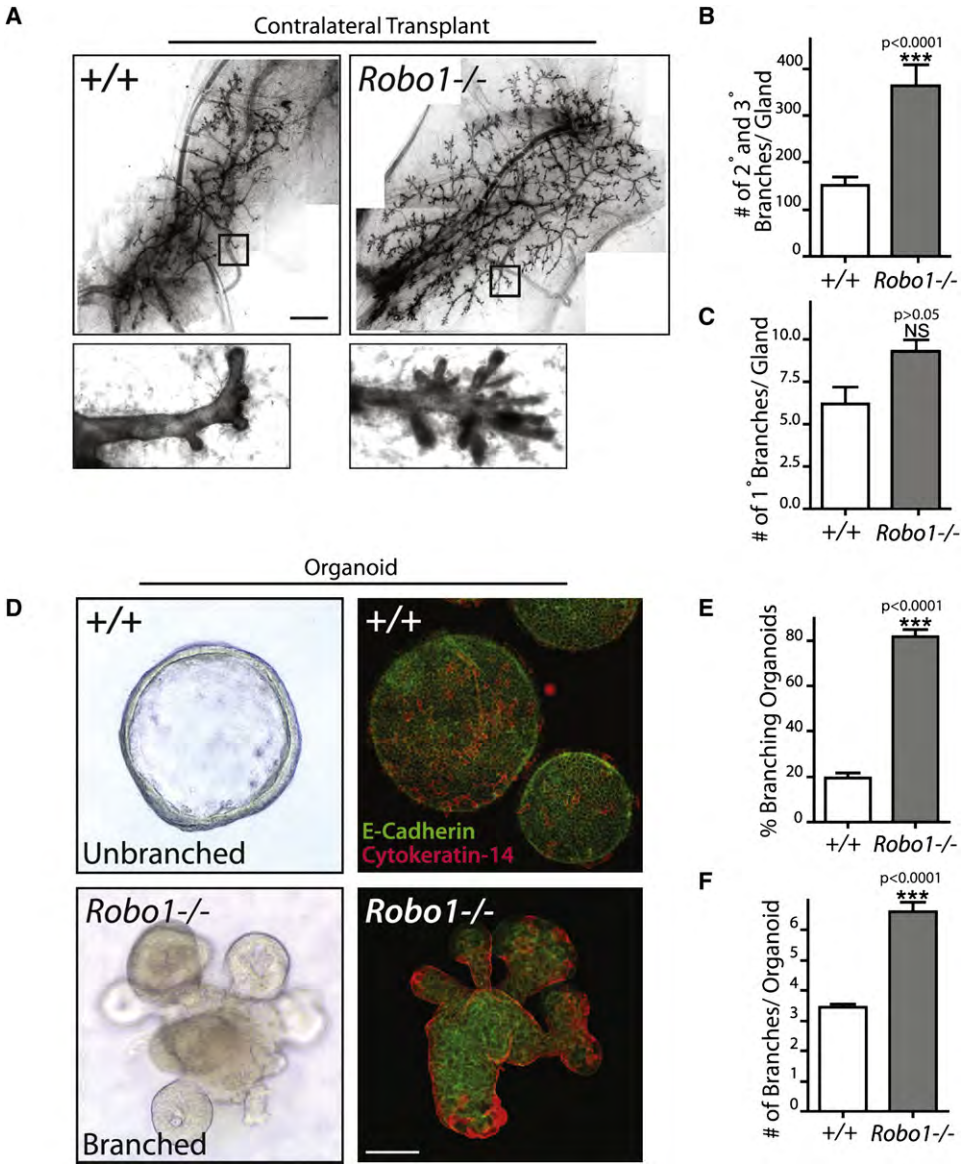

Figure 1. Loss of *Robo1* in Mammary Epithelium Leads to Excess Branching Morphogenesis

(A) Contralaterally transplanted, hematoxylin-stained, virgin WT and *Robo1*$^{-/-}$ outgrowths. Insets represent magnified images.

(B and C) Branchpoint analysis (n = 5 animals).

(D) Representative images of WT and *Robo1*$^{-/-}$ organoids obtained with phase contrast (left) and immunofluorescence using CK-14 (MECs) and E-cadherin (LECs) (right).

(E) Quantification of total branched *Robo1*$^{-/-}$ and WT organoids (n = 4 experiments, >300 organoids/genotype).

(F) Quantification of branches per *Robo1*$^{-/-}$ and WT organoid (n = 3 experiments, >300 organoids/genotype).

Scale bars represent 3 mm (A) and 30 μm (D). Asterisks indicate significance in a Student's t test (NS, not significant).

pathway, rather than Smad signaling, which does not depend on protein synthesis (Yue and Mulder, 2001).

We previously showed that *Robo1* is specifically expressed on cap cells and MECs during branching morphogenesis (Strickland et al., 2006). To assess whether this pattern is recapitulated in organoids, we assayed for β-galactosidase (β-gal) activity, taking advantage of *lacZ* inserted downstream of the *Robo1* promoter (Figures 3C–3E) (Long et al., 2004). As predicted by *Robo1* expression in vivo, we observed positive β-gal staining on the surface of organoids that coimmunostained with an MEC marker (Figure 3C). In a typical *Robo1*$^{-/-}$ organoid, ~30% of MECs stain positive for β-gal, and we considered this the threshold for positivity. Organoids were treated with TGF-β1 for 24 hr, resulting in significantly more β-gal-positive organoids (Figures 3D and 3E). To investigate whether this ROBO1 upregulation contributes to branch inhibition, we used HGF to elicit branching of WT organoids, followed by treatment with TGF-β1, SLIT2, or both (Figure 3F). TGF-β1 or SLIT2

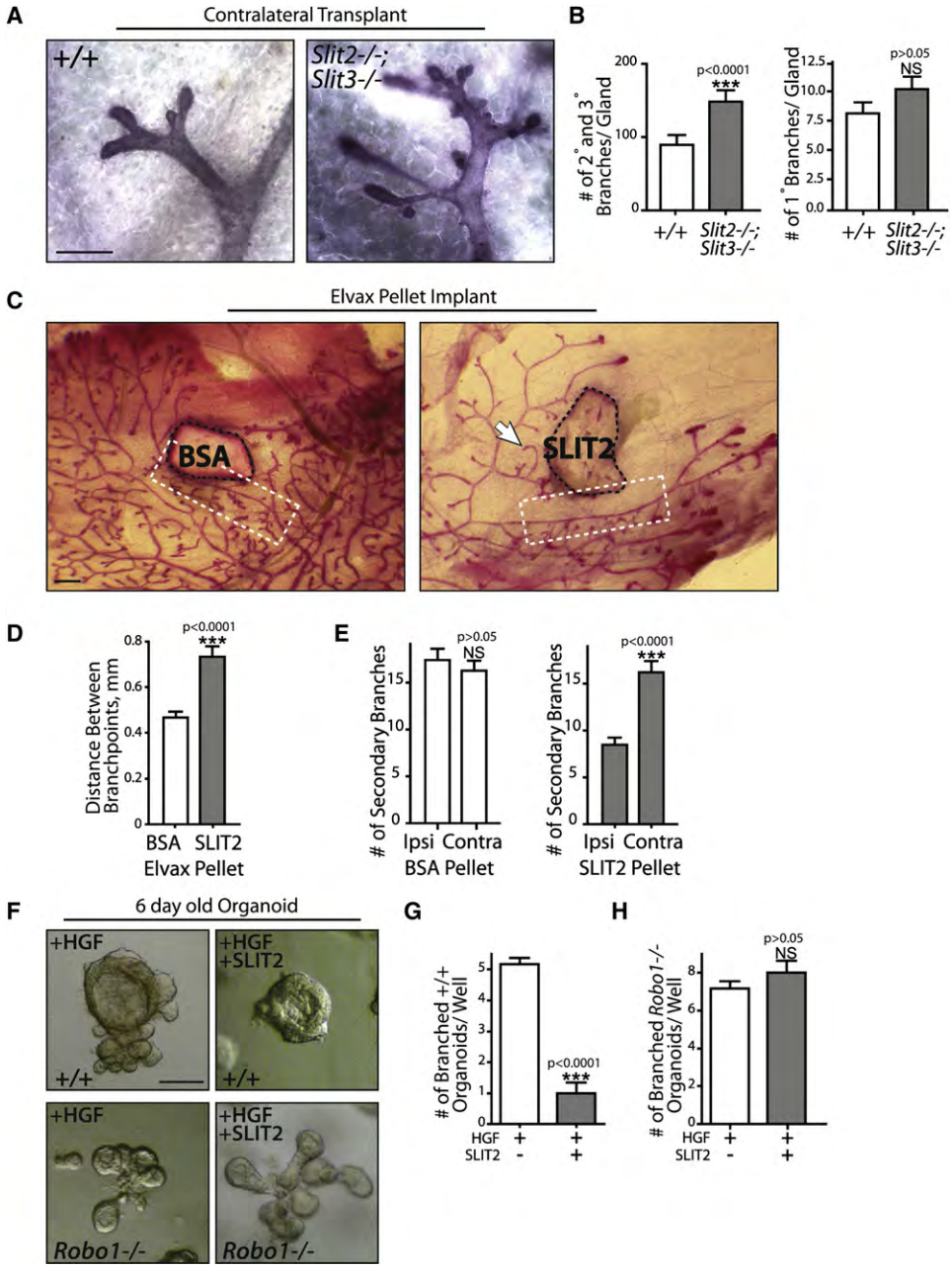

Figure 2. Loss of *Slit2* Results in Excess Branching; Conversely, Exogenous SLIT2 Treatment Results in Decreased Branching

(A) Contralaterally transplanted, hematoxylin-stained, virgin WT and *Slit2*$^{-/-}$;*Slit3*$^{-/-}$ outgrowths.

(B) Branchpoint analysis (n = 10 animals).

(C) Representative whole-mount images of carmine-stained glands contralaterally implanted with Elvax pellets containing either BSA or SLIT2. Black dashed lines outline pellets, white dashed boxes highlight areas near pellets, and the arrow points to an end bud turning away from SLIT2.

(D) Quantification of the distance between 2° branches (5 mm radius; n = 5 animals).

(E) Quantification of 2° branches ipsilateral or contralateral to the pellet (n = 5 animals).

(F) Representative phase-contrast images of WT or control *Robo1*$^{-/-}$ organoids induced to branch with HGF. After 24 hr, organoids were treated with HGF either alone or with SLIT2 and allowed to grow for 6 days.

(G and H) Quantification of the number of WT and *Robo1*$^{-/-}$ organoids in each condition that had three or more branches (n = 3 experiments, >100 organoids/ treatment).

Scale bars represent 1 mm (A and C) and 75 μm (F). Asterisks indicate significance in a Student's t test (NS, not significant).

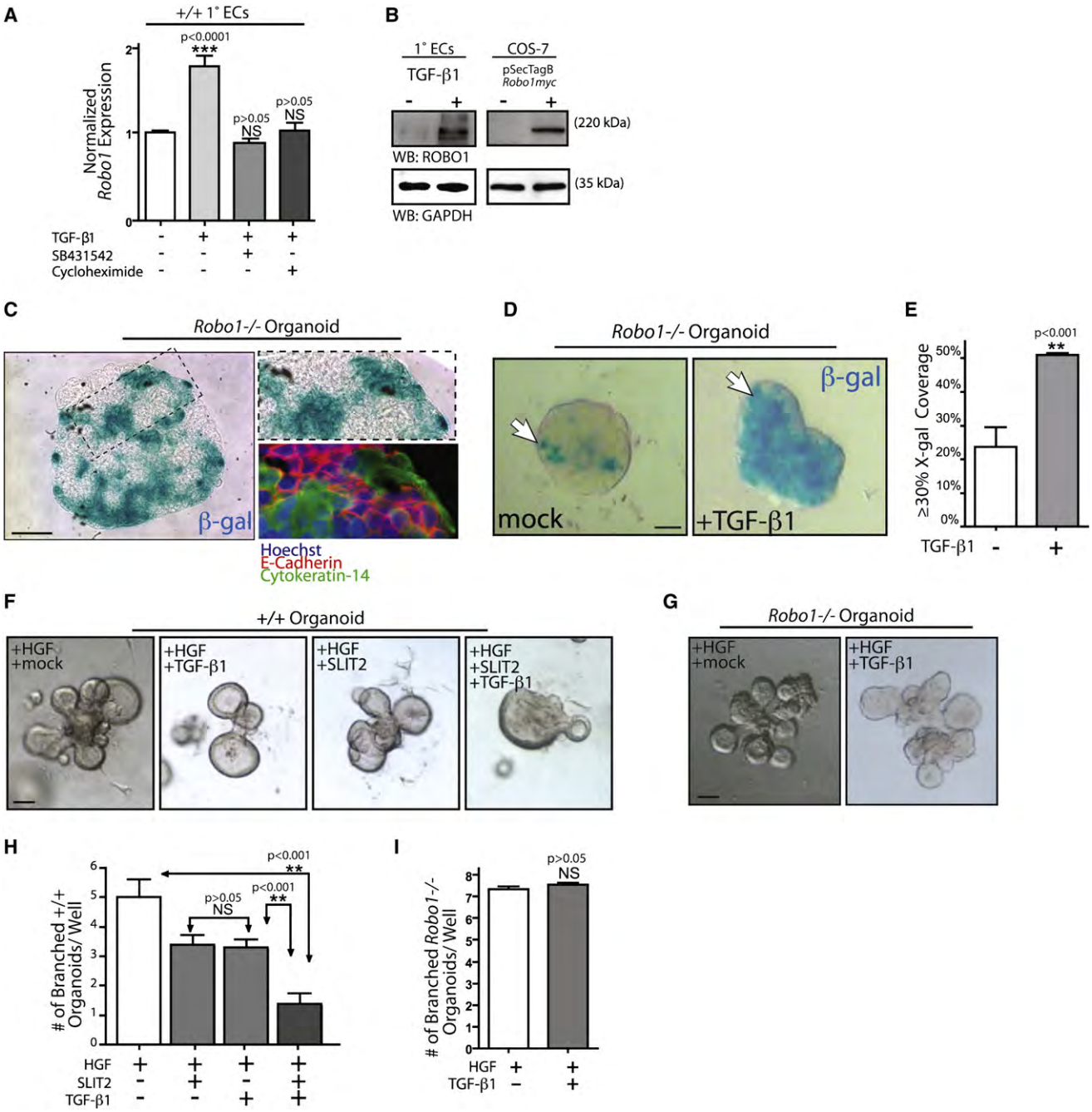

Figure 3. TGF-β1 Upregulates Robo1, Leading to Enhanced Branch Inhibition in Response to SLIT2

(A) *Robo1* levels after treatment with TGF-β1 alone or in combination with SB431542 or cycloheximide. Relative RT-qPCR analysis of ECs harvested from virgin mice (n = 3 independent RNA sets).

(B) ROBO1 protein levels after TGF-β1 treatment. Positive control is COS-7 cells expressing pSecTagB*Robo1myc*.

(C) Representative images of *Robo1*$^{-/-}$ organoids stained for β-gal (blue) (left) with a magnified image showing β-gal (upper) and coimmunostaining with CK-14 (green), E-cadherin (red), and nuclear marker Hoechst (blue) (lower).

(D and E) Representative phase-contrast images of β-gal-stained *Robo1*$^{-/-}$ organoids after mock or TGF-β1 treatment. The percentage of organoids containing ≥30% positive cells was quantified (n = 3 experiments, 100 organoids/treatment).

(F and G) WT and *Robo1*$^{-/-}$ organoids were stimulated to branch with HGF, treated with SLIT2, TGF-β1, or both, and imaged using bright-field microscopy (n = 3 experiments, >200 organoids/treatment).

(H and I) Quantification of WT and *Robo1*$^{-/-}$ organoids in each condition that had three or more branches (n = 3 experiments, >100 organoids/treatment).

Scale bars represent 30 μm (C, D, F, and G). Asterisks indicate significance in a Student's t test (E) or ANOVA (A and H) (NS, not significant).

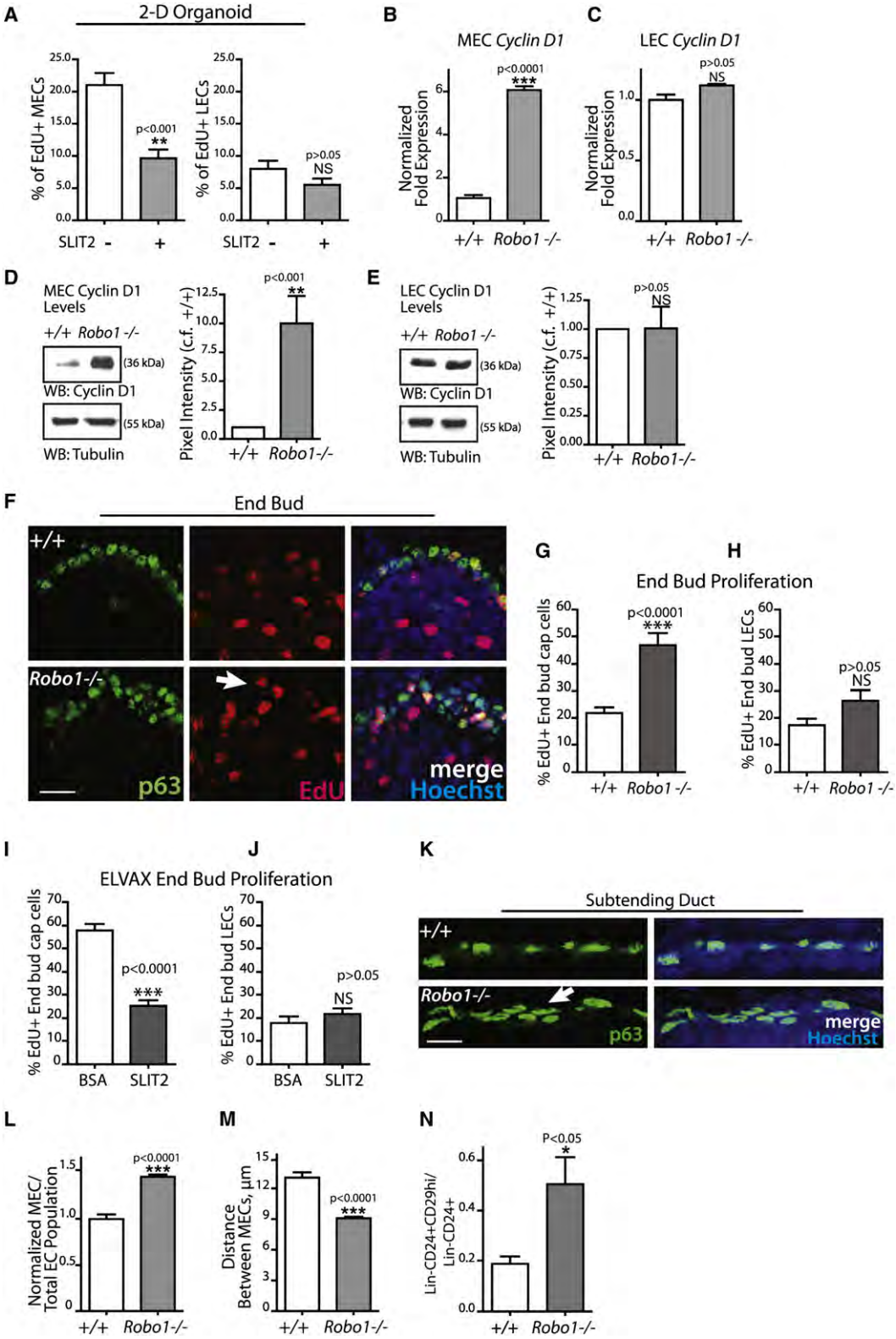

Figure 4. SLIT2/ROBO1 Signaling Inhibits the Proliferation of Basal Cap/Myoepithelial Cells

(A) Quantification of percentage of proliferating (EdU^+) cells in 2D organoids (n = 3 experiments, >500 cells).

(B–E) RT-qPCR and western blot analysis of *Cyclin D1* and Cyclin D1 levels, respectively, in WT and *Robo1*$^{-/-}$ MECs and LECs (RT-qPCR: n = 3 independent RNA sets; western blot: n = 3 experiments).

inhibited branching to a similar degree, but the effect was significantly enhanced upon treatment with both TGF-β1 and SLIT2 (Figures 3F and 3H). Moreover, *Robo1*$^{-/-}$ tissue was refractory to TGF-β1 treatment (Figures 3G and 3I), as it was to SLIT2 treatment (Figures 2F and 2H). These data support the notion that upregulation of ROBO1 in basal cells by TGF-β1 restricts branching by enhancing the inhibitory effects of SLIT.

SLIT/ROBO1 Signaling Regulates Basal Cell Proliferation

TGF-β1 inhibits mammary branching morphogenesis by reducing overall cellular proliferation (Ewan et al., 2002). To investigate whether SLIT/ROBO1 signaling similarly inhibits cell proliferation, but specifically in basal cells, we generated ductal fragments from WT glands and cultured them as 2D, bilayered, circular organoids (Figure S2A). SLIT2 treatment resulted in an ~50% reduction in MEC proliferation (Figure 4A; Figure S2B), similar to the reduction observed in a human MEC line, HME50 (Figures S2C and S2D), with no change in LEC proliferation (Figure 4A). These results suggest that only MECs are regulated by SLIT/ROBO1 signaling, consistent with the restricted expression of ROBO1 on these cells. However, LECs had a low basal index of proliferation, perhaps due to contact inhibition in the organoid center. To address this possibility, we separated WT and *Robo1*$^{-/-}$ MECs from LECs using differential trypsinization (Figures S2E–S2H) (Darcy et al., 2000), and examined a regulator of cell-cycle entry, Cyclin D1. There was a significant increase in *Cyclin D1* by RT-quantitative PCR (Figure 4B) and western blot (Figure 4D) in *Robo1*$^{-/-}$ MEC-enriched fractions, whereas no differences between genotypes were observed in LEC-enriched fractions (Figures 4C and 4E).

We also assessed cell proliferation in vivo in mammary glands by intraperitoneal injections of 5-ethynyl-2′-deoxyuridine (EdU) (Figure 4F). We initially focused on the mitotically active end buds and found an ~2-fold increase in cap cell proliferation in *Robo1*$^{-/-}$ glands and no significant change in LEC proliferation (Figures 4G and 4H), consistent with our data obtained in cell culture (Figures 4A–4E). Cap cell proliferation was also evaluated in glands containing SLIT2 and BSA Elvax pellets (Figures 4I and 4J), and a concordant ~2-fold decrease in cap cell proliferation was observed in end buds near SLIT2 pellets with, again, no significant difference in LEC proliferation.

We also examined subtending ducts to evaluate the consequences of having surplus cap cells, which differentiate into MECs. In agreement with previous studies (Bresciani, 1968), we found very few proliferating basal cells along WT or *Robo1*$^{-/-}$ ducts, suggesting that, unlike cap cells, differentiated MECs are refractory to the proproliferative consequences of losing SLIT/ROBO1 signaling (H.M., unpublished data). Evaluation of ductal morphology, however, revealed an overabundance of MECs in *Robo1*$^{-/-}$ ducts, suggesting that the consequence of exuberant cap cell proliferation is excess MECs (Figure 4K). We quantified both the number of MECs and the distance between them, and found that *Robo1*$^{-/-}$ glands have significantly more cells that are closer together (Figures 4L and 4M). We also used fluorescence-activated cell sorting (FACS) to examine the relative levels of basal cells in WT and *Robo*$^{-/-}$ glands and found a >2-fold increase in basal cells (Lin^{-}CD24^{+}CD29hi) in *Robo1*$^{-/-}$ tissue (Figure 4N). Together, these data show that SLIT2/ROBO1 signaling constrains cap cell proliferation, and that in its absence there is an excess of disorganized MECs.

The Number of Basal Cells Positively Influences the Number of Branches

These studies raise the question as to whether basal cell number alone influences branching. To investigate, we analyzed organoids (~100 μm diameter) that were either unbranched or contained one bud or branch. We observed MECs congregating at these bud/branch sites, with formation of a single bud/branch correlating with increased MEC number (Figures 5A and 5B; Figure S3A). To evaluate the consequences of MEC localization on bud growth, we generated and labeled WT organoids with EdU, and again analyzed similarly sized organoids containing a single bud (Figures 5C and 5D). Quantification of EdU^{+} cells in each quadrant revealed that bud-containing quadrants had ~2-fold more EdU^{+} cells (Figure 5E). Previous studies have shown that fibroblastic growth factor 2 (FGF2) is secreted from MECs and positively regulates mammary branching (Gomm et al., 1997). We evaluated *FGF2* levels in WT and *Robo1*$^{-/-}$ MECs and, while both populations express *FGF2*, *Robo1*$^{-/-}$ cells express significantly higher levels (Figure 5F).

Our data suggest that MEC number regulates mammary branching by supplying growth factors. To address this role for MECs, we performed mixing experiments in which we manipulated the ratio of MECs to LECs. First, we ensured that organoids in these assays arose from cell aggregates, rather than a single stem/progenitor cell, by mixing MECs from β-actin-EGFP mice with unlabeled LECs and documenting the formation of mixed-labeled organoids (Figure S3B). Next, we removed HGF from the culture media and manipulated the proportion of MECs to LECs, generating organoids that contained either a normal (~1:3) or high (~3:1) ratio of cells (Darcy et al., 2000). These ratios were confirmed by immunoblotting the input mixtures with MEC (CK-14) or LEC (E-cadherin) markers (Figure 5G). After 7 days, we categorized them as either branched or unbranched (Figure 5H), and quantified the number in each category (Figure 5I). A high ratio of MECs to LECs produced significantly more branched structures compared to a low ratio, which produced more unbranched structures, consistent with basal cell number having a corresponding influence on branch number (Figures 1, 2, and 4). Together, these data support a model in which SLIT/ROBO1 restricts the number of MECs by limiting cap cell

(F–H) Individual channel images of Hoechst-stained, EdU-labeled, p63-immunostained WT and *Robo1*$^{-/-}$ end buds (n = 3 animals).
(I and J) Quantification of MEC and LEC EdU^{+} nuclei in WT glands surrounding SLIT2 and BSA pellets (5 mm radius) (Figure 2C) (n = 3 animals).
(K) Individual and merged channel images of p63-immunostained and Hoechst-stained WT and *Robo1*$^{-/-}$ ducts.
(L) Quantification of MECs in *Robo1*$^{-/-}$ and WT ducts (n = 3 animals).
(M) Quantification of the distance between MECs in *Robo1*$^{-/-}$ and WT ducts (n = 3 animals).
(N) FACS analysis of the relative level of basal (Lin^{-}CD24^{+}CD29hi) to total (Lin^{-}CD24^{+}) epithelial cells in *Robo1*$^{-/-}$ and WT littermate glands.
Scale bars represent 20 μm (F and K). Asterisks indicate significance in a Student's t test (NS, not significant).

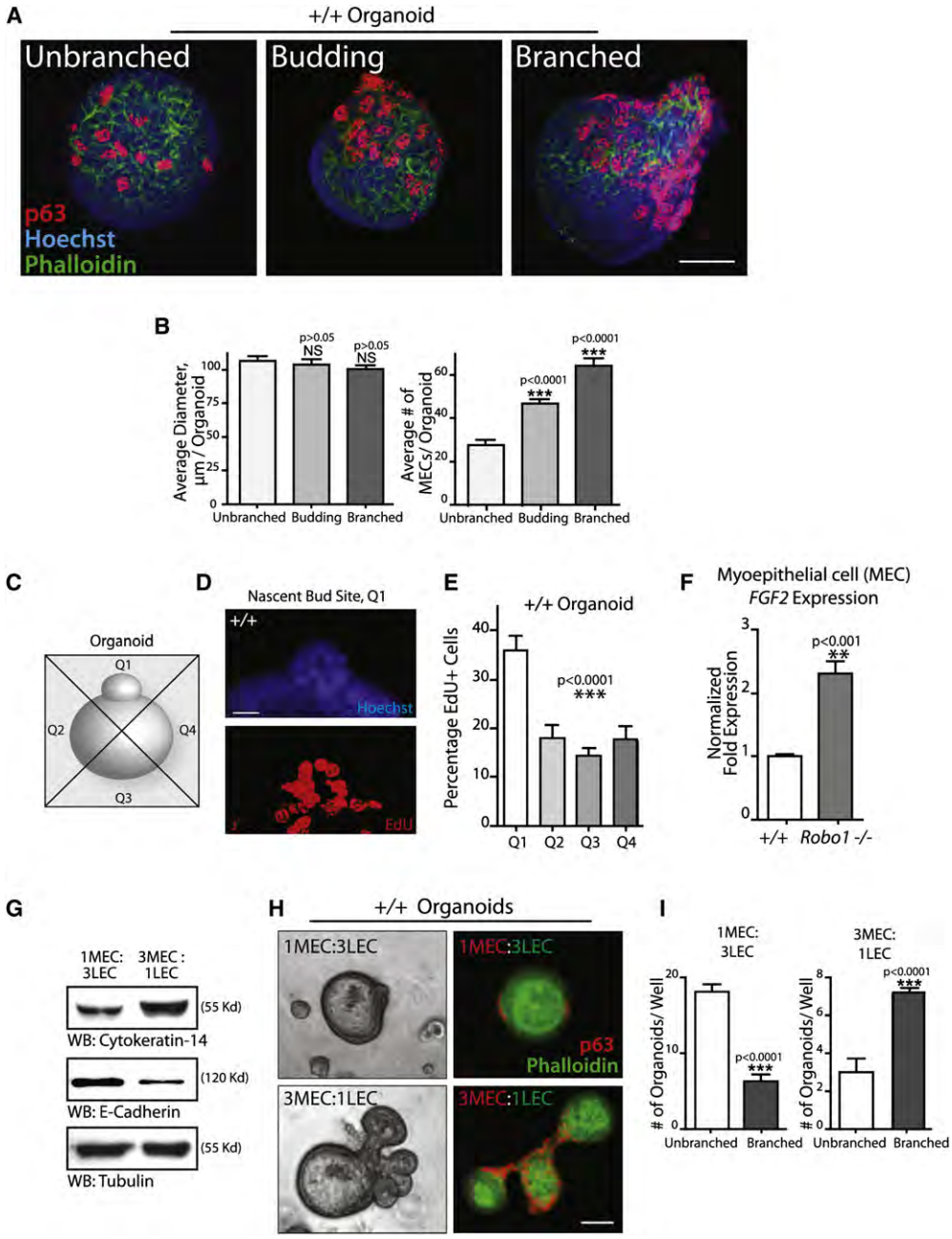

Figure 5. Basal Cell Number Influences Organoid Branching State

(A) Merged channel images of unbranched, budded, or branched WT organoids stained with Hoechst, phalloidin, and MEC marker p63.

(B) Quantification of organoid diameter and MEC number in budded, branched, and unbranched organoids (n = 3 experiments, >50 organoids/branching state).

(C) Cartoon model of an EdU-labeled organoid divided into quadrants with a bud containing a quadrant designated Q1.

(D and E) Quantification of quadrants from organoids labeled with EdU (red) and Hoechst (blue) (n = 3 experiments, >50 organoids/quadrant).

(F) Relative RT-qPCR analysis of *FGF2* levels in MECs harvested from WT and *Robo1*$^{-/-}$ glands (n = 3 independent RNA sets).

(G) Representative immunoblots from lysates of input cells at different MEC and LEC ratios: MEC marker, CK-14; LEC marker, E-cadherin; loading control, tubulin.

(H) Representative images of 1MEC:3LEC and 3MEC:1LEC organoids obtained with phase contrast (left) and immunofluorescence using p63 and phalloidin (right).

(I) Quantification of branched 3MEC:1LEC versus 1MEC:3LEC organoids (n = 3 experiments, >300 organoids/population).

Scale bars represent 30 μm (A, D, and H). Asterisks indicate significance in a Student's t test (NS, not significant).

proliferation. In the absence of SLIT/ROBO1 signaling, a surplus of MECs is generated that positively regulates branching by providing growth factors, such as FGF2.

SLIT/ROBO1 Signaling Regulates the Subcellular Localization of β-Catenin

Overexpression of activated β-catenin in the basal compartment of the mammary gland results in excess proliferation and hyperbranching (Teuliere et al., 2005), similar to the phenotype described in this study. It also produces basal-type hyperplasias similar to, but more severe than, phenotypes observed at later stages of development in *Robo1*$^{-/-}$ and *Slit2*$^{-/-}$;*Slit3*$^{-/-}$ outgrowths (Marlow et al., 2008) (Figures 1A and 2A). To investigate whether β-catenin is downstream of SLIT/ROBO1 in basal cells, we treated HME50 cells with SLIT2 and, using biochemical fractionation, detected a shift in β-catenin from the nuclear to the cytosolic/membrane fractions (Figure 6A). We confirmed this change in subcellular localization of β-catenin with immunocytochemistry. Figure 6B shows that SLIT2 treatment enhances the staining of β-catenin and E-cadherin at the membrane, with no change in the levels of total protein as assayed by immunoblot (Figure 6C). β-catenin was also activated in these cells using lithium chloride (LiCl) following SLIT2 treatment and, again, there was increased β-catenin membrane staining in SLIT2-treated samples and significantly decreased nuclear translocation (Figure S4A). Together, these studies suggest that SLIT/ROBO1 signaling influences β-catenin's subcellular localization. In cancer cells, this occurs through the Akt/PKB pathway (Prasad et al., 2008; Tseng et al., 2010), which negatively regulates glycogen synthase kinase 3-beta (GSK-3β) downstream of growth factor receptors (Cross et al., 1995). Similarly, we found that EGF and insulin (GF) treatment of primary MECs and LECs, as well as HME50 cells, increased the phosphorylation of Akt and GSK-3β (Figure 6D; Figure S4B). Pretreatment of cells with SLIT decreased this response in MECs and HME50 cells, but not in LECs. Decreased phosphorylation of GSK-3β activates it (Cross et al., 1995), favoring the accumulation of β-catenin in the cytosol and membrane of these cells (Figures 6A–6C).

Next, we probed whole MEC lysates with an antibody directed against active β-catenin (ABC) (Staal et al., 2002) and observed a decrease in this form upon SLIT2 treatment (Figure 6E). We used this antibody to examine the basal layer of WT organoids. In untreated organoids, there is modest positive staining in the nucleus. Treating cells with an activator of canonical WNT signaling dramatically increased the nuclear staining of unphosphorylated β-catenin, whereas treatment with SLIT2 reduced β-catenin's nuclear staining while increasing its membrane staining (Figure 6F). These data indicate that SLIT2 inhibits nuclear translocation of β-catenin, likely decreasing its transcriptional functions. To investigate, we evaluated LEF/TCF transcriptional targets by RT-qPCR and found increased expression of *Axin2*, *Cyclin D1*, and *Tcf1* mRNA in primary MECs harvested from *Robo1*$^{-/-}$ glands, and a concordant decrease in mRNA from WT MECs treated with SLIT2 (Figure 6G). One of these transcripts can also be monitored in vivo using *Axin2*$^{lacZ/+}$ mice. These mice faithfully reflect β-catenin signaling by reporting *Axin2* expression in multiple tissues (Lustig et al., 2002). During branching morphogenesis, there is robust β-gal staining in cap cells of the end bud and basal MECs of subtending ducts (Figure S4C) (Zeng and Nusse, 2010). We implanted SLIT2 and BSA pellets into *Axin2*$^{lacZ/+}$ glands and observed significantly reduced β-gal staining in MECs with SLIT2 but not BSA (Figure 6H). These data indicate that SLIT2 inhibits the proliferation of ROBO1-expressing basal cells by opposing the activation of β-catenin. Taken together, our data suggest a mechanism for restricting mammary branching morphogenesis by controlling cell number, specifically in the basal layer of the bilayered mammary gland (Figure 7).

DISCUSSION

Our studies define a mechanism governing mammary branching morphogenesis whereby SLIT/ROBO1 signaling inhibits lateral branch formation by controlling the proliferation of the basal cell layer. Specificity of signaling is achieved by restricting the expression of ROBO1 to the basal layer and regulating it with TGF-β1. This mechanism of SLIT regulating branching is different from the mechanisms identified in the nervous system, where an extracellular source of SLIT signals to ROBO receptors expressed on growth cones or axon shafts, resulting in cytoskeletal reorganization that leads to growth cone bifurcation or lateral extension of membrane away from the axonal shaft (Ypsilanti et al., 2010). In contrast, in the vasculature, a mechanism has been identified that is potentially similar to the one observed in the mammary gland. Here, SLIT is expressed by pericytes and signals through endothelial ROBO4 receptor to restrain sprouting angiogenesis by downregulating pathways activated by VEGF/VEGFR (Jones et al., 2008, 2009). VEGF increases the nuclear localization of β-catenin in endothelial cells (Ilan et al., 2003). If this drives sprouting angiogenesis, then SLIT/ROBO4 signaling could inhibit this process by sequestering β-catenin in the cytoplasm, similar to the effects observed in the mammary gland (Figure 6). Thus, the mechanism of SLIT/ROBO action in the mammary gland, via restricting β-catenin-dependent cell proliferation, may apply to vessel sprouting as well.

These studies highlight the importance of MECs as key regulators of breast development. MECs are responsible for producing components of the basal lamina and mediating interactions between ductal LECs and the extracellular environment. During development, they synthesize and secrete many key growth factors, including WNTs and FGFs (Figure 5F) (Gomm et al., 1997; Kouros-Mehr and Werb, 2006), which act as branching factors during morphogenesis (Lindvall et al., 2006; Lu et al., 2008). FGF does not promote MEC proliferation directly, but instead functions in a paracrine fashion to induce LEC proliferation (Figures 5C–5F) (Gomm et al., 1997). This distinction between basal and luminal cells, however, may not exist in the end bud. Instead, in this context, loss of FGF receptor 2 in a subset of cells leads to decreased proliferation of cap and luminal body cells (Lu et al., 2008), in addition to a hypobranching phenotype that highlights the positive contribution of cell proliferation in the end bud to branch formation (Lu et al., 2008; Parsa et al., 2008). Changes in branching are also observed upon constitutive activation of canonical WNT signaling, as demonstrated by overexpression of an N-terminally truncated, activated form of β-catenin in the basal cell layer that results in excess basal cells and precocious lateral bud formation (Teuliere et al., 2005). Furthermore, the opposite phenotype, fewer

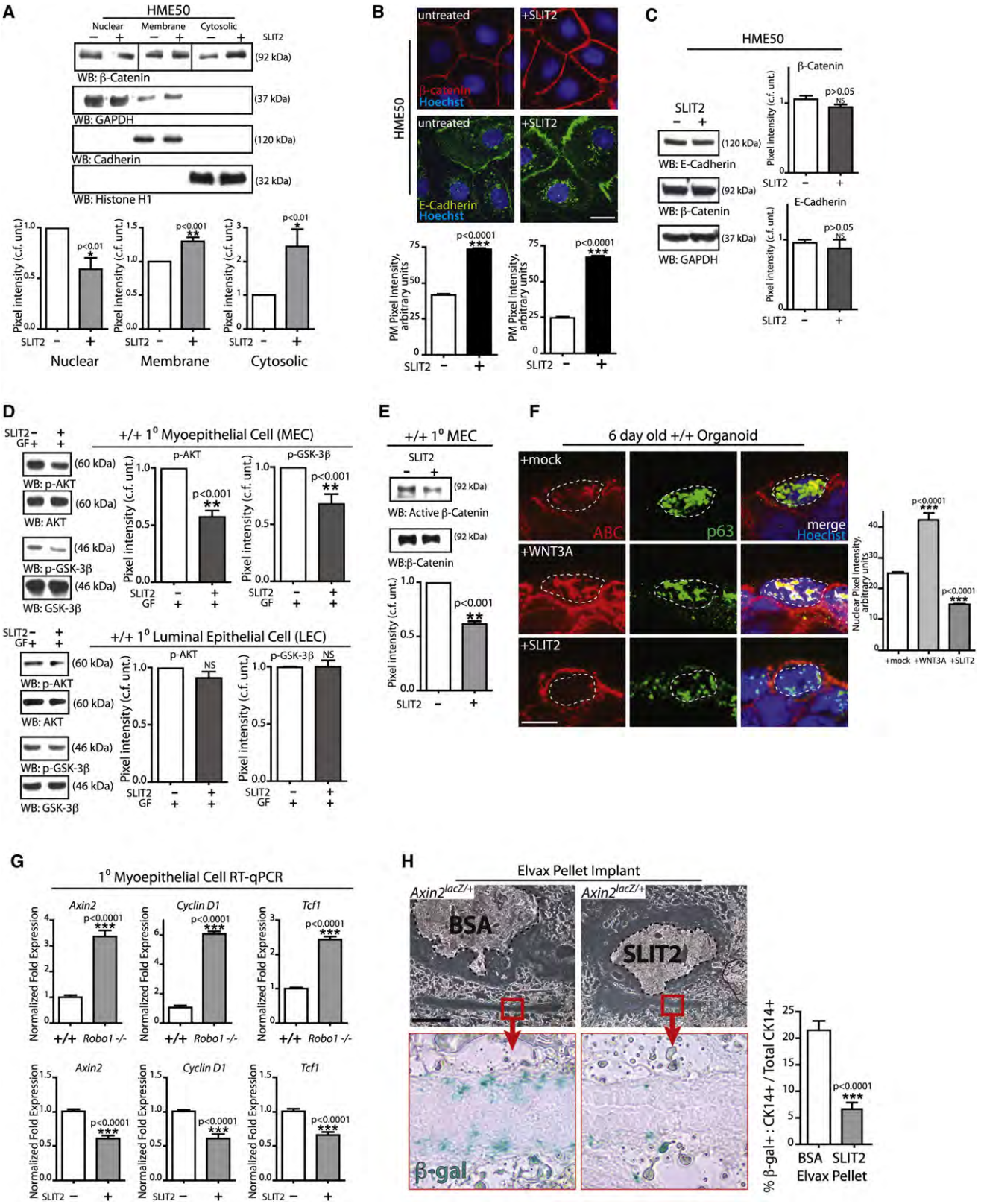

Figure 6. SLIT/ROBO1 Signaling Regulates the Subcellular Localization of β-Catenin

(A) Biochemical fractionation of HME50 cells treated with SLIT2. Top: representative immunoblots for β-catenin; nuclear loading control, histone H1; cytoplasmic loading control, GAPDH; membrane loading control, cadherin. Bottom: quantitative analysis of β-catenin (n = 3 experiments).

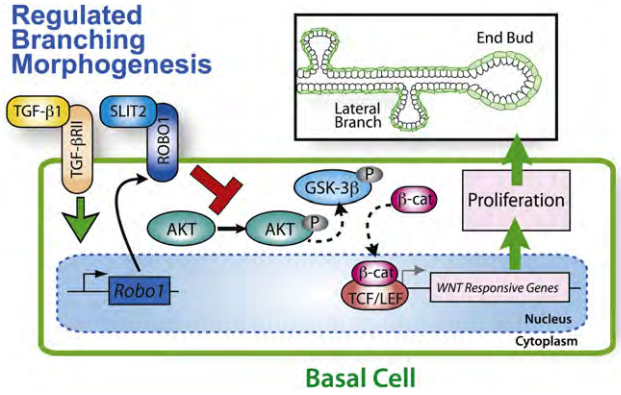

Figure 7. The SLIT/ROBO1 Signaling Axis Regulates Mammary Gland Branching Morphogenesis

Cartoon model of how the mammary basal layer promotes branching morphogenesis, and how this effect is countered by SLIT/ROBO1 signaling. From left to right, TGF-β1 elevates the expression of *Robo1* in basal cells. ROBO1 then interacts with ligand SLIT2 to inhibit the nuclear accumulation of β-catenin by inhibiting Akt activation. Inhibiting Akt results in unphosphorylated, activated GSK-3β, which phosphorylates β-catenin and favors its degradation or accumulation at the membrane (not pictured), thereby inhibiting its translocation to the nucleus and subsequent activation of transcription. Thus, by curbing basal cell proliferation, SLIT/ROBO1 signaling inhibits mammary gland branching morphogenesis.

terminal end buds and branches, is observed in glands heterozygous for the Lrp6 WNT receptor that also display reduced levels of β-catenin activation (Lindvall et al., 2009). Together, these studies highlight the importance of growth factor production by basal cells in enhancing branch formation.

We discovered that excessive mammary branching also occurs in the absence of SLIT/ROBO1 signaling due to both a surplus of basal cells, which provides high levels of growth factors, especially FGF2 (Figure 5F), and increased activation of canonical WNT signaling, due to aberrant localization of β-catenin (Figure 6). Taken together, our findings delineate an arm of the TGF-β1 pathway that restrains branching by negatively regulating progrowth signals in basal cells through two mechanisms: (1) directly, by inhibiting the activation of WNT signaling (Figure 6); and (2) indirectly, by limiting basal cell number and, consequently, the supply of positive factors (Figure 5). Without this growth control in the basal compartment, the mammary gland generates an overabundance of MECs, which produce an excess of growth factors that promote branching. These surplus MECs eventually invade the luminal population, creating a disruption in cell adhesion (Strickland et al., 2006). Moreover, over time, these excess growth factors, along with other changes that occur such as upregulation of CXCR4 and SDF1, spur the development of hyperplastic lesions with basal characteristics (Marlow et al., 2008). Thus, the loss of growth control in the basal compartment, identified in the current study, may provide the fundamental defect that is the basis for other disruptions occurring in mature and transplanted tissue in the absence of SLIT/ROBO1 signaling.

Our studies elucidate a new web of signaling that links TGF-β1 to the control of β-catenin through the SLIT/ROBO1 pathway. There is abundant research identifying roles for both WNT/β-catenin and TGF-β signaling pathways in tissue morphogenesis as regulators of cell proliferation, migration, and differentiation. That these pathways are directly connected is illustrated in the process of epithelial-to-mesenchymal transition (EMT) in which TGF-β1 induces the dissociation of β-catenin from cell contacts and promotes its subsequent translocation into the nucleus to drive transcription of LEF/TCF targets (Masszi et al., 2004; Medici et al., 2006). There is little evidence, however, that the reverse happens, with TGF-β1 supporting cell adhesion by increasing the association of β-catenin with cadherin. Our studies provide evidence that this occurs in a developmental context, and that by upregulating *Robo1*, TGF-β1 indirectly supports a mesenchymal-to-epithelial transition (MET) in which cap cells differentiate into MECs. This functional role for SLIT during MET is supported by studies in cancer cell lines where knockdown of SLIT, for example in a non-small-cell lung cancer line, activates Akt and inhibits GSK-3β. This, in turn, increases the levels of nuclear β-catenin and increases the expression of Snail, a crucial regulator of EMT/MET, resulting in decreased cadherin expression and increased cell migration (Tseng et al., 2010). Concordantly, in a study of breast cancer cells, SLIT overexpression inhibits Akt, activating GSK-3β, resulting in reduced nuclear accumulation of β-catenin and increased cadherin/β-catenin at the cell membrane (Prasad et al., 2008). Additionally, SLIT/ROBO1 signaling could regulate β-catenin directly through its inhibitory effect on Akt, which phosphorylates β-catenin on Ser552 and increases its nuclear translocation and activation of canonical WNT target genes (He et al., 2007). Thus, the ability of SLITs to function as tumor suppressors lies in their capacity to curb both cell motility and cell proliferation. Here we provide

(B) Merged channel images of Hoechst-, β-catenin- (top) or E-cadherin- (bottom) stained HME50 cells. Plasma membrane signals were recorded as mean pixel intensities over 5 μm of the highest-staining membrane (n = 3 experiments, >50 cells/treatment).

(C) Representative immunoblots and quantification of E-cadherin and β-catenin after SLIT2 treatment of HME50 cells (n = 3 experiments).

(D) Representative immunoblots and quantification for p-Akt (left) and p-GSK-3β (right) in HME50 cells treated with SLIT2 alone or in combination with growth factors (total Akt and GSK-3β as loading controls) (n = 2 experiments).

(E) Representative immunoblots and quantification for activated β-catenin (top) in MECs treated with SLIT2 (total β-catenin [bottom] as loading control) (n = 2 experiments).

(F) Individual and merged channel images of 6-day-old organoids stained with p63, ABC, and Hoechst after mock, WNT3A, or SLIT2 treatment. White dashed lines highlight nuclear area. Nuclear ABC levels were recorded as mean pixel intensities of 25^2 μm of nuclear area (n = 3 experiments, >50 cells/treatment).

(G) Relative RT-qPCR analysis of β-catenin target genes *Axin2*, *Cyclin D1*, and *Tcf1* in WT compared to *Robo1*$^{-/-}$ MECs (top), and WT compared to SLIT2-treated WT MECs (bottom) (n = 3 independent RNA sets).

(H) β-gal staining of *Axin2*$^{lacZ/+}$ mammary tissue in regions near SLIT2 (right) and BSA (left) Elvax pellets. Top panels reveal ductal proximity to Elvax pellets; bottom panels are magnified images of highlighted (red boxes) ductal area. Percentage of β-gal-positive MECs (CK14+) was quantified in ducts within 5 mm of the pellet (n = 3 experiments).

Scale bars represent 10 μm (B and F) and 0.5 mm (H). Asterisks indicate significance in a Student's t test (NS, not significant).

strong evidence for a developmental correlate of SLIT's role as a suppressor of tumor cell growth by showing its function in opposing canonical WNT signaling and limiting basal cell proliferation during mammary branching morphogenesis.

Recently, the basal cell population has been shown to contain a subpopulation of mammary stem cells (MaSCs) (Shackleton et al., 2006; Stingl et al., 2006) whose regenerative capacity is regulated by canonical WNT signaling (Badders et al., 2009; Zeng and Nusse, 2010). Because MaSCs have the potential to generate the repertoire and number of new cells necessary for branching, it is tempting to speculate that they are required for branch formation. Alternatively, it is possible that bipotent progenitor cells, which may not have a basal phenotype, are the operative cell type. In either case, it raises the possibility that SLIT affects branching by regulating the production of stem/progenitor cells. Indeed, recent data show that progesterone, which is responsible for side branching, initiates a series of events whereby LECs spur the proliferation of MaSCs by providing growth factors such as WNT4 and RANKL (Asselin-Labat et al., 2010; Joshi et al., 2010). Branching was not evaluated in these studies, and currently there is no evidence that MaSCs contribute directly to branching, but our studies have not excluded an effect of SLIT in countering the effects of progesterone and restricting the proliferation of MaSCs.

In conclusion, this report shows that SLIT/ROBO1 signaling is a central agent within a pathway that controls branching morphogenesis. Our studies provide mechanistic insight into how ROBO1 levels are influenced by a negative regulator, TGF-β1, and how this, in turn, curtails basal cell production by regulating the subcellular localization of β-catenin and inhibiting canonical WNT signaling. We propose that specification of basal cell number is a critical component regulating branch formation, with SLIT/ROBO1 acting to check growth factor signaling by curbing basal cell proliferation.

EXPERIMENTAL PROCEDURES

Animals

The study conformed to guidelines set by the University of California, Santa Cruz animal care committee (IACUC). Mouse *Slit2*, *Slit3*, *Robo1*, and *Axin2*$^{lacZ/+}$ knockouts were generated and genotyped as described (Lustig et al., 2002; Strickland et al., 2006). The promoters for *Robo1* and *Axin2* drive the expression of *lacZ* and was assessed by β-gal staining (Strickland et al., 2006).

Mammary Fat Pad Clearing, Transplantation, and Branching Analysis

Mammary anlage were rescued from knockout embryos and transplanted into precleared fat pads of *Foxn1*^{nu} mice (Strickland et al., 2006). Contralateral outgrowths were harvested 4 weeks posttransplant and subjected to whole-mount hematoxylin staining. Primary branches were defined as ducts extending from the nipple and terminating in an end bud. Secondary and tertiary branches were defined as bifurcating from primary ducts or secondary branches, respectively.

Primary Mouse Mammary Epithelial Cell Culture

Glands were digested with collagenase and dispase (Figures S2E–S2H) (Darcy et al., 2000). Differential trypsinization was performed to obtain purified MEC and LEC fractions (Darcy et al., 2000). For mammary cell sorting, single-cell suspensions from thoracic and inguinal mammary glands were prepared as previously described (Shackleton et al., 2006). FACS analysis was performed using a FACSAria (Becton Dickinson).

RNA Extraction and RT-PCR Analysis

RNA was extracted using a PureLink RNA Mini kit (Invitrogen). cDNA was prepared using an iScript cDNA synthesis kit (Bio-Rad). PCR was performed in triplicate and quantified using a Rotor Gene 6000 real-time PCR machine and software (Corbett Research) to assay SYBR green fluorescence (Bio-Rad) (Livak and Schmittgen, 2001). Results were normalized to that of *GAPDH*.

In Vitro Branching Morphogenesis Assays

Three-dimensional primary cultures were generated as previously described (Lee et al., 2007). Briefly, to generate organoids, we embedded 10,000 ECs in 100 μl of growth factor-reduced Matrigel (BD Biosciences)/0.7 cm^2. Fragment organoids were obtained by embedding purified epithelial fragments into Matrigel (Ewald et al., 2008), and stimulated with 2.5 nM bFGF (Sigma).

Elvax Slow-Release Pellet Preparation and Surgical Implantation

Elvax pellets containing 271 ng of SLIT2 and 0.45 mg of BSA or only 0.45 mg of BSA (control) were contralaterally implanted at the forefront of the growing ductal tree in wild-type CD1 mice and harvested after 7 days (Silberstein and Daniel, 1987).

Antibodies, Reagents, and Cell Lines

Antibodies used were as follows: CK-14 (Covance); E-cadherin (R&D Systems); p63 (Santa Cruz Biotechnology); ROBO1 (Abcam); Myc (9E10); tubulin (Sigma); GAPDH (Santa Cruz Biotechnology); β-catenin (610154) (BD Biosciences); ABC (8E7) (Millipore); histone H1 (Santa Cruz Biotechnology); and Akt, p-Akt (Thr308), GSK-3β, and p-GSK-3β (Ser9) (Cell Signaling). Nonantibody markers used were: Alexa Fluor 546 phalloidin for filamentous actin (Invitrogen), Hoechst (Invitrogen) for nuclei, and EdU (Invitrogen) to label proliferating cells. HME50 cells were cultured in DMEM-F12 supplemented with 100× mammary epithelial cell growth supplement (Cascade Biologics).

Western Blot and Cellular Fractionation

Tissue protein lysates were prepared and analyzed by western blot as described (Marlow et al., 2008). For cellular fractionation, HME50 cells were treated with SLIT2 for 4 hr and then fractionated using the Qproteome Cell Compartment kit (QIAGEN).

Proliferation Assays

In vitro cultures were treated with 10 μM EdU for 1 hr before detection. In vivo labeling was accomplished by intraperitoneal injections of EdU (25 ng/g of body weight) followed by harvest 2 hr postinjection. Samples were subjected to Click-iT chemistry (Invitrogen).

Statistical Analysis

Statistical tests and p values are indicated in the figure legends. Graph columns represent the mean and error bars represent the standard error of the mean.

SUPPLEMENTAL INFORMATION

Supplemental Information includes four figures and can be found with this article online at doi:10.1016/j.devcel.2011.05.012.

ACKNOWLEDGMENTS

We thank Marisela Marinez and Fay Davidson for technical assistance; Gary Silberstein (University of California, Santa Cruz), Mark Sternlicht (FibroGen), and Dr. Yi Arial Zeng (Shanghai Institutes for Biological Sciences), who also supplied WNT3, for thoughtful comments on the manuscript; Susan Strome for use of a confocal microscope (NIH grants GM46295 and GM34059); and Santa Cruz Biotechnology for their generous donation of antibodies. *Slit3*$^{-/-}$ mice were kindly provided by Dr. David Ornitz (Washington University); *Slit2*$^{-/-}$ and *Robo1*$^{-/-}$ mice by Dr. Marc Tessier-Lavigne (Genentech); and *Axin2*$^{lacZ/+}$ by Dr. Walter Birchmeier (Max Delbrueck Center) and Roel Nusse (Stanford University). We acknowledge grants from the NIH (R01 CA-128902), Congressionally Directed Medical Research Program (W81XWH-08-1-0380), Santa Cruz Cancer Benefit Group, Initiative for Maximizing Student Diversity

(NIH GM058903) (H.M.), and Center for Biomolecular Science and Engineering (5P41HG002371-09) (H.M.) for funding this research.

Received: November 30, 2010
Revised: April 12, 2011
Accepted: May 16, 2011
Published: June 13, 2011

REFERENCES

Andrew, D.J., and Ewald, A.J. (2010). Morphogenesis of epithelial tubes: insights into tube formation, elongation, and elaboration. Dev. Biol. *341*, 34–55.

Asselin-Labat, M.L., Vaillant, F., Sheridan, J.M., Pal, B., Wu, D., Simpson, E.R., Yasuda, H., Smyth, G.K., Martin, T.J., Lindeman, G.J., et al. (2010). Control of mammary stem cell function by steroid hormone signalling. Nature *465*, 798–802.

Badders, N.M., Goel, S., Clark, R.J., Klos, K.S., Kim, S., Bafico, A., Lindvall, C., Williams, B.O., and Alexander, C.M. (2009). The Wnt receptor, Lrp5, is expressed by mouse mammary stem cells and is required to maintain the basal lineage. PLoS One *4*, e6594.

Barsky, S.H., and Karlin, N.J. (2006). Mechanisms of disease: breast tumor pathogenesis and the role of the myoepithelial cell. Nat. Clin. Pract. Oncol. *3*, 138–151.

Bresciani, F. (1968). Topography of DNA synthesis in the mammary gland of the CH3 mouse and its control by ovarian hormones: an autoradiographic study. Cell Tissue Kinet. *1*, 51–63.

Brose, K., Bland, K.S., Wang, K.H., Arnott, D., Henzel, W., Goodman, C.S., Tessier-Lavigne, M., and Kidd, T. (1999). Slit proteins bind Robo receptors and have an evolutionarily conserved role in repulsive axon guidance. Cell *96*, 795–806.

Cross, D.A., Alessi, D.R., Cohen, P., Andjelkovich, M., and Hemmings, B.A. (1995). Inhibition of glycogen synthase kinase-3 by insulin mediated by protein kinase B. Nature *378*, 785–789.

Dallol, A., Dickinson, R.E., and Latif, F. (2005). Epigenetic disruption of the SLIT-ROBO interactions in human cancer. In DNA Methylation, Epigenetics and Metastasis, R.J. Ablin, W.G. Jiang, and M. Esteller, eds. (New York: Springer Netherlands), pp. 191–214.

Darcy, K.M., Zangani, D., Lee, P.-P.L., and Ip, M. (2000). Isolation and Culture of Normal Rat Mammary Epithelial Cells (New York: Kluwer Academic/Plenum Press).

Ewald, A.J., Brenot, A., Duong, M., Chan, B.S., and Werb, Z. (2008). Collective epithelial migration and cell rearrangements drive mammary branching morphogenesis. Dev. Cell *14*, 570–581.

Ewan, K.B., Shyamala, G., Ravani, S.A., Tang, Y., Akhurst, R., Wakefield, L., and Barcellos-Hoff, M.H. (2002). Latent transforming growth factor-β activation in mammary gland: regulation by ovarian hormones affects ductal and alveolar proliferation. Am. J. Pathol. *160*, 2081–2093.

Gomm, J.J., Browne, P.J., Coope, R.C., Bansal, G.S., Yiangou, C., Johnston, C.L., Mason, R., and Coombes, R.C. (1997). A paracrine role for myoepithelial cell-derived FGF2 in the normal human breast. Exp. Cell Res. *234*, 165–173.

Grieshammer, U., Le, M., Plump, A.S., Wang, F., Tessier-Lavigne, M., and Martin, G.R. (2004). SLIT2-mediated ROBO2 signaling restricts kidney induction to a single site. Dev. Cell *6*, 709–717.

Gudjonsson, T., Adriance, M.C., Sternlicht, M.D., Petersen, O.W., and Bissell, M.J. (2005). Myoepithelial cells: their origin and function in breast morphogenesis and neoplasia. J. Mammary Gland Biol. Neoplasia *10*, 261–272.

He, X.C., Yin, T., Grindley, J.C., Tian, Q., Sato, T., Tao, W.A., Dirisina, R., Porter-Westpfahl, K.S., Hembree, M., Johnson, T., et al. (2007). PTEN-deficient intestinal stem cells initiate intestinal polyposis. Nat. Genet. *39*, 189–198.

Holliday, D.L., Brouilette, K.T., Markert, A., Gordon, L.A., and Jones, J.L. (2009). Novel multicellular organotypic models of normal and malignant breast: tools for dissecting the role of the microenvironment in breast cancer progression. Breast Cancer Res. *11*, R3.

Ilan, N., Tucker, A., and Madri, J.A. (2003). Vascular endothelial growth factor expression, β-catenin tyrosine phosphorylation, and endothelial proliferative behavior: a pathway for transformation? Lab. Invest. *83*, 1105–1115.

Ingman, W.V., and Robertson, S.A. (2008). Mammary gland development in transforming growth factor β1 null mutant mice: systemic and epithelial effects. Biol. Reprod. *79*, 711–717.

Jones, C.A., London, N.R., Chen, H., Park, K.W., Sauvaget, D., Stockton, R.A., Wythe, J.D., Suh, W., Larrieu-Lahargue, F., Mukouyama, Y.S., et al. (2008). Robo4 stabilizes the vascular network by inhibiting pathologic angiogenesis and endothelial hyperpermeability. Nat. Med. *14*, 448–453.

Jones, C.A., Nishiya, N., London, N.R., Zhu, W., Sorensen, L.K., Chan, A.C., Lim, C.J., Chen, H., Zhang, Q., Schultz, P.G., et al. (2009). Slit2-Robo4 signalling promotes vascular stability by blocking Arf6 activity. Nat. Cell Biol. *11*, 1325–1331.

Joshi, P.A., Jackson, H.W., Beristain, A.G., Di Grappa, M.A., Mote, P.A., Clarke, C.L., Stingl, J., Waterhouse, P.D., and Khokha, R. (2010). Progesterone induces adult mammary stem cell expansion. Nature *465*, 803–807.

Kouros-Mehr, H., and Werb, Z. (2006). Candidate regulators of mammary branching morphogenesis identified by genome-wide transcript analysis. Dev. Dyn. *235*, 3404–3412.

Labbe, E., Lock, L., Letamendia, A., Gorska, A.E., Gryfe, R., Gallinger, S., Moses, H.L., and Attisano, L. (2007). Transcriptional cooperation between the transforming growth factor-β and Wnt pathways in mammary and intestinal tumorigenesis. Cancer Res. *67*, 75–84.

Lee, G.Y., Kenny, P.A., Lee, E.H., and Bissell, M.J. (2007). Three-dimensional culture models of normal and malignant breast epithelial cells. Nat. Methods *4*, 359–365.

Lindvall, C., Evans, N.C., Zylstra, C.R., Li, Y., Alexander, C.M., and Williams, B.O. (2006). The Wnt signaling receptor Lrp5 is required for mammary ductal stem cell activity and Wnt1-induced tumorigenesis. J. Biol. Chem. *281*, 35081–35087.

Lindvall, C., Zylstra, C.R., Evans, N., West, R.A., Dykema, K., Furge, K.A., and Williams, B.O. (2009). The Wnt co-receptor Lrp6 is required for normal mouse mammary gland development. PLoS One *4*, e5813.

Livak, K.J., and Schmittgen, T.D. (2001). Analysis of relative gene expression data using real-time quantitative PCR and the $2(-\Delta\Delta C(T))$ method. Methods *25*, 402–408.

Long, H., Sabatier, C., Ma, L., Plump, A., Yuan, W., Ornitz, D.M., Tamada, A., Murakami, F., Goodman, C.S., and Tessier-Lavigne, M. (2004). Conserved roles for Slit and Robo proteins in midline commissural axon guidance. Neuron *42*, 213–223.

Lu, P., Ewald, A.J., Martin, G.R., and Werb, Z. (2008). Genetic mosaic analysis reveals FGF receptor 2 function in terminal end buds during mammary gland branching morphogenesis. Dev. Biol. *321*, 77–87.

Lustig, B., Jerchow, B., Sachs, M., Weiler, S., Pietsch, T., Karsten, U., van de Wetering, M., Clevers, H., Schlag, P.M., Birchmeier, W., et al. (2002). Negative feedback loop of Wnt signaling through upregulation of conductin/axin2 in colorectal and liver tumors. Mol. Cell. Biol. *22*, 1184–1193.

Marlow, R., Strickland, P., Lee, J.S., Wu, X., Pebenito, M., Binnewies, M., Le, E.K., Moran, A., Macias, H., Cardiff, R.D., et al. (2008). SLITs suppress tumor growth in vivo by silencing Sdf1/Cxcr4 within breast epithelium. Cancer Res. *68*, 7819–7827.

Marlow, R., Binnewies, M., Sorensen, L.K., Monica, S.D., Strickland, P., Forsberg, E.C., Li, D.Y., and Hinck, L. (2010). Vascular Robo4 restricts proangiogenic VEGF signaling in breast. Proc. Natl. Acad. Sci. USA *107*, 10520–10525.

Masszi, A., Fan, L., Rosivall, L., McCulloch, C.A., Rotstein, O.D., Mucsi, I., and Kapus, A. (2004). Integrity of cell-cell contacts is a critical regulator of TGF-β1-induced epithelial-to-myofibroblast transition: role for β-catenin. Am. J. Pathol. *165*, 1955–1967.

Medici, D., Hay, E.D., and Goodenough, D.A. (2006). Cooperation between Snail and LEF-1 transcription factors is essential for TGF-β1-induced epithelial-mesenchymal transition. Mol. Biol. Cell *17*, 1871–1879.

Nelson, C.M., Vanduijn, M.M., Inman, J.L., Fletcher, D.A., and Bissell, M.J. (2006). Tissue geometry determines sites of mammary branching morphogenesis in organotypic cultures. Science *314*, 298–300.

Parsa, S., Ramasamy, S.K., De Langhe, S., Gupte, V.V., Haigh, J.J., Medina, D., and Bellusci, S. (2008). Terminal end bud maintenance in mammary gland is dependent upon FGFR2b signaling. Dev. Biol. *317*, 121–131.

Pavlovich, A.L., Boghaert, E., and Nelson, C.M. (2011). Mammary branch initiation and extension are inhibited by separate pathways downstream of TGFβ in culture. Exp. Cell Res., in press. Published online April 1, 2011. 10.1016/j.yexcr.2011.03.017.

Prasad, A., Paruchuri, V., Preet, A., Latif, F., and Ganju, R.K. (2008). Slit-2 induces a tumor-suppressive effect by regulating β-catenin in breast cancer cells. J. Biol. Chem. *283*, 26624–26633.

Roarty, K., and Serra, R. (2007). Wnt5a is required for proper mammary gland development and TGF-β-mediated inhibition of ductal growth. Development *134*, 3929–3939.

Roarty, K., Baxley, S.E., Crowley, M.R., Frost, A.R., and Serra, R. (2009). Loss of TGF-β or Wnt5a results in an increase in Wnt/β-catenin activity and redirects mammary tumour phenotype. Breast Cancer Res. *11*, R19.

Shackleton, M., Vaillant, F., Simpson, K.J., Stingl, J., Smyth, G.K., Asselin-Labat, M.L., Wu, L., Lindeman, G.J., and Visvader, J.E. (2006). Generation of a functional mammary gland from a single stem cell. Nature *439*, 84–88.

Silberstein, G.B. (2001). Postnatal mammary gland morphogenesis. Microsc. Res. Tech. *52*, 155–162.

Silberstein, G.B., and Daniel, C.W. (1987). Investigation of mouse mammary ductal growth regulation using slow-release plastic implants. J. Dairy Sci. *70*, 1981–1990.

Staal, F.J., van Noort, M., Strous, G.J., and Clevers, H.C. (2002). Wnt signals are transmitted through N-terminally dephosphorylated β-catenin. EMBO Rep. *3*, 63–68.

Stingl, J., Eirew, P., Ricketson, I., Shackleton, M., Vaillant, F., Choi, D., Li, H.I., and Eaves, C.J. (2006). Purification and unique properties of mammary epithelial stem cells. Nature *439*, 993–997.

Strickland, P., Shin, G.C., Plump, A., Tessier-Lavigne, M., and Hinck, L. (2006). Slit2 and netrin 1 act synergistically as adhesive cues to generate tubular bi-layers during ductal morphogenesis. Development *133*, 823–832.

Teuliere, J., Faraldo, M.M., Deugnier, M.A., Shtutman, M., Ben-Ze'ev, A., Thiery, J.P., and Glukhova, M.A. (2005). Targeted activation of β-catenin signaling in basal mammary epithelial cells affects mammary development and leads to hyperplasia. Development *132*, 267–277.

Tseng, R.C., Lee, S.H., Hsu, H.S., Chen, B.H., Tsai, W.C., Tzao, C., and Wang, Y.C. (2010). SLIT2 attenuation during lung cancer progression deregulates β-catenin and E-cadherin and associates with poor prognosis. Cancer Res. *70*, 543–551.

Wang, K.H., Brose, K., Arnott, D., Kidd, T., Goodman, C.S., Henzel, W., and Tessier-Lavigne, M. (1999). Biochemical purification of a mammalian Slit protein as a positive regulator of sensory axon elongation and branching. Cell *96*, 771–784.

Williams, J.M., and Daniel, C.W. (1983). Mammary ductal elongation: differentiation of myoepithelium and basal lamina during branching morphogenesis. Dev. Biol. *97*, 274–290.

Yang, X.M., Han, H.X., Sui, F., Dai, Y.M., Chen, M., and Geng, J.G. (2010). Slit-Robo signaling mediates lymphangiogenesis and promotes tumor lymphatic metastasis. Biochem. Biophys. Res. Commun. *396*, 571–577.

Ypsilanti, A.R., Zagar, Y., and Chedotal, A. (2010). Moving away from the midline: new developments for Slit and Robo. Development *137*, 1939–1952.

Yue, J., and Mulder, K.M. (2001). Transforming growth factor-β signal transduction in epithelial cells. Pharmacol. Ther. *91*, 1–34.

Zeng, Y.A., and Nusse, R. (2010). Wnt proteins are self-renewal factors for mammary stem cells and promote their long-term expansion in culture. Cell Stem Cell *6*, 568–577.

Vascular Robo4 restricts proangiogenic VEGF signaling in breast

Rebecca Marlow[a], Mikhail Binnewies[a], Lise K. Sorensen[b], Stefanie D. Monica[a], Phyllis Strickland[a], E. Camilla Forsberg[c], Dean Y. Li[b], and Lindsay Hinck[a,1]

[a]Department of Molecular, Cell and Developmental Biology, University of California, Santa Cruz, CA 95064; [b]Department of Oncological Sciences, University of Utah, Salt Lake City, UT 84112; and [c]Department of BioMolecular Engineering, University of California, Santa Cruz, CA 95064

Edited* by Gail Martin, University of California, San Francisco, CA, and approved April 28, 2010 (received for review February 16, 2010)

Formation of the vascular system within organs requires the balanced action of numerous positive and negative factors secreted by stromal and epithelial cells. Here, we used a genetic approach to determine the role of SLITs in regulating the growth and organization of blood vessels in the mammary gland. We demonstrate that vascularization of the gland is not affected by loss of *Slit* expression in the epithelial compartment. Instead, we identify a stromal source of SLIT, mural cells encircling blood vessels, and show that loss of *Slit* in the stroma leads to elevated blood vessel density and complexity. We examine candidate SLIT receptors, *Robo1* and *Robo4*, and find that increased vessel angiogenesis is phenocopied by loss of endothelial-specific *Robo4*, as long as it is combined with the presence of an angiogenic stimulus such as preneoplasia or pregnancy. In contrast, loss of *Robo1* does not affect blood vessel growth. The enhanced growth of blood vessels in *Robo4*$^{-/-}$ endothelium is due to activation of vascular endothelial growth factor (VEGF)-R2 signaling through the Src and FAK kinases. Thus, our studies present a genetic dissection of SLIT/ROBO signaling during organ development. We identify a stromal, rather than epithelial, source of SLITs that inhibits blood vessel growth by signaling through endothelial ROBO4 to down-regulate VEGF/VEGFR2 signaling.

angiogenesis | ROBO | SLIT | mammary gland | organogenesis

Recent studies on the SLIT family of axon guidance molecules have demonstrated a conserved role in regulating development of the vascular system. However, a comprehensive understanding of their vascular function has been hampered by contradictory findings (1). SLITs have been shown to both attract (2–6) and repel (7–9) endothelial cells. ROBO1, which binds directly to SLITs, has been shown to promote endothelial cell motility, either alone (2, 6, 10) or as a heterodimeric partner with ROBO4 (5, 9). In contrast, ROBO4 binds SLITs at either very low affinity or not at all and likely requires a coreceptor, such as ROBO1 or a Syndecan, to signal (5, 11, 12). ROBO4 has been assigned the repellent functions of SLITs (7, 8) and, more recently, an alternative role in countering the effects of vascular endothelial growth factor (VEGF) to provide vascular stabilization (13, 14). One experimental variable that may be responsible for these contradictory findings is that many studies were performed in vitro using recombinant SLIT protein prepared in a variety of ways (2, 5, 6, 8, 13, 15). Here, we circumvent the requirement for recombinant protein by taking a genetic approach to address the function of SLIT in a biological context using the mammary gland as a model system. Such an approach provides insight into the role of endogenous SLIT/ROBO signaling in mammary development and angiogenesis.

During postnatal mammary gland development, the epithelium elaborates a bilayered, tree-like structure as it grows from the nipple subdermally through the surrounding stromal environment (16). The stroma is composed of adipocytes, fibroblasts, immune cells and a limited number of principal arteries supplying the capillary plexuses that envelop ducts. The gland undergoes stereotyped cycles of cell growth and differentiation under the influence of estrus and pregnancy hormones. In the virgin, the estrus cycle does not cause expansion of the vasculature, but pregnancy is accompanied by robust capillary sprouting that provides increased blood supply to promote lobulo-alveolar expansion (17, 18). Classic studies on vascular patterning of the gland demonstrated the importance of the epithelium because its absence resulted in only the major vessels and none of the duct-associated capillary plexuses (17). One explanation for this observation is that the epithelium acts as an important source of vascular endothelial growth factor (VEGF) (19–22) and possibly other factors, such as guidance cues. VEGF is also up-regulated in breast tumors, stimulating angiogenesis and fueling cancer cell growth (23). Thus, epithelial VEGF plays an important role in regulating angiogenesis in the mammary gland. In contrast, little is known about the role of guidance cues such as SLITs in directing blood vessel growth and organization during organ development.

We previously demonstrated the expression of SLITs in mammary gland epithelium (24). Here, we identify a second source of SLIT, mural cells associated with blood vessels. We use transplantation experiments to determine the compartment, epithelial or stromal, in which SLIT/ROBO signaling occurs. We show that stromal, but not epithelial, SLITs inhibit vessel growth by down-regulating VEGFR signaling through ROBO4; ROBO1 is not required for this inhibition. However, loss of the inhibitory action of SLIT, alone, does not stimulate vessel growth. This requires additional positive factors such as SDF1 or VEGF, and we demonstrate that preneoplasia or pregnancy supplies these proangiogenic molecules. Together, these studies elucidate a role for SLIT/ROBO signaling in maintaining vascular homeostasis during mammary morphogenesis.

Results

Loss of Global, but Not Epithelial, *Slit* Expression Leads to Increased Blood Vessel Number and Complexity. To determine SLIT function during mammary gland development, we initially focused on epithelial SLITs as a target-derived source because previous studies have reported directional migration of endothelial cells in response to exogenous or tumor-supplied SLIT protein (2, 4, 7, 8). Only *Slit2* and *Slit3* are expressed by mammary epithelia (24); therefore, to evaluate the consequences of losing epithelial SLIT expression, we generated *Slit2*$^{-/-}$;*Slit3*$^{-/-}$ chimeric mammary outgrowths by transplantation because the *Slit2*$^{-/-}$ mutation is perinatal lethal (Fig. 1*A*) (25). This technique involved placing small fragments of adult epithelium into contralateral fat

Author contributions: R.M., M.B., P.S., and L.H. designed research; R.M., M.B., L.K.S., S.D.M., and P.S. performed research; E.C.F. and D.Y.L. contributed new reagents/analytic tools; R.M., M.B., L.K.S, S.D.M., P.S., E.C.F, D.Y.L, and L.H. analyzed data; and R.M. and L.H. wrote the paper.

Conflict of interest statement: D.Y.L. is employed by the University of Utah, which has filed intellectual property surrounding the therapeutic uses of targeting Robo4 and with the intent to license this body of intellectual property for commercialization.

*This Direct Submission article had a prearranged editor.

[1]To whom correspondence should be addressed. E-mail: hinck@biology.ucsc.edu.

This article contains supporting information online at www.pnas.org/lookup/suppl/doi:10.1073/pnas.1001896107/-/DCSupplemental.

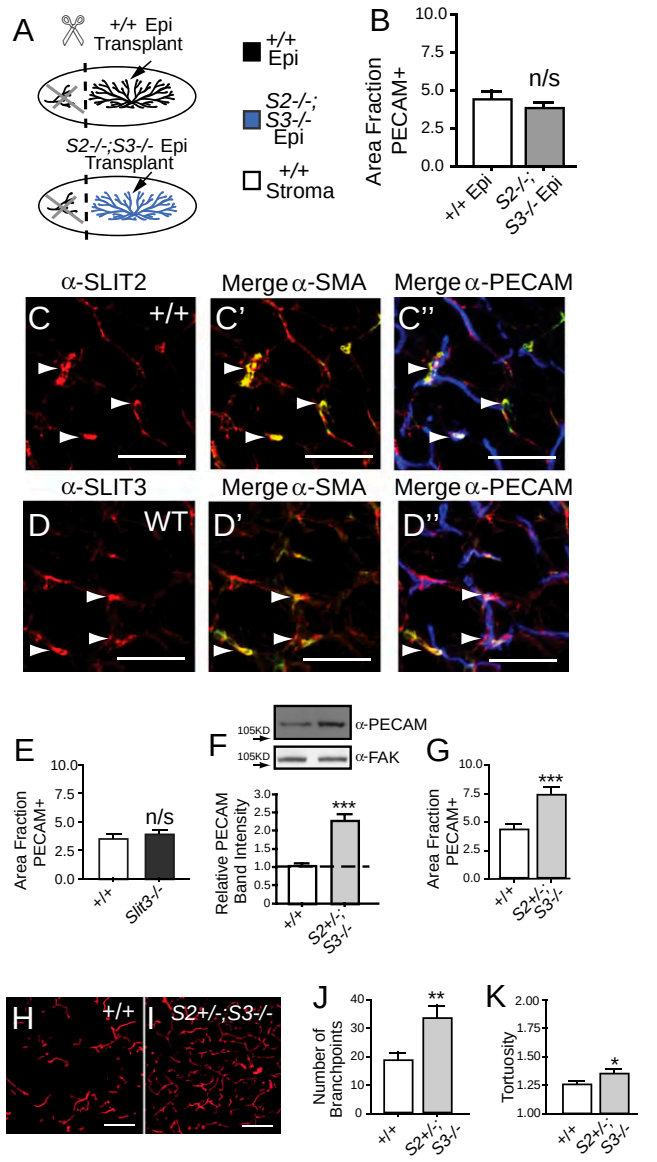

Fig. 1. Loss of global, but not epithelial *Slits*, enhances blood vessel growth. (*A*) Diagram illustrating transplants that generate chimeric mammary glands with *Slit2*$^{-/-}$;*Slit3*$^{-/-}$ epithelium (blue) and contralateral WT epithelium (black), transplanted into immunocompromised (*Foxn1*^{nu}) hosts (white) that have been precleared of their WT epithelium (black). (*B*) Lack of *Slit* in the epithelium does not alter blood vessel density in outgrowths. Quantitative analysis of PECAM-positive pixel area (n = 3 contralateral outgrowths, 15 fields of view (FOV)/outgrowth). Error bars = SEM. n/s = not significant. (*C* and *D*) Mural cells express SLIT2 and SLIT3. Representative images of sections immunostained for PECAM (blue), SMA (green), and SLIT2 or SLIT3 (red). Arrows indicate mural cell localization. (Scale bar, 50 μm.) (*E*) Lack of *Slit3* does not increase blood vessel number in the mammary gland. Quantitative analysis of PECAM-positive pixel area (n = 3 animals, 15 FOV/gland). Error bars = SEM. n/s = not significant. (*F–K*) Global lack of *Slit* significantly increases blood vessel number and network complexity. (*F*) Representative PECAM immunoblots on WT and *Slit2*$^{+/-}$;*Slit3*$^{-/-}$ mammary lysates (50 μg loaded; FAK immunoblot is loading control). Bar graph represent quantitative analysis of PECAM band intensity (ImageJ) (n = 3). Error bars = SEM, ***$P < 0.001$ unpaired t test. (*G*) Quantitative analysis of PECAM-positive pixel area (n = 3 animals, 15 FOV/animal). Error bars = SEM. *** $P < 0.001$ unpaired t test. (*H* and *I*) Representative images of WT (*H*) and *Slit2*$^{+/-}$;*Slit3*$^{-/-}$ (*I*) mammary sections immunostained with anti-PECAM (red). (Scale bar = 50 μm.) (*J*) Number of branchpoints and (*K*) tortuosity of blood vessels were quantified. Error bars = SEM, ***$P < 0.001$, **$P < 0.005$, *$P < 0.01$ unpaired t test.

pads of immunocompromised (*Foxn1*$^{nu-/-}$) host mice that have been precleared to remove endogenous epithelium (26). After 10 weeks, the fragments have grown into mature epithelial trees and the entire gland was harvested. Blood vessel density was analyzed by immunostaining for blood vessel marker PECAM and quantified. We observed no significant difference in blood vessel density between transplants containing WT or *Slit2*$^{-/-}$;*Slit3*$^{-/-}$ epithelium (Fig. 1*B* and Fig. S1 *A* and *B*), suggesting that endothelial cells are refractory to the loss of epithelial SLIT.

It has been reported that *Slit2* and *Slit3* are expressed in cells surrounding the vasculature (6, 13), suggesting the presence of a stromal source for SLITs, at least in some tissues. We performed immunohistochemistry on sections of adult mammary gland with antibodies directed against SLIT2 or SLIT3, PECAM, and the mural cell marker, SMA. We observe strong colocalization of SMA with both SLITs, demonstrating expression of SLIT in support cells surrounding blood vessels. We also observe weaker colocalization of SLITs with PECAM that may reflect cell-associated SLIT, either secreted from surrounding support cells or a consequence of low level SLIT expression by endothelial cells (Fig. 1 *C* and *D* and Fig. S1 *C* and *D*). These studies identify a stromal source of SLITs that may exert a local effect on vessel growth and organization.

To evaluate the consequences of knocking out *Slit3* in both the epithelia and stroma, we examined intact, adult glands of mice that were homozygous null for *Slit3* and observed no changes in blood vessel density (Fig. 1*E* and Fig. S1 *E* and *F*). This suggests that, unlike the embryonic diaphragm (6), SLIT3 functions redundantly with SLIT2 in the adult mammary gland. To evaluate the consequences of depleting both *Slits*, we examined intact glands of mice that are homozygous for *Slit3* and heterozygous for *Slit2* because the *Slit2* null mutation is lethal (*Slit2*$^{+/-}$; *Slit3*$^{-/-}$). In these glands, we observe an approximately two-fold increase in blood vessel density and a significant increase in the complexity of the vessel network (Fig. 1 *F–K*). This analysis shows that a single functional allele of *Slit2* is insufficient to supply the SLIT required to restrict blood vessel growth in the mammary gland. Together with the absence of phenotype in transplanted *Slit2*$^{-/-}$;*Slit3*$^{-/-}$ glands in which *Slits* are knocked out in the epithelium alone (Fig. 1*B*), the data suggest that stromal SLITs function at short-range to restrain the growth of mammary gland endothelial cells.

Combined Loss of *Robo1* and *Robo4* Leads to Increased Vessel Density. To evaluate the roles of ROBO1 and ROBO4 in mammary gland vasculature, we examined their loss-of-function phenotypes because phenocopy of *Slit2*$^{+/-}$;*Slit3*$^{-/-}$ defects provides strong genetic evidence that one, or both, of these receptors functions in the same pathway. ROBO4 has been identified as an endothelial specific mediator of SLIT signaling and its removal is not lethal to the animal (13, 14). To evaluate its loss-of-function phenotype, we analyzed intact, adult *Robo4*$^{-/-}$ and WT glands and did not observe a significant difference in the number of blood vessels (Fig. 2*A* and Fig. S2 *A* and *B*).

Next, we examined the expression of ROBO1 in blood vessels because it is unclear whether it is expressed by all types of endothelial cells (2, 7). We performed immunohistochemical analysis on WT glands using anti-ROBO1 (27) and found it colocalized in a membrane-associated pattern with PECAM (Fig. 2*B*). We confirmed these results by taking advantage of the expression of LacZ in knockout tissue under the control of the endogenous *Robo1* promoter and found positive staining in *Robo1*$^{-/-}$ blood vessels (Fig. S2 *C* and *D*). Thus, in our system, ROBO1 is expressed on blood vessels and may serve as a SLIT receptor. To investigate, we evaluated the loss-of-function phenotype in intact, adult *Robo1*$^{-/-}$ and WT glands and did not observe a significant difference in blood vessel number (Fig. 2*C*).

Because analysis of the single knock-out *Robo1* and *Robo4* glands did not yield a phenotype, we generated and analyzed

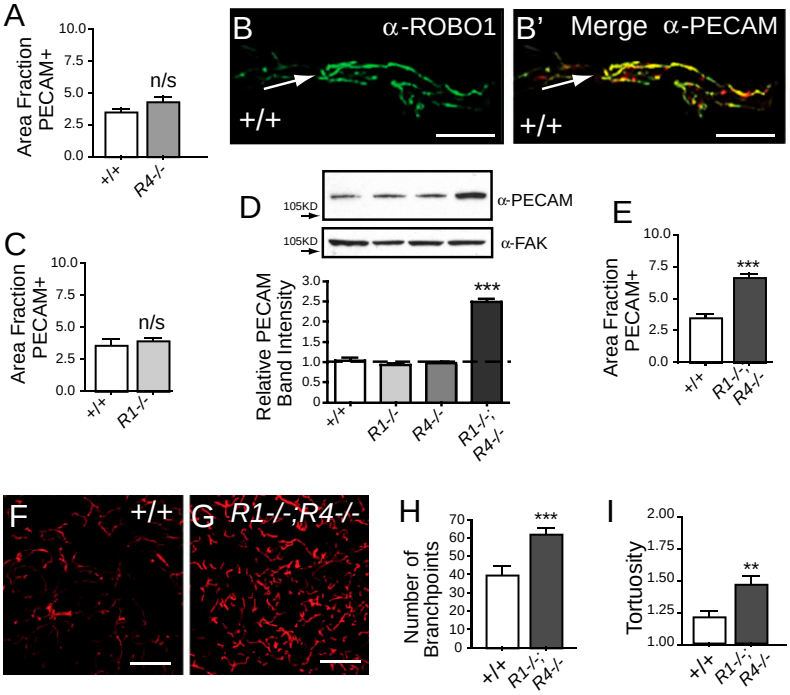

Fig. 2. Loss of ROBO1 and ROBO4 enhances blood vessel growth. (*A*) Lack of *Robo4* does not alter blood vessel density in the mammary gland. Quantitative analysis of PECAM-positive pixel area ($n = 3$ animals, 15 FOV/animal). Error bars = SEM. n/s = not significant. (*B*) ROBO1 is expressed by blood vessels. Representative images of ROBO1 (green) and PECAM (red) immunostaining on WT mammary sections. (Scale bar, 20 μm.) (*C*) Lack of *Robo1* does not alter blood vessel density in the mammary gland. Quantitative analysis of PECAM-positive pixel area ($n = 3$ animals, 15 FOV/animal). Error bars = SEM. n/s = not significant. (*D–I*) Lack of both *Robo1* and *Robo4* significantly increases blood vessel density and network complexity in the mammary gland. (*D*) Representative PECAM immunoblots on WT, Robo1$^{-/-}$, Robo4$^{-/-}$, and *Robo1*$^{-/-}$;*Robo4*$^{-/-}$ mammary lysates (50 μg loaded; FAK immunoblot is loading control). Bar graph represent quantitative analysis of PECAM band intensity (ImageJ) ($n = 3$). Error bars = SEM, ***$P < 0.001$ ANOVA. (*E*) Quantitative analysis of PECAM-positive pixel area ($n = 4$ animals, 15 FOV/animal). ***$P < 0.001$ unpaired *t* test. (*F* and *G*) Representative images of WT (*F*) and *Robo1*$^{-/-}$;*Robo4*$^{-/-}$ (*G*) mammary sections immunostained with anti-PECAM (red). (Scale bar, 50 μm.) (*H* and *I*) Quantification of branchpoint number (*H*) and tortuosity (*I*). Error bars = SEM. ***$P < 0.001$, **$P < 0.005$ unpaired *t* test.

Robo1$^{-/-}$;*Robo4*$^{-/-}$ mice. We discovered an approximately twofold increase in blood vessel density and complexity in *Robo1*$^{-/-}$;*Robo4*$^{-/-}$ glands (Fig. 2 *D–I* and Fig. S2 *E* and *F*) that was similar to the increase observed in *Slit2*$^{+/-}$;*Slit3*$^{-/-}$ glands (Fig. 1 *F–K*). These results demonstrate that loss of both SLIT receptors is required to achieve increased blood vessel density.

***Robo4*$^{-/-}$ Blood Vessels Display Enhanced Angiogenesis in Response to SDF1 and VEGF.** Our studies show that generating a blood vessel surplus, similar to that observed in *Slit2*$^{+/-}$;*Slit3*$^{-/-}$ glands, requires loss of both *Robo1* and *Robo4*. One explanation for this requirement is that each receptor compensates for the other in restraining vessel growth and only loss of both ROBO receptors leads to increased density. Alternatively, there may be an epithelial effect because these analyses were performed on intact, rather than transplanted, glands. ROBO1 is expressed in the epithelium (24), as well as the endothelium (Fig. 2*B* and Fig S2 *C* and *D*), raising the possibility that loss of *Robo1* in the epithelium contributes to the observed increase in blood vessel density in the *Robo1*$^{-/-}$;*Robo4*$^{-/-}$ mice. Indeed, we previously showed that epithelial loss of *Robo1* generates disorganized, hyperplastic tissue that is characterized by up-regulation of the chemokine CXCL12, also known as stromal derived factor-1 (SDF1) (27).

SDF1 induces the expression of VEGF in breast cancer cell lines (28) and normal breast epithelium (Fig. S3*A*). Therefore, we evaluated the expression of SDF1 and VEGF in *Robo1*$^{-/-}$ tissue and found that loss of *Robo1*, either alone or in combination with *Robo4*, resulted in up-regulation of both SDF1 and VEGF-A in mammary epithelium (Fig. 3 *A* and *B* and Fig. S3 *B–J*). To determine whether the angiogenic phenotype in *Robo1*$^{-/-}$;*Robo4*$^{-/-}$ glands is attributable to the loss of *Robo1* in the epithelium and consequent up-regulation of proangiogenic factors, we generated chimeric mammary glands by transplantation. First, we transplanted *Robo1*$^{-/-}$ and WT epithelial fragments into WT fat pads (Fig. 3*C*). After 10 weeks of outgrowth, we examined the number and complexity of blood vessels and observed no difference between the outgrowths (Fig. 3*D* and Fig S3 *K* and *L*), suggesting that loss of epithelial *Robo1*, alone, is insufficient to increase blood vessel density.

Next, we examined the angiogenic phenotype in glands that combined loss of epithelial *Robo1* with loss of stromal *Robo4*. We generated these chimeric glands by transplanting *Robo1*$^{-/-}$ and contralateral WT epithelium into *Robo4*$^{-/-}$ fat pads and examined the number and complexity of blood vessels after 10 weeks of outgrowth (Fig. 3*E*). We found a significant increase in blood vessel density in glands containing *Robo1*$^{-/-}$ epithelium combined with *Robo4*$^{-/-}$ stroma (Fig. 3 *F–H* and Fig S3 *M* and *N*), similar to the increase observed in *Robo1*$^{-/-}$;*Robo4*$^{-/-}$ (Fig. 2 *D–I*) and *Slit2*$^{+/-}$;*Slit3*$^{-/-}$ glands (Fig. 1 *F–K*). Together, these data show that the presence of ROBO1 in the endothelium does not compensate for the loss of ROBO4. Instead, ROBO4 appears to function alone in the endothelium as an angiogenesis inhibitor. To examine whether there are other contexts in which ROBO4 mediates SLIT signaling in the absence of ROBO1, we performed migration assays on Human Lung MicroVascular Endothelial Cells-Lung (HMVEC-L) (Fig. 3*I*). These cells express low levels of *Robo1* and robust levels of *Robo4*, both of which could be selectively knocked down using siRNAs. We observed that VEGF stimulated migration of these cells was reduced by the N-terminal fragment of SLIT2, a reduction that occurred upon knockdown of *Robo1*, but not *Robo4*, providing another example where ROBO4 transduces a SLIT signal, even when *Robo1* expression is greatly diminished or absent.

Together, our studies suggest that ROBO1 contributes to the *Robo1*$^{-/-}$;*Robo4*$^{-/-}$angiogenic phenotype through its role in the epithelium as a negative regulator of SDF1 and VEGF-A (Fig. 3 *A* and *B* and Fig. S3 *B–J*). The up-regulation of proangiogenic cues that occurs in *Robo1*$^{-/-}$ mammary epithelium generates a pre-pathological environment. However, this alone was insufficient to increase angiogenesis because we found that, in addition, loss of *Robo4* was also necessary (Figs. 2 *D–I* and 3 *D–I*). This process of pathological angiogenesis in response to proangiogenic cues has previously been documented in the visual system of *Robo4*$^{-/-}$ animals (13). However, it is unknown whether the loss of *Robo4*, alone, will result in increased angiogenesis during normal developmental processes, in part because there are few examples of robust blood vessel growth in the adult animal. In the mammary gland, however, there is a normal developmental event, pregnancy, associated with exuberant sprouting angiogenesis (18) that is driven by VEGF-A

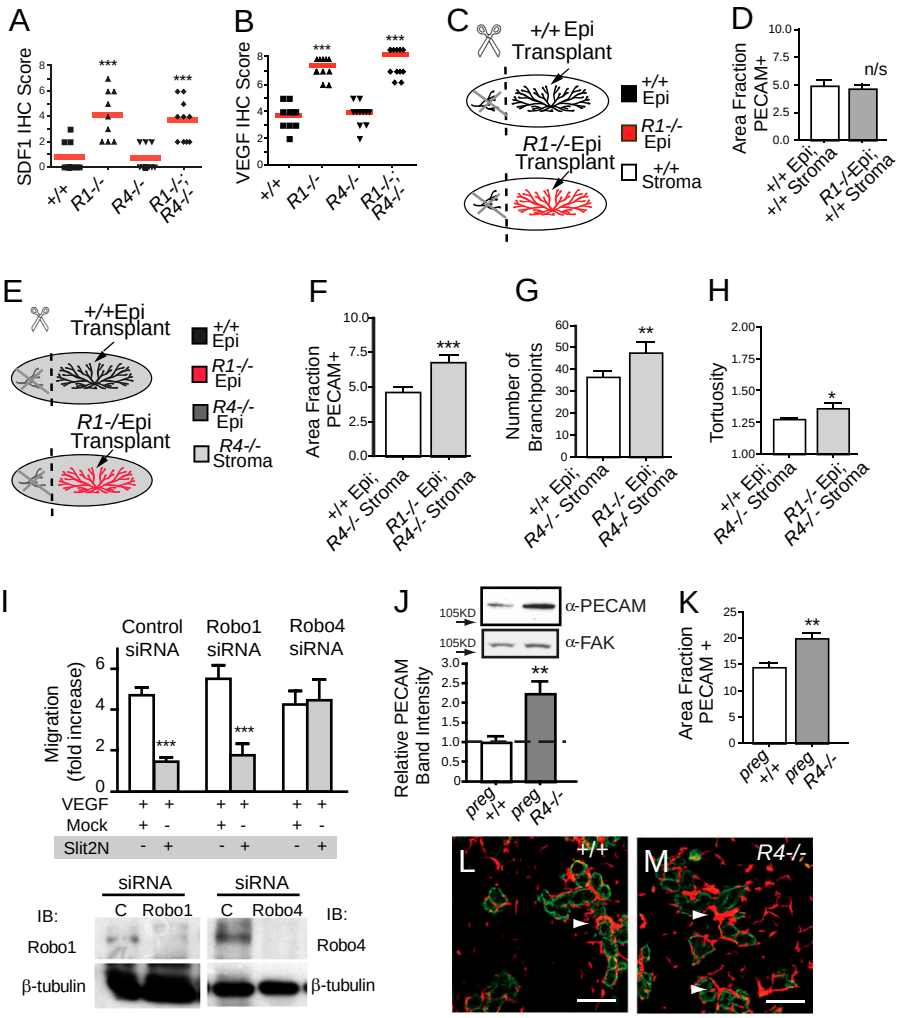

Fig. 3. The proangiogenic factor, VEGF, emanating from *Robo1*$^{-/-}$ and pregnant epithelium increases angiogenesis in *Robo4*$^{-/-}$ glands. (*A* and *B*) SDF1 (*A*) and VEGF-A (*B*) are expressed at higher levels by *Robo1*$^{-/-}$ and *Robo1*$^{-/-}$;*Robo4*$^{-/-}$, compared to WT or *Robo4*$^{-/-}$, mammary glands. Immunostained sections were scored according to cell percent positivity and staining intensity ($n = 3$ animals, 10 FOV/animal). Scores were plotted on a vertical scatter plot and red bars indicate average score. ***$P < 0.001$ ANOVA. (*C*) Diagram illustrating generation of chimeric glands with *Robo1*$^{-/-}$ epithelium (red) and contralateral WT epithelium (black), transplanted into immunocompromised (*Foxn1*^{nu}) hosts (white) that have been cleared of their WT epithelium (black) (*D*) Lack of *Robo1* in the epithelium does not alter blood vessel density in outgrowths. Quantification of PECAM-positive pixel area [$n = 7$ contralateral outgrowths, 15 FOV/outgrowth]. Error bars = SEM. n/s = not significant. (*E*) Diagram illustrating generation of chimeric glands with *Robo1*$^{-/-}$ epithelium (red) and contralateral WT epithelium (black) into syngeneic *Robo4*$^{-/-}$ background (light gray) that have been cleared of their host *Robo4*$^{-/-}$ epithelium (dark gray). (*F–H*) Increased blood vessel density with loss of *Robo1* in the epithelium combined with the loss of *Robo4*. (*F*) Quantitative analysis of PECAM-positive pixel area ($n = 3$ contralateral outgrowths, 15 FOV/outgrowth). Quantification of branchpoint number (*G*) and tortuosity (*H*). Error bars = SEM, **$P < 0.005$, *$P < 0.01$ unpaired *t* test. (*I*) *Robo4* is necessary for SLIT2N-mediated inhibition of VEGF-induced human microvascular endothelial cells-lung (HMVEC-L) migration. HMVEC-L cells were subjected to control, *Robo1*, or *Robo4* siRNA and allowed to migrate in response to VEGF in the presence of Mock or SLIT2N ($n > 3$, *** $P < 0.001$ ANOVA). Western blot analysis confirmed knockdown of *Robo1* or *Robo4* expression. (*J–M*) Pregnancy increases blood vessel density in *Robo4-/-* glands compared to WT. (*J*) Representative immunoblots of anti-PECAM on WT and *Robo4*$^{-/-}$mammary lysates (50 μg loaded; FAK immunoblot is loading control). Bar graph represents quantification of PECAM band intensity (ImageJ) ($n = 3$). Error bars = SEM, ***$P < 0.001$ unpaired *t* test. (*K*) Quantitative analysis of PECAM-positive pixel area ($n = 3$ animals, 10 FOV/animal). Error bars = SEM, **$P < 0.005$ unpaired *t* test. (*L* and *M*) Representative images of WT (*L*) and *Robo4*$^{-/-}$ (*M*) mammary sections from animals at pregnancy day 12.5 immunostained with anti-PECAM (red) and anti-CK14 (green), a marker for myoepithelial cells. Arrowheads indicate capillary baskets surrounding alveoli. (Scale bar, 50 μm.)

(19, 20) (Fig. S3*O*). To evaluate the consequences of *Robo4* loss in this context, we analyzed midpregnant *Robo4*$^{-/-}$ glands and found a significant increase in blood vessel density (Fig. 3*J–M*). These data show that a normal developmental event, pregnancy, results in excessive sprouting angiogenesis in the absence of *Robo4*.

ROBO4 Restrains VEGF/VEGFR Signaling. One model proposed for SLIT/ROBO4 signaling is that it functions to restrain pathologic angiogenesis by inhibiting VEGF/VEGFR2 signaling (13). We examined the activation of VEGFR2 by evaluating its autophosphorylation status in *Robo4*$^{-/-}$ glands under two proangiogenic conditions: hyperplasia, due to loss of *Robo1*$^{-/-}$, and pregnancy. We observed an approximately twofold increase in phosphorylation in extracts from *Robo1*$^{-/-}$;*Robo4*$^{-/-}$ glands, compared to WT, *Robo1*$^{-/-}$, or *Robo4*$^{-/-}$ gland extracts (Fig. 4*A*). Moreover, a similar increase in VEGFR2 activation was observed in extracts from pregnant *Robo4*$^{-/-}$, compared to pregnant WT, glands (Fig. 4*B*). We confirmed this increase in VEGFR2 signaling by immunohistochemistry using anti-PY1175 VEGFR2 (Fig. 4*C* and Fig. S4 *A–D*). Next, we examined whether this increase in VEGFR phosphorylation activated downstream signaling pathways by immunoblotting for phospho-Src (PY416) (Fig. 4*D*) and immunostaining for phospho-FAK (PY-397) (Fig. 4*E* and Fig. S4 *E–H*). We

found up-regulated VEGFR2 signaling in hyperplastic *Robo1*$^{-/-}$;*Robo4*$^{-/-}$ and pregnant *Robo4*$^{-/-}$ glands. Altogether the data show that loss of *Robo4* under conditions that favor angiogenesis, tissue hyperplasia or pregnancy, leads to increased VEGF/VEGFR2 signaling (Fig. 4) and increased angiogenesis (Figs. 2 *D–I* and 3 *F–H*, *L*, and *M*).

Discussion

Here, we took advantage of a relatively simple, but highly manipulable, model system of organ development to examine the role of SLIT guidance cues in regulating vascular development during postnatal mammogenesis. This involves the elaboration of an extensive vascular bed and the generation of ductal capillary plexuses, concomitant with expansive growth of the epithelial mammary tree (18). There have been many conflicting reports describing the response of cultured endothelial cells to SLIT, but few studies examining the role of SLIT/ROBO signaling in regulating angiogenesis and vascular remodeling in vivo (6, 13). Our data show that blood vessels respond to a stromal source of SLIT that signals through a ROBO4-mediated pathway to counter VEGF/VEGFR signaling and restrain angiogenesis (Fig. S5). In contrast, ROBO1 on endothelial cells does not appear to restrain vessel growth. Taken together, our studies support a recently proposed model for SLIT/ROBO4 function based on studies of pathologic angiogenesis in the retina (13). Both in this context and in the mammary gland, there are two requirements for increased angiogenesis (1): elimination of the restraining function of ROBO4 and (2) provision of a proangiogenic cue such as VEGF (Figs. 2 *D–G*, 3 *F–H* and *J–M*, 4, and Fig S5).

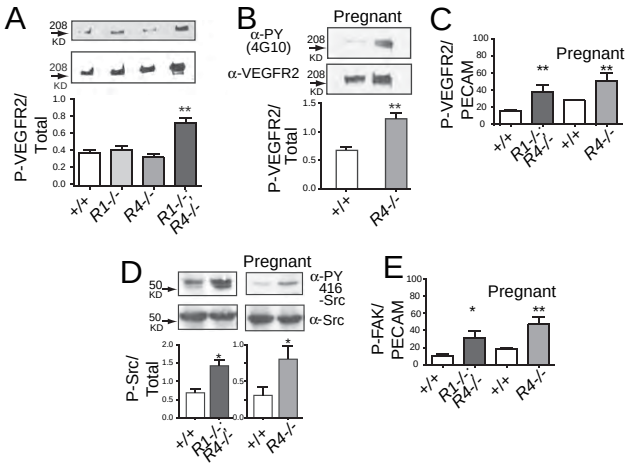

Fig. 4. ROBO4 functions to restrain VEGF/VEGFR2 signaling in the mammary gland. (*A*) Increased activation of VEGFR2 in *Robo1*$^{-/-}$;*Robo4*$^{-/-}$ but not WT, *Robo1*$^{-/-}$ or *Robo4*$^{-/-}$ glands. Immunoblotting for VEGFR2 and phosphotyrosine (4G10) after immunoprecipitation of VEGFR2 from adult gland lysates. Bar graph represents quantification of phospho-VEGFR2 relative to total VEGFR2 (ImageJ) ($n = 4$ per stage and per genotype). Error bars = SEM, $^{**}P < 0.005$ unpaired *t* test. (*B*) Increased activation of VEGFR2 in *Robo4*$^{-/-}$ in pregnant glands (day 12.5) compared to WT. Bar graph represents quantification of phospho-VEGFR2 relative to total VEGFR2 (ImageJ) ($n = 3$). Error bars = SEM, $^{**}P < 0.005$ unpaired *t* test. (*C*) Increased activation of VEGFR2 in *Robo1*$^{-/-}$;*Robo4*$^{-/-}$ adult glands and *Robo4*$^{-/-}$ pregnant glands, compared to WT controls. Bar graphs represent area fraction of pixels positive for PY1175-VEGFR2 divided by the area fraction positive for PECAM ($n = 4$ animals/genotype, 10 FOV/animal). Error bars = SEM, $^{**}P < 0.005$ ANOVA. (*D*) Increased activation of Src in *Robo1*$^{-/-}$;*Robo4*$^{-/-}$ adult virgin glands and *Robo4*$^{-/-}$ pregnant (day 12.5) glands, compared to WT controls. Representative immunoblots for Src and P-Y416-Src on mammary lysates (50 μg loaded). Bar graph represent quantitative analysis of Src and P-Y416-Src band intensity (ImageJ) ($n = 3$). Error bars = SEM, $^{*}P < 0.01$ unpaired *t* test. (*E*) Increased activation of FAK in *Robo1*$^{-/-}$;*Robo4*$^{-/-}$ adult virgin glands and *Robo4*$^{-/-}$ pregnant (day 12.5) glands compared to WT controls. Bar graphs represent the area fraction of pixels positive for PY397-FAK divided by the area fraction positive for PECAM ($n = 4$ animals, 10 FOV/animal). Error bars = SEM, $^{*}P < 0.01$, $^{**}P < 0.005$ ANOVA.

The identity of the SLIT receptor on blood vessels is unclear because both ROBO1 and ROBO4 have been implicated in endothelial cell migration (2, 7, 10, 29). Surprisingly, we found in mammary gland that loss of neither *Robo4* nor *Robo1*, alone, affected blood vessel growth but, instead, the absence of both ROBO receptors was required to generate the increased angiogenesis observed in *Slit2*$^{+/-}$;*Slit3*$^{-/-}$ glands. This was perplexing because the current model for SLIT/ROBO signaling in endothelium proposes the formation of a heterodimeric complex of receptors, with ROBO1 responsible for SLIT binding and ROBO4 functioning in signal transduction (5). If this heterodimeric complex were present on mammary blood vessels, then we would expect loss of either *Robo1* or *Robo4* to yield a phenotype, because both would be required to transduce the SLIT signal.

One of the authors (D.Y.L.) and coworkers, however, recently showed using the retina as an in vivo model system that loss of *Robo4*, alone, yielded a phenotype in the adult animal during the process of pathological angiogenesis (13). In this study, no phenotype was found in *Robo4*$^{-/-}$ animals during development that occurred normally with no apparent defects in vasculogenesis or angiogenesis. When evaluating the mammary gland phenotypes generated by loss of both *Robo1* and *Robo4*, we realized that loss of either *Slit* or *Robo1* in our mammary model system causes a secondary, potentially proangiogenic effect: up-regulation of SDF1 and VEGF (Fig. 3 *A* and *B* and Fig. S3 *A–J*) (27). There is growing evidence that SDF1 and VEGF collaborate to stimulate neoangiogenesis occurring in response to tumors, wounds, and chronic inflammatory disorders (28, 30, 31). Together, these factors contribute to the rapid proliferation of blood vessels observed during pathological angiogenesis. Our data show that up-regulation of these proangiogenic cues, due to loss of *Slit* or *Robo1*, functions as a "stimulatory cue" in our model system (Fig. 3 *A*, *B*, *F–H*, *J–M* and Fig. S3). Absent of this effect, ROBO1 does not appear to play a significant role transducing the inhibitory SLIT signal in blood vessels as evidenced by (*i*) the lack of phenotype in *Robo1*$^{-/-}$ glands (Figs. 2*C* and 3*D* and Figs. S2 *E* and *F* and S3 *K* and *L*), and (*ii*) the increase in vessel density in chimeric glands containing *Robo1*$^{-/-}$ epithelium and *Robo4*$^{-/-}$ endothelium (Fig. 3 *F–H* and Fig. S3 *M* and *N*).

Our data show a clear genetic interaction between SLITs and ROBO4. Moreover, there is recently published evidence that SLITs activate a ROBO4-initiated downstream signaling cascade (6, 14). However, it is still unclear whether SLITs bind directly to ROBO4. Direct interactions have been demonstrated by coimmunoprecipitation assays (6, 7), but the interaction cannot be duplicated with recombinant protein in Biacore assays (15). Thus, it seems likely that a coreceptor is required to transmit SLIT binding into ROBO4 activation. In some contexts, ROBO1 may fulfill this function (5), whereas in other contexts it may be served by receptors such as a Syndecan (11, 12).

Datasets from microarray analyses on human breast tumor samples show decreased *Robo4* expression in human breast cancer (32), colorectal cancer (33), and prostate tumors (34). Our study suggests one explanation for this finding. Environments that require growth, such as tumor microenvironments, may down-regulate *Robo4* expression to enhance the blood supply to cancerous cells because SLIT/ROBO4 signaling inhibits VEGF-mediated angiogenesis. These studies suggest that one way a proangiogenic tumor environment reduces SLIT/ROBO4 signaling and releases the brake on VEGF/VEGFR signaling is by downregulating *Robo4* expression.

The recent model proposed for ROBO4 action, in which it counters the activation of VEGF/VEGFR signaling, limited its role to pathological processes in the retina. Here, we present evidence that ROBO4 also restrains blood vessel growth during

the nonpathological expansion of epithelium and endothelium occurring in mammary gland in preparation for milk production and delivery. VEGF-A is the prime candidate for mediating this rapid increase in capillary number achieved by sprouting angiogenesis (19, 20, 35), but an unanswered question is how its actions are regulated during this short burst of pregnancy-associated angiogenesis that is coupled with rapid epithelial expansion. This period of development must be tightly regulated to prevent loss of growth control that would contribute to tumor development (36). We find that loss of *Robo4* during mid-pregnancy, when VEGF-A expression is at its highest (19), leads to a significant increase in the vascular density of the gland (Fig. 3 *J–M*). This corresponds to increased VEGFR2 autophosphorylation and activation of downstream signaling pathways (Fig. 4). Thus, down-regulation or silencing of *Robo4* expression during pregnancy or involution, periods of active tissue remodeling, could contribute to a tumor microenvironment and may play a role in the transient increase in breast cancer risk observed following pregnancy (37). Taken together, our results indicate a guardianship role for *Robo4* in normal development, when we propose it functions to restrain VEGF/VEGFR2 signaling during sprouting angiogenesis that generates alveolar blood supply.

In conclusion, the findings presented in this report identify the importance of locally-derived SLIT in restraining vascular growth during pregnancy and early stages of breast transformation. This study comprehensively addresses the contribution of both SLIT and their ROBO receptors to vascular development during mammalian organogenesis. Our data support a role for this signaling axis in inhibiting endothelial cell proliferation by downregulating the activation of downstream Src and FAK family kinases and, consequently, counteracting VEGF-VEGFR signaling.

Materials and Methods

Animals. All mice were harvested as adults (10- to 12-wk-old). The study conformed to guidelines set by the Institutional Animal Care and Use Committee (IACUC) at the University of California, Santa Cruz. *Slit2*, *Slit3*, *Robo1*, and *Robo4* null mice were generated as described (13, 24). Transplant techniques, antibodies, immunohistochemistry, migration assays, RT-PCR, immunoprecipitation, immunoblotting, image processing, statistical analyses and determination of blood vessel density, branchpoints and tortuosity are described in detail in *SI Materials and Methods*.

ACKNOWLEDGMENTS. We thank Hector Macias and Jennifer Compton for critical reading of the manuscript and Jennifer Compton and Angel Moran for genotyping. *Slit3*$^{-/-}$ mice were generously provided by Dr. Ornitz (Washington University, St. Louis, MO) and *Slit2*$^{-/-}$ and *Robo1*$^{-/-}$ mice by Dr. Tessier-Lavigne (Genentech Inc., South San Francisco, CA). This research was funded by the National Institutes of Health (RO1 CA-128902), Congressionally Directed Medical Research Program (W81XWH-08-1-0380), and Santa Cruz Cancer Benefit Group.

1. Klagsbrun M, Eichmann A (2005) A role for axon guidance receptors and ligands in blood vessel development and tumor angiogenesis. *Cytokine Growth Factor Rev* 16: 535–548.
2. Wang B, et al. (2003) Induction of tumor angiogenesis by Slit-Robo signaling and inhibition of cancer growth by blocking Robo activity. *Cancer Cell* 4:19–29.
3. Kaur S, et al. (2006) Robo4 signaling in endothelial cells implies attraction guidance mechanisms. *J Biol Chem* 281:11347–11356.
4. Howitt JA, Clout NJ, Hohenester E (2004) Binding site for Robo receptors revealed by dissection of the leucine-rich repeat region of Slit. *EMBO J* 23:4406–4412.
5. Sheldon H, et al. (2009) Active involvement of Robo1 and Robo4 in filopodia formation and endothelial cell motility mediated via WASP and other actin nucleation-promoting factors. *FASEB J* 23:513–522.
6. Zhang B, et al. (2009) *Repulsive Axon Guidance Molecule Slit3 Is a Novel Angiogenic Factor.* Blood 114:4300–4309.
7. Park KW, et al. (2003) Robo4 is a vascular-specific receptor that inhibits endothelial migration. *Dev Biol* 261:251–267.
8. Seth P, et al. (2005) Magic roundabout, a tumor endothelial marker: Expression and signaling. *Biochem Biophys Res Commun* 332:533–541.
9. Kaur S, et al. (2008) Silencing of directional migration in roundabout4 knockdown endothelial cells. *BMC Cell Biol* 9:61.
10. Wang LJ, et al. (2008) Targeting Slit-Roundabout signaling inhibits tumor angiogenesis in chemical-induced squamous cell carcinogenesis. *Cancer Sci* 99: 510–517.
11. Hu H (2001) Cell-surface heparan sulfate is involved in the repulsive guidance activities of Slit2 protein. *Nat Neurosci* 4:695–701.
12. Steigemann P, Molitor A, Fellert S, Jäckle H, Vorbrüggen G (2004) Heparan sulfate proteoglycan syndecan promotes axonal and myotube guidance by slit/robo signaling. *Curr Biol* 14:225–230.
13. Jones CA, et al. (2008) Robo4 stabilizes the vascular network by inhibiting pathologic angiogenesis and endothelial hyperpermeability. *Nat Med* 14:448–453.
14. Jones CA, et al. (2009) Slit2-Robo4 signalling promotes vascular stability by blocking Arf6 activity. *Nat Cell Biol* 11:1325–1331.
15. Suchting S, Heal P, Tahtis K, Stewart LM, Bicknell R (2005) Soluble Robo4 receptor inhibits in vivo angiogenesis and endothelial cell migration. *FASEB J* 19:121–123.
16. Hinck L, Silberstein GB (2005) Key stages in mammary gland development: The mammary end bud as a motile organ. *Breast Cancer Res* 7:245–251.
17. Soemarwoto IN, Bern HA (1958) The effect of hormones on the vascular pattern of the mouse mammary gland. *Am J Anat* 103:403–435.
18. Djonov V, Andres AC, Ziemiecki A (2001) Vascular remodelling during the normal and malignant life cycle of the mammary gland. *Microsc Res Tech* 52:182–189.
19. Pepper MS, et al. (2000) Regulation of VEGF and VEGF receptor expression in the rodent mammary gland during pregnancy, lactation, and involution. *Dev Dyn* 218: 507–524.
20. Hovey RC, Goldhar AS, Baffi J, Vonderhaar BK (2001) Transcriptional regulation of vascular endothelial growth factor expression in epithelial and stromal cells during mouse mammary gland development. *Mol Endocrinol* 15:819–831.
21. Rossiter H, et al. (2007) Inactivation of VEGF in mammary gland epithelium severely compromises mammary gland development and function. *FASEB J* 21:3994–4004.
22. Qiu Y, et al. (2008) Mammary alveolar development during lactation is inhibited by the endogenous antiangiogenic growth factor isoform, VEGF165b. *FASEB J* 22: 1104–1112.
23. Fox SB, Generali DG, Harris AL (2007) Breast tumour angiogenesis. *Breast Cancer Res* 9:216.
24. Strickland P, Shin GC, Plump A, Tessier-Lavigne M, Hinck L (2006) Slit2 and netrin 1 act synergistically as adhesive cues to generate tubular bi-layers during ductal morphogenesis. *Development* 133:823–832.
25. Plump AS, et al. (2002) Slit1 and Slit2 cooperate to prevent premature midline crossing of retinal axons in the mouse visual system. *Neuron* 33:219–232.
26. Robinson GW, Accili D, Hennighausen L (2000) *Rescue of Mammary Epithelium of Early Lethal Phenotypes by Embryonic Mammary Gland Transplantation as Exemplified with Insulin Receptor Null Mice* (Kluwer Academic/Plenum Press, New York), pp 307–316.
27. Marlow R, et al. (2008) SLITs suppress tumor growth in vivo by silencing Sdf1/Cxcr4 within breast epithelium. *Cancer Res* 68:7819–7827.
28. Liang Z, et al. (2007) CXCR4/CXCL12 axis promotes VEGF-mediated tumor angiogenesis through Akt signaling pathway. *Biochem Biophys Res Commun* 359: 716–722.
29. Huminiecki L, Gorn M, Suchting S, Poulsom R, Bicknell R (2002) Magic roundabout is a new member of the roundabout receptor family that is endothelial specific and expressed at sites of active angiogenesis. *Genomics* 79:547–552.
30. Grunewald M, et al. (2006) VEGF-induced adult neovascularization: Recruitment, retention, and role of accessory cells. *Cell* 124:175–189.
31. Lima e Silva R, et al. (2007) The SDF-1/CXCR4 ligand/receptor pair is an important contributor to several types of ocular neovascularization. *FASEB J* 21:3219–3230.
32. Richardson AL, et al. (2006) X chromosomal abnormalities in basal-like human breast cancer. *Cancer Cell* 9:121–132.
33. Gröne J, et al. (2006) Robo1/Robo4: Differential expression of angiogenic markers in colorectal cancer. *Oncol Rep* 15:1437–1443.
34. Latil A, et al. (2003) Quantification of expression of netrins, slits and their receptors in human prostate tumors. *Int J Cancer* 103:306–315.
35. Goldhar AS, Vonderhaar BK, Trott JF, Hovey RC (2005) Prolactin-induced expression of vascular endothelial growth factor via Egr-1. *Mol Cell Endocrinol* 232:9–19.
36. McDaniel SM, et al. (2006) Remodeling of the mammary microenvironment after lactation promotes breast tumor cell metastasis. *Am J Pathol* 168:608–620.
37. Schedin P (2006) Pregnancy-associated breast cancer and metastasis. *Nat Rev Cancer* 6:281–291.

SLITs Suppress Tumor Growth *In vivo* by Silencing *Sdf1/Cxcr4* within Breast Epithelium

Rebecca Marlow,[1] Phyllis Strickland,[1] Ji Shin Lee,[3] Xinyan Wu,[3] Milana PeBenito,[1] Mikhail Binnewies,[1] Elizabeth K. Le,[1] Angel Moran,[1] Hector Macias,[1] Robert D. Cardiff,[2] Saraswati Sukumar,[3] and Lindsay Hinck[1]

[1]Department of Molecular, Cell and Developmental Biology, University of California, Santa Cruz, California; [2]University of California Davis Center of Comparative Medicine, Davis, California; and [3]Sidney Kimmel Comprehensive Cancer Center, Johns Hopkins University School of Medicine, Baltimore, Maryland

Abstract

The genes encoding *Slits* and their *Robo* receptors are silenced in many types of cancer, including breast, suggesting a role for this signaling pathway in suppressing tumorigenesis. The molecular mechanism underlying these tumor-suppressive effects has not been delineated. Here, we show that loss of *Slits*, or their *Robo1* receptor, in murine mammary gland or human breast carcinoma cells results in coordinate up-regulation of the *Sdf1* and *Cxcr4* signaling axis, specifically within mammary epithelium. This is accompanied by hyperplastic changes in cells and desmoplastic alterations in the surrounding stroma. A similar inverse correlation between *Slit* and *Cxcr4* expression is identified in human breast tumor tissues. Furthermore, we show in a xenograft model that *Slit* overexpression down-regulates CXCR4 and dominantly suppresses tumor growth. These studies classify *Slits* as negative regulators of *Sdf1* and *Cxcr4* and identify a molecular signature in hyperplastic breast lesions that signifies inappropriate up-regulation of key prometastatic genes. [Cancer Res 2008;68(19):7819–27]

Introduction

The multistep model for breast carcinogenesis postulates that invasive carcinoma arises by way of intermediate hyperplastic lesions that progress in severity through stages of atypia to *in situ* and finally invasive carcinoma. It is generally recognized that there are clinically significant differences between various hyperplastic lesions, with some containing cellular and molecular changes that confer higher risk of progression to invasive disease. Pathologists identify clinically relevant differences later in disease progression, but early breast lesions are not well defined and further subclassification of their tumor potential by morphologic criteria is likely to be impossible. Consequently, assessing the potential risks associated with premalignant breast disease will rely on refining our understanding of the molecular signatures that confer increased risk of progression from epithelial hyperplasia to invasive carcinoma.

Up-regulation of CXCR4 is an example of one molecular change in breast cancer cells that is associated with poor prognosis (1, 2). Its role in directing metastasizing breast cancer cells to target sites is well established (3). Little is known, however, about the role of CXCR4 during breast cancer progression, although it is up-regulated early during cellular transformation (1, 4), along with SDF1 (5), which is produced by cancer-associated fibroblasts (CAF) and is in the local environment (6, 7). Recent studies have identified roles for this signaling pathway in primary breast tumors (8, 9), and in this context, one possibility is that signaling through the CXCR4/SDF1 axis drives proliferation, conferring selective advantage to cells as they transform into metastasizing carcinomas. Several mechanisms up-regulate CXCR4 during tumor metastasis (10–13), but there is little information about mechanisms regulating the SDF1/CXCR4 chemokine axis in organs at early stages of transformation.

SLITs (*Slit1, Slit2*, and *Slit3*) are a family of secreted proteins that mediate positional interactions between cells and their environment during development by signaling through ROBO receptors (*Robo1, Robo2, Robo3*, and *Robo4*; ref. 14). SLIT/ROBO signaling, however, is not restricted to development, and loss of these cues likely plays an important role during tumor progression. *Slits* and *Robos* are considered candidate tumor suppressor genes because their promoters are frequently hypermethylated in epithelial cancers (15–18). In ~50% of sampled human breast tumors, *Slit2* or *Slit3* gene expression is silenced (15, 19).

Cross-talk between SLIT/ROBO and CXCR4/SDF1 signaling has been observed in several systems, with the regulatory effect occurring downstream of the receptors and involving modulation of intracellular signaling intermediates. In leukocytes and human breast cancer cell lines, SLIT impedes SDF1-induced chemotaxis (20, 21). In breast cancer cells, this deterring effect occurs via SLIT-mediated inhibition of SDF1-induced activation of signaling pathways involved in motility (21). Similarly, in the nervous system, a reciprocal regulation of SLIT-mediated axonal repulsion by SDF1 is exerted through modulation of cyclic nucleotide signaling intermediates (22). These studies show an intriguing interrelationship between these signaling axes but do not address the consequences of losing the function of one of these signaling systems, such as occurs in breast during tumor progression when *Slit* expression is silenced.

Here, we investigate the consequences of losing SLIT/ROBO1 signaling in murine mammary gland, human breast cancer cells, and human tumors. We identify *Sdf1* and *Cxcr4* as critical targets of SLIT/ROBO1 regulation. Exploiting the ability to transplant knockout mammary epithelium into host mammary fat pads, we determine the compartment, epithelial or stromal, in which SLIT/ROBO1 signaling occurs, and how loss of signaling in one location leads to alterations across the epithelial/stromal boundary. Finally, we explore the tumor-suppressive capabilities of *Slits* using a xenograft model of human breast cancer.

Note: Supplementary data for this article are available at Cancer Research Online (http://cancerres.aacrjournals.org/).

R. Marlow and P. Strickland contributed equally to this work.

Requests for reprints: Lindsay Hinck, Department of Molecular, Cell and Developmental Biology, University of California, Santa Cruz, CA 95064. Phone: 831-459-5253; Fax: 831-459-3139; E-mail: hinck@biology.ucsc.edu.

doi:10.1158/0008-5472.CAN-08-1357

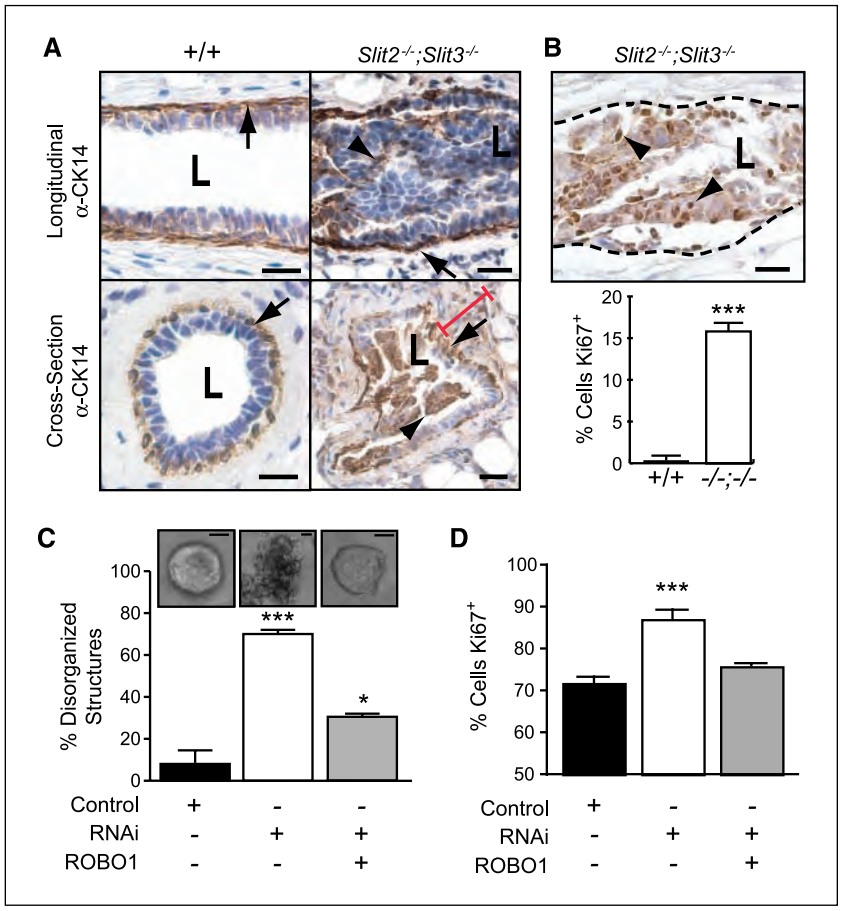

Figure 1. Loss of *Slit2* and *Slit3* expression in mammary epithelium leads to the formation of hyperplastic disorganized lesions. *A,* lack of SLIT in the epithelium leads to lesion formation. Immunostaining with anti-CK14 on longitudinal sections and cross-sections through +/+ and *Slit2*$^{-/-}$;*Slit3*$^{-/-}$ mammary outgrowths. *Arrows,* ductal myoepithelial cell layer; *arrowheads,* CK14-positive cells abnormally located in the lumen. *Red bar,* condensed desmoplastic stroma. *L*, lumen. *B,* lack of SLIT leads to hyperplasia. Representative lesion with dashed line indicating epithelial/stromal interface. *Arrowheads,* Ki67^{+} cells. *Columns,* mean percentage [n = 3 animals at 12 wk of age, 15 fields of view/animal (5×)]; *bars,* SD. ***, $P < 0.0001$, unpaired t test. *C,* lack of ROBO1 leads to a disorganized phenotype in three-dimensional culture. After transfection, MCF7 cells were grown in Matrigel. After 5 d, colonies were photographed (5×) and percentage of disorganized structures was counted. Representative images of colonies are shown. *Scale bar,* 10 μm. *Columns,* mean percentage; *bars,* SD. ***, $P < 0.0001$, ANOVA. *RNAi,* RNA interference. *D,* lack of ROBO1 increases the cell proliferation index. *Columns,* mean percentage of Ki67^{+} cells; *bars,* SD. **, $P < 0.001$, ANOVA.

Materials and Methods

Clinical samples. Frozen or formalin-fixed paraffin-embedded tissue specimens were collected at Johns Hopkins University (Baltimore, MD). All human tissue was collected using protocols approved by the Institutional Review Board. Informed consent was obtained from each individual who provided tissue linked with clinical data.

Animals. The study conformed to guidelines set by University of California at Santa Cruz animal care committee (Chancellor's Animal Research Committee). Mouse Slit2, Slit3, and Robo1 nulls were generated and genotyped as described (23).

Transplant techniques. Mammary anlage was rescued from E16-20 embryos and transplanted into precleared fat pads of athymic nude mice (24). Tissue fragments from the resulting outgrowths were contralaterally transplanted to generate knockout and wild-type tissue controls (25).

Implantation of Elvax beads. Elvax, an ethylene vinyl copolymer capable of sustained slow release of bioactive molecules, was prepared as described (26), with pellets containing 225 ng SDF1 and 0.45 mg bovine serum albumin (BSA) for control. Pellets were contralaterally implanted into the fat pad of wild-type CD1 mice (n = 3), and tissue was harvested after 6 d.

Cell lines, DNA constructs, and antibodies. MCF7 and MDA-MB-231 cells were maintained in DMEM supplemented with 10% FCS. pGL-CXCR4(−375) contains CXCR4 between −357 and +51 relative to the transcription site followed by the luciferase gene (12). pCRII-SDF1 (for riboprobes) contains 538-nucleotide fragment of the mouse *Sdf1* cDNA (27). Mouse image clone 3385804 (American Type Culture Collection). Small interfering RNA (siRNA) directed against *Robo1* was from Santa Cruz Biotechnology. pSecTagB-*hSlit3*-C-myc was from Dr. Roy Bicknell (University of Birmingham, Birmingham, United Kingdom). The following antibodies were used: anti-CK14 (AF64, Covance), anti-SMA (1A4, Sigma), anti-Ki67 (Santa Cruz Biotechnology), anti-CXCR4 (Abcam), anti-SDF1 (Santa Cruz Biotechnology), anti-SLIT3 (Chemicon), anti-SLIT2 (Chemicon), anti-HA (Dr. Doug Kellog, University of California, Santa Cruz, CA), anti-Myc (9E10), anti-ROBO1 (Abcam), and anti-extracellular signal-regulated kinase (Santa Cruz Biotechnology).

Generation of stable cell lines. MDA-MB-231 cells were transfected with pSecTagB-Slit2-HA and pSecTagB-Slit3-Myc and selected in zeocin (Invitrogen). n = 3 lines were generated expressing SLIT2-HA and n = 2 lines expressing SLIT3-Myc.

Tumor generation. Stable cell lines (10^6 cells) were injected into precleared fat pads of nude mice. Tumor volume was calculated using the formula $(\text{length} \times \text{width})^2/2$.

Immunohistochemistry. Tissue was fixed in 4% paraformaldehyde. Paraffin-embedded tissue was sectioned at 6 μm and serially mounted. Standard protocols were used and avidin-biotin complex method (Vector Labs) was used for amplification.

Scoring of immunohistochemistry. Immunostaining was scored according to percentage positive cells (P) and staining intensity (I). Score equals P + I. P scores 0 (none), 1 (<1%), 2 (1–10%), 3 (10–30%), 4 (30–60%), and 5 (>60%). I scores 0 (none), 1 (weak), 2 (intermediate), and 3 (strong).

siRNA transfection. MCF7 cells were transiently transfected using *Robo1* siRNA (Santa Cruz Biotechnology) and Lipofectamine 2000 (Invitrogen) according to the manufacturers' instructions. For three-dimensional culture, the "on-top" method was used (28). For luciferase assay, 48 h before harvest, cells were cotransfected with pGL-CXCR4(−375) (F-luciferase) and pRL-TK (R-luciferase). Cells were lysed using passive lysis buffer and assay was carried out in triplicate using the Dual-Luciferase Assay System (Promega) and Wallac Victor Luminometer (Perkin-Elmer Life Sciences) according to the manufacturers' instructions. F-luciferase activity was normalized to R-luciferase activity (transfection efficiency).

Western blotting. Western blotting was performed using standard procedures (29). Band intensity was scanned using Typhoon 9410 imager and quantified using ImageQuant 5 software.

Quantitative real-time reverse transcription-PCR analysis. Real-time reverse transcription-PCR (RT-PCR) analysis was done as previously described (30). Data were first analyzed using the Sequence Detector Software SDS 2.0 (Applied Biosystems). Results were calculated and normalized relative to glyceraldehyde-3-phosphate dehydrogenase (GAPDH) control. All of the PCR assays were done in triplicate, and mean values are shown in figures.

***In situ* hybridization.** *In situ* hybridization was carried out as described previously (23, 25).

Primary cell isolation. Primary mammary epithelial cells were prepared from mild collagenase and dispase digestion, as described (23). Cells were plated overnight and then trypsinized and placed onto Matrigel-coated coverslips.

Chemotaxis assay. Chemotaxis was examined as described before (29). Phase-contrast images were acquired at 0 and 60 min. The change in cell area in the directed quadrant was calculated using ImageJ.

Statistical analysis. We used factorial design ANOVA, unpaired t tests, or Mann-Whitney tests to analyze data as appropriate. Significant ANOVA values were subsequently subjected to post-test using the Tukey-Kramer comparison. We report P values for each statistical test; all P values were <0.05.

Results

Loss of *Slit* or *Robo1* in mammary epithelium leads to the formation of hyperplastic, disorganized lesions. Given the expanding role of SLITs in epithelial biology, we hypothesized a tumor-suppressive function for *Slits* in breast. We previously showed that two *Slit* family members, *Slit2* and *Slit3*, are expressed in murine mammary gland (23). The homozygous *Slit2*$^{-/-}$ mutation causes perinatal lethality. Therefore, to investigate the consequence of its loss in mature mammary gland, we generated *Slit2*$^{-/-}$;*Slit3*$^{-/-}$ outgrowths by contralateral transplantation of knockout and wild-type anlage into cleared fat pads of immunocompromised mice (24).

We examined mature *Slit2*$^{-/-}$;*Slit3*$^{-/-}$ mammary outgrowths for morphology. Compared with the open lumens and organized bilayers of ducts in control outgrowths, *Slit2*$^{-/-}$;*Slit3*$^{-/-}$ ducts displayed striking abnormalities (Fig. 1*A*). The phenotype was 100% penetrant, with ~30% of ducts having lesions extending between 0.3 and 5.0 mm. We categorized the lesions as mild and severe. Mild lesions contained cells in the luminal space (10.1% ± SE 1.9; n = 621 ducts; 5 outgrowths), and many of these cells were peeled away from the myoepithelial layer, similar to an adhesive defect previously described in *Ntn1*$^{-/-}$;*Slit2*$^{-/-}$ glands (23). In severe lesions (17.8% ± SE 8.1; n = 621 ducts; 5 outgrowths), ductal lumens were occluded with a disorganized mass of cells (Fig. 1*A*). These excess cells suggested disrupted growth control due to either increased proliferation and/or decreased apoptosis. We labeled proliferating cells and observed a significant increase in the percentage of Ki67^{+} cells in *Slit2*$^{-/-}$;*Slit3*$^{-/-}$, compared with +/+, ducts (Fig. 1*B*). This increase is responsible for the excess cells

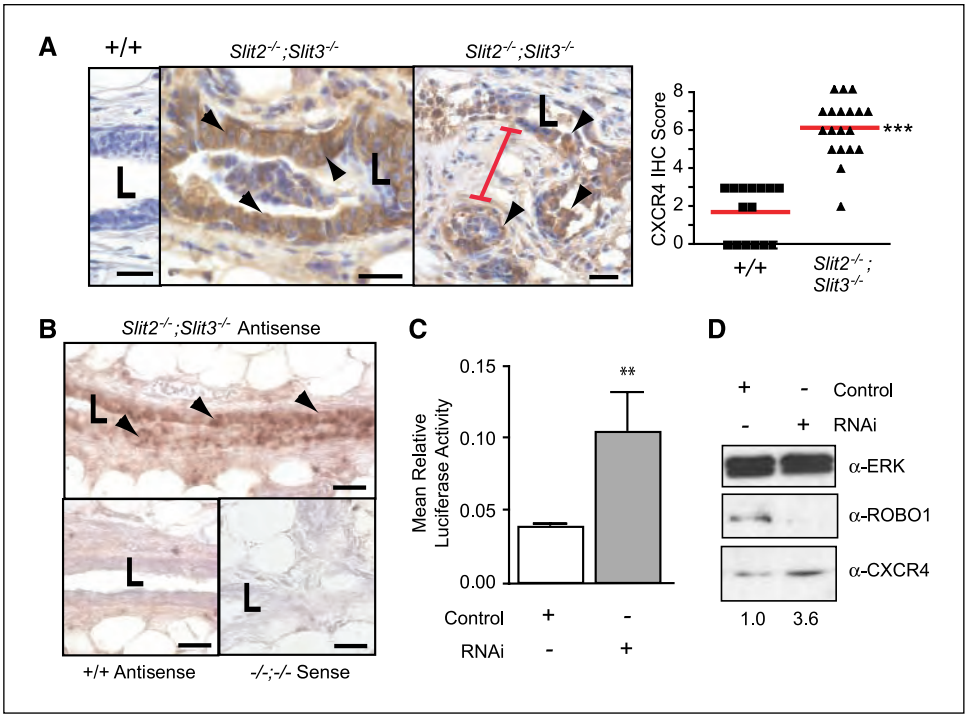

Figure 2. Loss of *Slit2* and *Slit3* causes up-regulation of CXCR4 in mouse mammary gland and human MCF7 cells. *A,* in *Slit2*$^{-/-}$;*Slit3*$^{-/-}$ outgrowths, CXCR4 protein expression is localized to epithelia, with desmoplastic stroma between lesions. Representative immunostaining with anti-CXCR4 on +/+ and *Slit2*$^{-/-}$;*Slit3*$^{-/-}$ mammary outgrowths. *Arrowheads,* positive epithelial cells. *Red bar,* condensed desmoplastic stroma. *Scale bar,* 20 μm. CXCR4 immunostaining was scored according to positivity and staining intensity and plotted on a vertical scatter plot. *Red bars,* average score. Significantly more CXCR4 staining is seen in *Slit2*$^{-/-}$;*Slit3*$^{-/-}$ outgrowths. ***, P < 0.0001, Mann-Whitney. *B, Cxcr4* mRNA is specifically present in the epithelium of *Slit2*$^{-/-}$;*Slit3*$^{-/-}$ outgrowths. *In situ* hybridization on +/+ and *Slit2*$^{-/-}$;*Slit3*$^{-/-}$ outgrowths using antisense probes reveals *Cxcr4* mRNA in *Slit2*$^{-/-}$;*Slit3*$^{-/-}$, but not +/+, cells. *Arrowheads,* positive epithelial cells. Sense probes show little or no background staining. *Scale bar,* 20 μm. *L,* lumen. *C,* loss of SLIT/ROBO signaling in MCF7 cells leads to up-regulation of *Cxcr4* gene expression. Cells were treated with control or *Robo1* siRNA and then cotransfected with pGL-CXCR4(−375), which contains the *Cxcr4* promoter region coupled to the F-luciferase gene and pRL-TK (R-luciferase). Cells were lysed after 36 h and luciferase activity was measured in triplicate. Activities were normalized for transfection efficiency. *Columns,* mean relative luciferase activity; *bars,* SE. **, P = 0.0095, Mann-Whitney test. *D,* loss of SLIT/ROBO signaling in MCF7 cells leads to increased levels of CXCR4 protein. Representative immunoblots (n = 4). *Numbers,* CXCR4 band intensity.

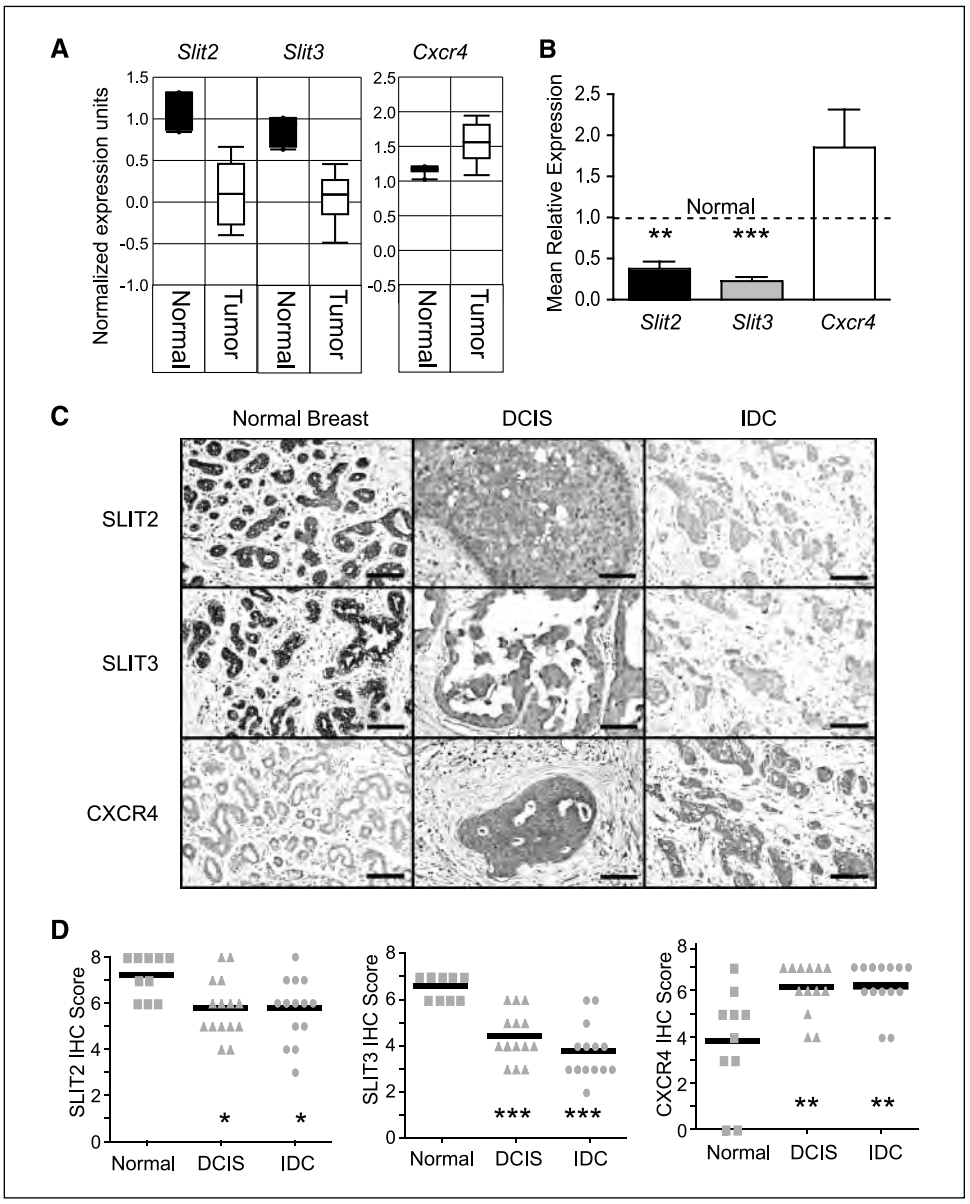

Figure 3. Loss of *Slit* expression in human tumors correlates with up-regulation of *Cxcr4*. *A,* box plots of data from the Richardson microarray data set were drawn using the Oncomine Cancer Profiling Database (32). *Slit2* ($P = 2.6E{-}10$) and *Slit3* ($P = 7.1E{-}9$) expression is significantly reduced in tumors, whereas *Cxcr4* ($P = 1.8E{-}5$) expression is elevated. Normal, $n = 7$; tumor, $n = 40$; P values from t test. *B,* expression levels, by quantitative PCR, of *Slit2, Slit3*, and *Cxcr4* were obtained from a panel of tumors, with values normalized against internal control *GAPDH*. The data were then normalized to values obtained from normal breast ($n = 6$). A value of 1 equals expression level of the gene in average normal breast. Seventeen of 25 tumor samples (68%) showed elevated *Cxcr4* expression compared with normal breast. In these tumors, this elevation corresponded with significantly reduced expression of *Slit2* or *Slit3*. *Columns,* mean relative expression; *bars,* SE. *Slit2* versus *Cxcr4*: **, $P < 0.011$; *Slit3* versus *Cxcr4*: ***, $P < 0.001$, ANOVA. *C,* SLIT expression is decreased in tumors, whereas CXCR4 levels increase. Normal breast, DCIS, and IDC tissue sections were immunostained with anti-SLIT2, anti-SLIT3, and anti-CXCR4. Representative images are shown. *Scale bar,* 100 μm. *D,* immunostained sections were scored according to cell percentage positivity and staining intensity. Scores were plotted on a vertical scatter plot. *Black bars,* average score. Both SLIT2 (*, $P = 0.01$, ANOVA) and SLIT3 (***, $P < 0.0001$, ANOVA) exhibit decreased expression in DCIS and IDC compared with normal breast. In contrast, CXCR4 is expressed at very low levels in normal breast, but its expression increases in DCIS and IDC (**, $P = 0.0005$, ANOVA).

because we evaluated apoptosis using activated caspase-3 staining and observed no difference (data not shown). Histopathologic analyses concurred with our observations that *Slit2*$^{-/-}$;*Slit3*$^{-/-}$ tissue contains hyperplasias. Condensed and desmoplastic stroma surrounding the lesions were also noted in the diagnosis (Fig. 1*A*), as was a large influx of immune infiltrates in the knockout, compared with wild-type, tissue.

ROBO1 is a SLIT receptor that could mediate the observed effects in the gland (23). *Robo1*$^{-/-}$ animals are viable so we evaluated the loss-of-function phenotype using intact glands. Ducts in *Robo1*$^{-/-}$ glands were hyperplastic and disorganized, displaying a phenotype that was indistinguishable from *Slit2*$^{-/-}$;*Slit3*$^{-/-}$ ductal lesions (Supplementary Fig. S1). As was the case for *Slit2*$^{-/-}$;*Slit3*$^{-/-}$ tissue, the penetrance of the phenotype was 100%, with ~30% of ducts displaying lesions that extended between 0.3 and 5.0 mm.

To investigate whether a similar phenotype occurred when SLIT/ROBO1 signaling was disrupted in human breast cells, we used the MCF7 line that retains several characteristics of differentiated mammary epithelium, including expression of *Slit2, Slit3*, and *Robo1* (data not shown; ref. 31). Cells were treated with *Robo1* siRNA to down-regulate SLIT/ROBO1 signaling (Supplementary Fig. S2) and then cultured in Matrigel. MCF7 cells formed smooth, nonpolarized colonies without central lumens. In contrast, the siRNA-treated colonies were large and disorganized, a phenotype that was rescued by reexpression of *Robo1* (Fig. 1*C*). Immunostaining with Ki67 revealed a significantly higher fraction of proliferating cells in colonies treated with *Robo1* siRNA compared with control (Fig. 1*D*). This was similar to the elevated proliferation observed in *Slit2*$^{-/-}$;*Slit3*$^{-/-}$ outgrowths and *Robo1*$^{-/-}$ glands (Fig. 1*B*; Supplementary Fig. S2). Together, these data show that a consequence of *Slit/Robo1* loss is elevated proliferation leading to hyperplastic lesions.

Loss of *Slit* up-regulates *Cxcr4* expression. We sought candidates whose misexpression in the absence of SLIT/ROBO1 signaling is responsible for the observed hyperplastic phenotype.

One candidate is CXCR4 because it is expressed early during breast tumorigenesis (1, 4), and blocking its expression or function inhibits breast tumor growth (8, 9). Western blots of whole gland lysates showed elevated CXCR4 expression in *Slit2*$^{-/-}$;*Slit3*$^{-/-}$, compared with +/+, tissue (Supplementary Fig. S3). Immunohistochemistry revealed CXCR4 expression in a large fraction of cells in *Slit2*$^{-/-}$;*Slit3*$^{-/-}$ epithelium, with little or no expression in +/+ epithelium (Fig. 2*A*). We also observed condensed and desmoplastic stroma surrounding these CXCR4-positive lesions (Fig. 2*A*). Because CXCR4 is regulated by transcriptional and posttranscriptional mechanisms, we performed *in situ* hybridization studies and observed *Cxcr4* in *Slit* knockout, but not wild-type, epithelium (Fig. 2*B*). A transcriptional mechanism also occurred in *Robo1* siRNA-treated MCF7 cells because we observed increased *Cxcr4*

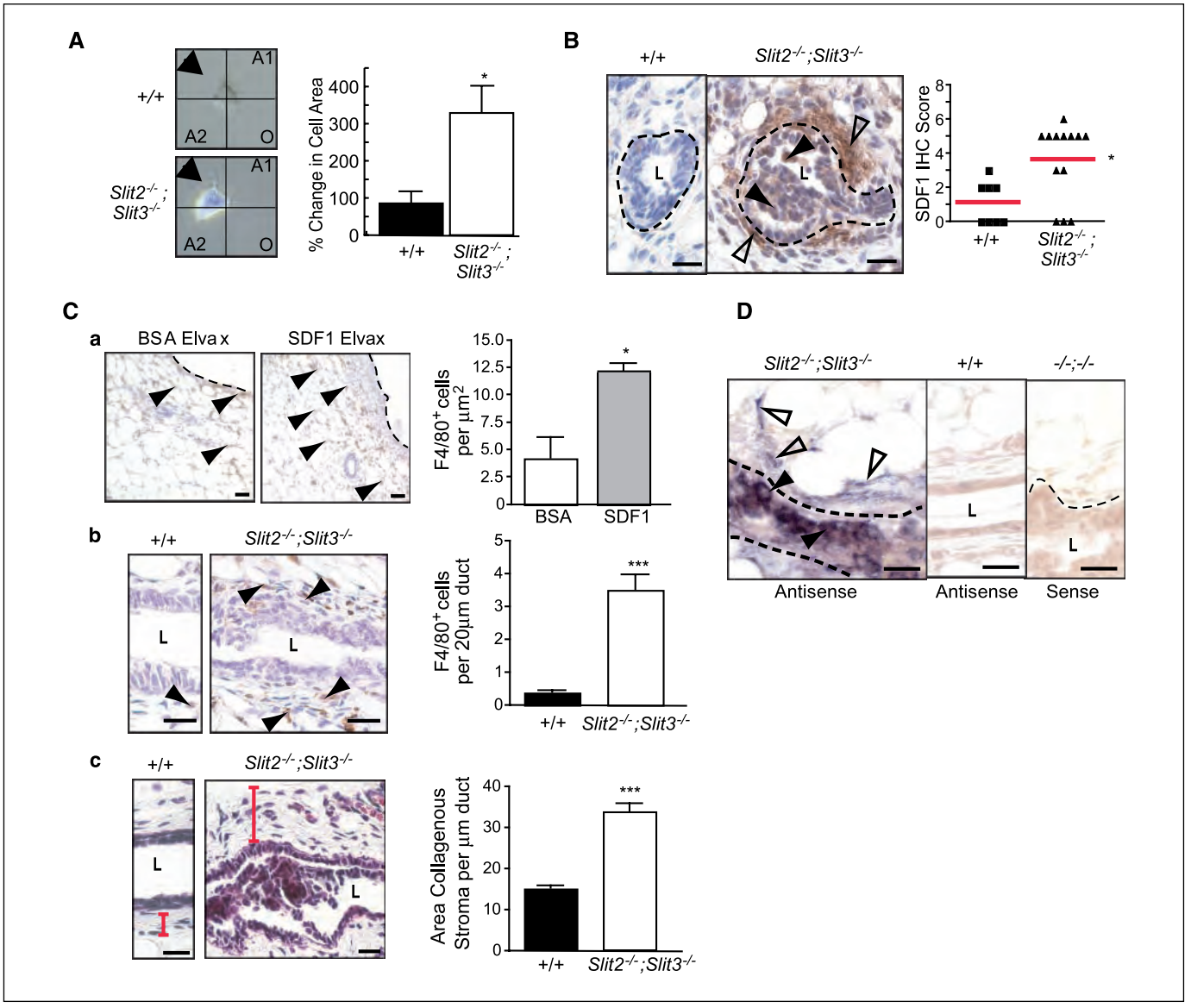

Figure 4. Loss of *Slit* expression results in coordinate up-regulation of SDF1 and the formation of desmoplastic stroma. *A, Slit2*$^{-/-}$;*Slit3*$^{-/-}$, but not +/+, cells respond to a point source of SDF1. Primary epithelial cells were prepared from outgrowths and placed in stable liquid gradients of SDF1 (29). Phase-contrast images were acquired at 0 and 60 min. Using ImageJ, the change in cell area in the source quadrant (*arrow*) was calculated. *Columns,* mean percentage change ($n = 7$); *bars,* SE. *, $P = 0.0018$, Mann-Whitney. *B,* SDF1 protein is present in the stroma surrounding *Slit2*$^{-/-}$;*Slit3*$^{-/-}$ outgrowths. Representative immunostaining with anti-SDF1 on +/+ and *Slit2*$^{-/-}$;*Slit3*$^{-/-}$ mammary outgrowths. *Dotted lines,* epithelial/stromal interface. *Open arrowheads,* positive staining in stroma; *arrowheads,* epithelial cells expressing SDF1. *Scale bar,* 20 μm. SDF1 immunostaining was scored according to positivity and intensity. Scores were plotted on a vertical scatter plot. *Red bars,* average score. Significantly more SDF1 staining is seen in *Slit2*$^{-/-}$;*Slit3*$^{-/-}$ outgrowths. *, $P = 0.018$, Mann-Whitney. *C,* SDF1 attracts macrophages. *a,* representative images of F4/80 staining in fat pads containing BSA versus SDF1 Elvax pellets. The number of F4/80$^+$ cells surrounding pellets was counted and expressed as the number of F4/80$^+$ cells per μm^2. *Columns,* average; *bars,* SD. *, $P = 0.0086$, unpaired *t* test. Macrophages surround *Slit2*$^{-/-}$;*Slit3*$^{-/-}$ ducts. *b,* representative images of F4/80 staining in +/+ versus *Slit2*$^{-/-}$;*Slit3*$^{-/-}$ tissue. Duct length was measured and the number of F4/80$^+$ cells was counted (ImageJ software). *Columns,* average; *bars,* SD. ***, $P < 0.0001$, unpaired *t* test ($n = 3$ animals, 10 fields of view/animal). Stroma surrounding *Slit2*$^{-/-}$;*Slit3*$^{-/-}$ ducts is desmoplastic. *c,* representative images of Masson's trichrome staining of +/+ versus *Slit2*$^{-/-}$;*Slit3*$^{-/-}$ tissue. *Red bar,* width of stroma. Longitudinal images of ducts were taken and duct length and positively stained areas were measured (ImageJ software). *Columns,* average; *bars,* SD. ***, $P < 0.0001$, unpaired *t* test. *Scale bar,* 20 μm. *D, Sdf1* mRNA is specifically present in subpopulations of elongated stromal cells (*open arrowheads*) and epithelial cells (*closed arrowheads*) in *Slit2*$^{-/-}$;*Slit3*$^{-/-}$ outgrowths. *In situ* hybridization on +/+ and *Slit2*$^{-/-}$;*Slit3*$^{-/-}$ outgrowths using antisense probes reveals *Sdf1* mRNA in *Slit2*$^{-/-}$;*Slit3*$^{-/-}$, but not +/+, cells. Sense probes show no or little background staining. *Scale bar,* 20 μm.

reporter gene activity and increased levels of CXCR4 in treated, compared with control, cells (Fig. 2*C* and *D*). Together, our results show that SLIT/ROBO1 signaling negatively regulates *Cxcr4* expression, with loss of this regulation leading to elevated levels of CXCR4 in murine tissue and human breast cancer cells.

If *Slits* silence *Cxcr4* in normal breast, we hypothesize that loss of *Slits* in tumors will correspond with elevated *Cxcr4.* To investigate, we analyzed microarray data sets from human breast tumor samples available at Oncomine.org (32) and found an inverse correlation between *Slit* and *Cxcr4* expression (Fig. 3*A*). We confirmed this by performing quantitative RT-PCR on a panel of human tumors; in 68% of tumors with elevated *Cxcr4* expression, *Slit2* or *Slit3* levels were significantly reduced compared with their expression in normal tissue (Fig. 3*B*). We further verified these observations at the protein level using immunohistochemistry on samples of normal breast, ductal carcinoma *in situ* (DCIS), and infiltrating ductal carcinoma (IDC; Fig. 3*C* and *D*). Again, there were robust levels of SLIT2 and SLIT3 in normal tissue that significantly decreased with increasing tumor grade. In contrast, and as previously shown (1, 4), little or no CXCR4 was detectable in normal breast, but its expression significantly increased with higher tumor grade.

Loss of *Slit* expression results in coordinate up-regulation of SDF1. Although CXCR4 is up-regulated in the vast majority of sampled premalignant lesions, studies on human breast cancer cell lines have suggested that it is only active in metastatic cells (33). To evaluate CXCR4 activity in *Slit2*$^{-/-}$;*Slit3*$^{-/-}$ cells, we performed chemotaxis assays. *Slit2*$^{-/-}$;*Slit3*$^{-/-}$ cells did not exhibit robust migration as expected of primary cells harvested from premalignant tissue but instead responded to SDF1 by reorganizing their cell membrane and sending membranous projections toward a point source (Fig. 4*A*). Wild-type cells were unresponsive to SDF1. This result suggested that CXCR4 expressed on *Slit2*$^{-/-}$;*Slit3*$^{-/-}$ cells is active and reacts to its ligand.

This raised the question of whether SDF1 surrounded *Slit2*$^{-/-}$;*Slit3*$^{-/-}$ lesions because recent studies have placed it in the tumor microenvironment (6, 7). We found abundant SDF1 expression in the epithelium and the surrounding stroma of knockout, but not wild-type, tissue (Fig. 4*B*). The presence of SDF1 is consistent with the histopathologic diagnosis that noted the infiltration of immune cells within desmoplastic stroma surrounding *Slit2*$^{-/-}$;*Slit3*$^{-/-}$ lesions. Macrophages, which express CXCR4, represent a major component of immune infiltrates surrounding tumors and play a key role in promoting the angiogenic switch during malignant transition (34). To determine whether macrophages are attracted to SDF1, we implanted point sources of SDF1 or vehicle (BSA) into wild-type mammary glands (Fig. 4*C, a*). Significantly more macrophages (F4/80^{+}) infiltrated into the tissue surrounding SDF1, compared with control, showing that SDF1 is a chemoattractant for macrophages and suggesting a role in recruiting these immune cells to tumors (Fig. 4*C, a*). Next, we

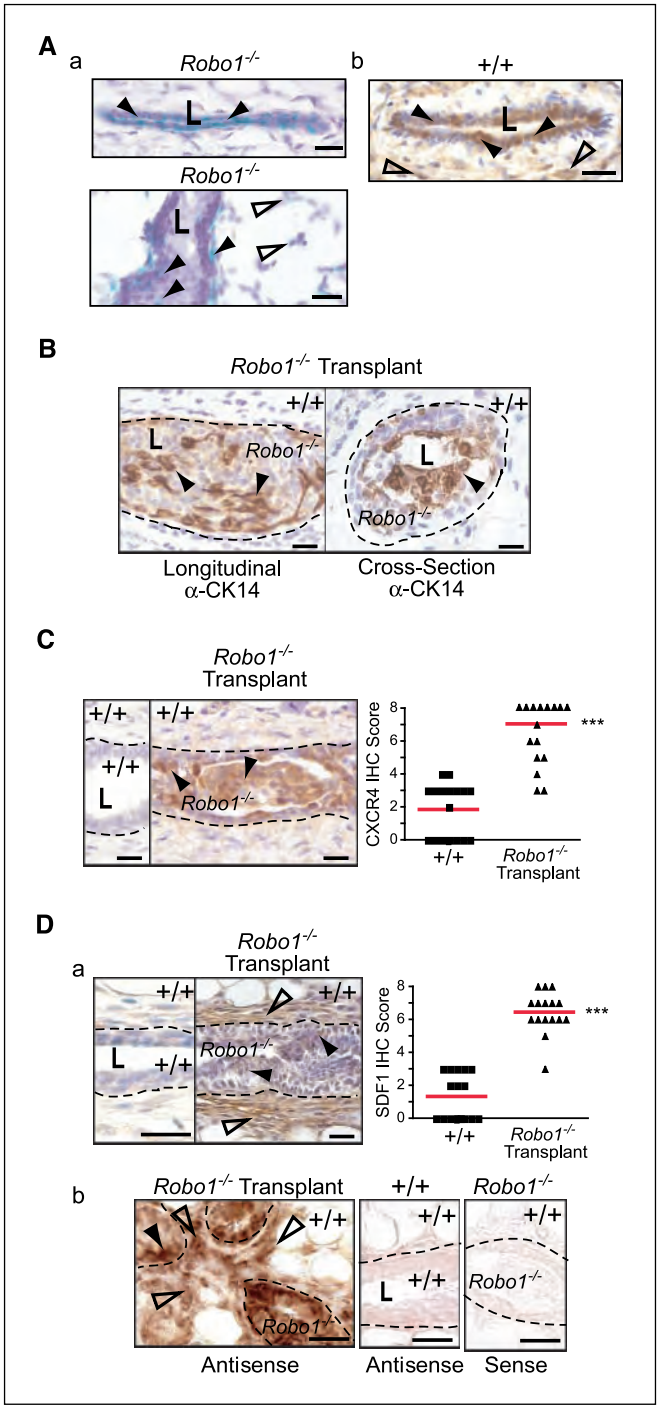

Figure 5. Coordinate up-regulation of CXCR4 and SDF1 is due to lack of SLIT/ROBO1 signaling within mammary epithelia. *A,* to examine *Robo1* gene expression, we took advantage of the *lacZ* gene under the control of the endogenous *Robo1* promoter in −/− tissue. *a,* longitudinal sections of *Robo1*$^{-/-}$ ducts stained for β-galactosidase activity. *b,* longitudinal section of +/+ duct immunostained with anti-ROBO1. *Open arrows,* positive stromal staining; *arrowheads,* positive epithelial cells. *Scale bar,* 20 μm. *L*, lumen. *B,* transplanted *Robo1*$^{-/-}$ mammary outgrowths show severe ductal defects similar to those observed in *Slit2*$^{-/-}$;*Slit3*$^{-/-}$ outgrowths. *Scale bar,* 20 μm. *C,* CXCR4 protein is specifically expressed in the epithelium of *Robo1*$^{-/-}$ outgrowths. Representative immunostaining with anti-CXCR4 on +/+ stroma/+/+ epithelia and +/+ stroma/*Robo1*$^{-/-}$ epithelia. *Arrows,* positive cells. *Scale bar,* 20 μm. CXCR4 immunostaining was scored and plotted on a vertical scatter plot. *Red bars,* average score. Significantly more CXCR4 staining is seen in *Robo1*$^{-/-}$ outgrowths. ***, $P < 0.0001$, Mann-Whitney test. *D,* SDF1 is present in the stroma surrounding *Robo1*$^{-/-}$ epithelial outgrowths (*a*; *open arrowheads*) and in a subpopulation of epithelial cells (*arrowheads*). Representative immunostaining with anti-SDF1 on +/+ stroma/+/+ epithelia and +/+ stroma/*Robo1*$^{-/-}$ epithelia. SDF1 immunostaining was scored and plotted on a vertical scatter plot. *Red bars,* average score. Significantly more SDF1 staining is seen in *Robo1*$^{-/-}$ outgrowths. ***, $P < 0.0001$, Mann-Whitney test. *Sdf1* mRNA is present in subpopulations of stromal fibroblasts (*b*; *open arrowheads*) and epithelial cells (*arrowheads*) in *Robo1*$^{-/-}$ outgrowths. *In situ* hybridization on +/+ stroma/+/+ epithelia and +/+ stroma/*Robo1*$^{-/-}$ epithelia outgrowths using antisense probes reveals *Sdf1* mRNA in +/+ stroma/*Robo1*$^{-/-}$ epithelia but not +/+ stroma/+/+ epithelia cells. Sense probes show little or no background staining. *Scale bar,* 20 μm.

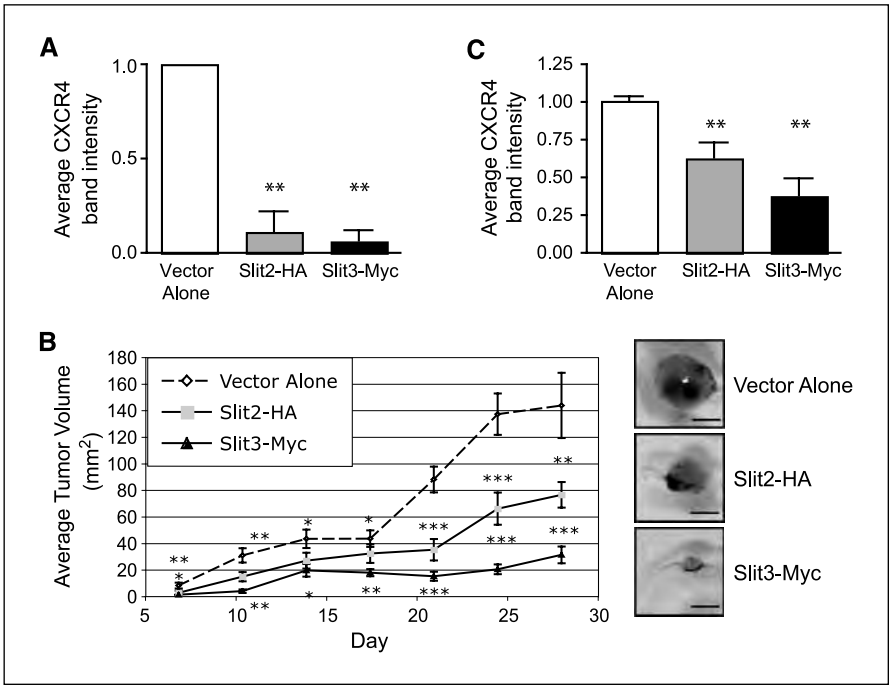

Figure 6. *Slit* expression in MDA-MB-231 cells blocks tumor growth by reducing CXCR4 expression. *A, Slit2*-HA and *Slit3*-Myc stable cell lines express low levels of CXCR4 compared with vector alone control lines. Stable *Slit2*-HA ($n = 3$) and *Slit3*-myc ($n = 2$) cell lines were generated by clonal selection. Stable cell line extracts were probed with anti-CXCR4. *Columns,* mean CXCR4 band intensity ($n = 2$ for each line); *bars,* SE. **, $P < 0.001$, ANOVA. *B,* expression of *Slit2* or *Slit3* resulted in smaller tumor size. Tumors were generated using *Slit* and control stable cell lines. $n = 12$ mice for each line. *Points,* mean tumor volume at each day; *bars,* SE. ***, $P < 0.0001$; **, $P < 0.001$; *, $P < 0.05$, ANOVA. Representative images of orthotopic tumors are shown. *Scale bar,* 0.25 mm. *C,* tumors expressing *Slit2* or *Slit3* contain significantly less CXCR4 protein compared with control tumors. *Columns,* mean CXCR4 immunoblot band intensity from $n = 3$ tumors; *bars,* SE. **, $P = 0.01$, ANOVA.

performed F4/80 immunohistochemistry on $Slit2^{-/-};Slit3^{-/-}$ and control tissue and found a significant increase in macrophages surrounding knockout tissue (Fig. 4*C, b*). We also evaluated the stromal expression of collagen, a major constituent of desmoplastic stroma (Fig. 4*C, c*). Stroma surrounding $Slit2^{-/-};Slit3^{-/-}$ epithelium contained significantly more condensed, collagenous stroma, compared with +/+, consistent with the histopathologic analysis. To define the cellular source of SDF1, we performed *in situ* hybridization analyses and discovered *Sdf1* in a fraction of epithelial cells and in a subset of elongated stromal cells that are likely to be fibroblasts based on their morphology (Fig. 4*D*). Thus, both CXCR4 and SDF1 are initially up-regulated in the epithelium, as has been recently observed in a xenograft model of DCIS (5). A local source of SDF1 may function to transform myoepithelial cells into CAFs or to recruit CAFs from circulating cells (35).

Epithelial regulation of CXCR4/SDF1 chemokine signaling axis. Together, the data show that loss of *Slit* expression leads to the coordinate up-regulation of *Cxcr4* in epithelia and *Sdf1* in both epithelia and stroma. This suggests that SLIT/ROBO1 signaling keeps SDF1/CXCR4 expression in check, but the regulatory networks may be complicated. *Slit* genes are expressed in the epithelia, but they encode a secreted cue that may act on any cell type expressing ROBO1 receptors. During mammary development, ROBO1 is expressed on myoepithelial cells (23), but as the gland matures, we observed a switch in its expression to include a subpopulation of luminal cells (Fig. 5*A*). ROBO1 was also expressed on stromal fibroblasts (Fig. 5*A*). Consequently, loss of *Slit* expression could regulate *Sdf1* and *Cxcr4* independently by disrupting ROBO1 signaling in both the stromal and epithelial compartments. Alternatively, loss of SLIT/ROBO1 signaling in just one compartment could up-regulate *Sdf1* and *Cxcr4* in both compartments.

To investigate, we eliminated SLIT/ROBO1 signaling selectively in the epithelial compartment by transplanting $Robo1^{-/-}$ epithelium into wild-type stroma. In these chimeric glands, we observed disorganized, hyperplastic epithelial lesions (Fig. 5*B*), which were similar in phenotype, penetrance (100%), and expressivity (19.64% ± SE 9.77; $n = 669$ ducts; 6 outgrowths) to those seen in $Slit2^{-/-};Slit3^{-/-}$ transplants (Fig. 1*A*). We evaluated the chemokine axis and again found up-regulation of CXCR4 in $Robo1^{-/-}$ epithelium (Fig. 5*C*), and coordinate up-regulation of SDF1 in the surrounding +/+ stroma (Fig. 5*D, a*), which was desmoplastic and contained immune infiltrates similar to stroma surrounding $Slit2^{-/-}Slit3^{-/-}$ tissue (data not shown). These data show that loss of SLIT/ROBO1 signaling in the epithelial compartment, alone, up-regulates SDF1 and CXCR4. This leads to phenotypic changes similar to those occurring in $Slit2^{-/-};Slit3^{-/-}$ transplants in which SLIT/ROBO1 signaling is disrupted in both compartments. To define the source of SDF1 in the transplanted tissue, we performed *in situ* hybridization studies and found *Sdf1* mRNA in cell subpopulations in the epithelia and stroma (Fig. 5*D, b*), suggesting that loss of SLIT/ROBO1 signaling in breast epithelia at early stages of transformation both generates a local source of *Sdf1* and up-regulates *Cxcr4*. We therefore conclude that loss of SLIT/ROBO1 signaling in the epithelia, alone, is sufficient to drive the observed morphologic and molecular changes, resulting in hyperplastic lesions, surrounded by desmoplastic stroma.

SLITs suppress CXCR4 expression and inhibit tumor growth. Given that SLITs exert this regulatory function by inhibiting the expression of *Sdf1* and *Cxcr4* within the mammary epithelium, we wondered whether overexpression of *Slits* in human breast carcinoma cells would suppress *Cxcr4* expression and inhibit tumor growth. Previous studies have shown that the metastatic human cell line MDA-MB-231 expresses CXCR4, but not SDF1 (36), and that inhibiting CXCR4 expression or function in these cells blocks primary tumor growth (8, 9). Because MDA-MB-231 cells express ROBO1 and ROBO2 (21),[4] signaling through these receptors could down-regulate CXCR4 expression and suppress tumor formation. To investigate, we transiently expressed *Myc-Slit2*

[4] R. Marlow, unpublished data.

or *Myc-Slit3* in MDA-MB-231 cells and documented decreased CXCR4 expression (Supplementary Fig. S4). Next, we generated stable cell lines expressing *Slit2* ($n = 3$) or *Slit3* ($n = 2$) and again found reduced CXCR4 levels (Fig. 6*A*). We also observed that *Slit*-expressing cells formed significantly fewer colonies, compared with control, when cultured in Matrigel (Supplementary Fig. S5). This suggested a general inhibition of cell growth, so we pursued the observation by establishing orthotopic xenograft tumors in immunocompromised hosts. We found that *Slit*-expressing cells formed significantly smaller tumors over time, with *Slit3* producing the most dramatic effect (Fig. 6*B*). We confirmed sustained down-regulation of CXCR4 in *Slit*-expressing tumors after 28 days of *in vivo* incubation (Fig. 6*C*; Supplementary Fig. S6). Thus, expression of *Slits* in MDA-MB-231 cells both down-regulates CXCR4 and inhibits tumor growth. Together with the observation that targeting CXCR4 reduces tumor growth in numerous organs (37, 38), our results suggest that SLITs suppress tumor growth by inhibiting the proliferative consequences of elevated CXCR4 expression.

Discussion

There is extensive literature on the molecular and genetic alterations that occur in invasive breast carcinoma and signify poor prognosis, but relatively little progress has been made in defining the genetic changes occurring in premalignant lesions. Here, we report that loss of *Slit* expression early during tumor progression up-regulates a key chemokine signaling axis and generates hyperplastic changes in the epithelium, along with desmoplastic changes in the stroma. Expression of CXCR4 was originally thought to occur late during tumor progression, generating cells that are ready to metastasize and home to organs expressing high levels of SDF1 (3). This restricted view of CXCR4 function, however, has been called into question because 93% of studied cases of atypical ductal carcinoma display high levels of CXCR4 (4), suggesting a role for CXCR4 in mediating earlier aspects of cellular transformation. Our data show that changes, loss and gain, in *Slit* expression function as a switch in the epithelium that up-regulate and down-regulate *Cxcr4*, leading to attendant changes in proliferation. We also show that loss of *Slits* results in the coordinate up-regulation of *Sdf1* in both the epithelium and surrounding stroma and this is accompanied by changes in the local microenvironment consistent with transformation.

The importance of the tumor microenvironment is well established, but it is unclear how it is generated. Our studies show that loss of SLIT/ROBO1 signaling exclusively in the epithelia is sufficient to increase expression of both *Cxcr4* and *Sdf1* (Fig. 5). The establishment of an initial SDF1/CXCR4 signaling loop within the epithelium is supported by recent studies using human MCF10DCIS.com cells in a xenograft model (5). Both CXCR4 and SDF1 are expressed at low levels in early MCF10DCIS lesions. CXCR4 expression remains epithelial, but during intermediate stages of transformation, SDF1 is switched on in the activated stroma. Once the ductal carcinoma becomes invasive, SDF1 expression is extinguished in the epithelia and is exclusively expressed by CAFs in the activated stroma. The origin of these CAFs is currently unknown. Some may be transformed from normal fibroblasts by aberrant signals from cancerous epithelial cells, whereas others may be transformed after being recruited from circulating bone marrow–derived cells (35). In either case, the transformation of these cells seems to be a consequence of their interaction with the cancerous epithelium. Our data raise the possibility that up-regulation of epithelial SDF1, accompanying *Slit* loss, contributes to the recruitment and/or transformation of CAFs, and support the model that genetic changes in the tumor epithelium, alone, are sufficient to drive transformation of cells and the surrounding microenvironment (7).

Our data also provide *in vivo* evidence that the SDF1/CXCR4 axis is fully functional within the epithelium during preinvasive stages of breast transformation and that it promotes cell survival and proliferation. We show that loss of SLIT/ROBO1 signaling results in the development of hyperplastic lesions (Fig. 1) with the coordinate up-regulation of both CXCR4 and SDF1 in the mammary epithelium (Figs. 2, 4, and 5). This type of autocrine stimulation of cell growth by SDF1/CXCR4 has been documented in human breast cancer cells on overexpression of SDF1 (39) and was also observed in the MCF10DCIS.com cells, described above, in which intraepithelial SDF1/CXCR4 signaling gives way to signaling across the epithelial/stromal boundary as the tumor microenvironment becomes established (5). Numerous pathways have been implicated in the mitogenic activity of SDF1/CXCR4 and may be responsible for the hyperplastic lesions observed in $Slit2^{-/-};Slit3^{-/-}$ tissue (40). We are currently investigating the pathways that drive proliferation because targeting these pathways could provide therapies that arrest cellular proliferation in early stages of transformation.

The molecular mechanism through which cells acquire SDF1 and CXCR4 expression during the evolution of tumors is unclear. At later stages of cellular transformation, CXCR4 expression is up-regulated by several mechanisms (40). Our studies reveal a transcriptional mechanism during early stages of transformation that occurs within breast epithelia (Figs. 2, 4, and 5). We show that SLITs signal through their ROBO1 receptor to negatively regulate *Cxcr4* and *Sdf1*. Negative transcriptional regulation of both *Cxcr4* and *Sdf1* has been shown in renal cells where hypoxia-inducible factors 1 and 2 (Hif1 and Hif2) are targeted for degradation by von Hippel-Lindau (VHL) proteins (11). It has been shown that loss of VHL leads to stabilization of Hifs and subsequent up-regulation of both *Sdf1* and *Cxcr4* due to the Hif response elements contained in their promoters (41). Hifs are frequently up-regulated during breast transformation (42) and can drive the inappropriate proliferation of cells even under conditions of normal oxygen (43). Thus, Hifs or VHL proteins may be targeted by SLIT/ROBO1 signaling, and we are currently investigating their expression profiles in $Slit2^{-/-};Slit3^{-/-}$ and $Robo1^{-/-}$ glands.

Numerous studies show epigenetic inactivation of *Slits* in multiple types of cancer (15, 16, 18, 19), and in breast, this loss of *Slit* also correlates with increasing tumor grade (44). Our histopathologic analyses of $Slit2^{-/-};Slit3^{-/-}$ and $Robo1^{-/-}$ mammary epithelium revealed hyperplastic lesions with no nuclear atypia (Fig. 1), a type of lesion that can be found in ~30% of women with benign proliferative breast disease (45). Epidemiologic studies show that identification of such lesions confers a 2-fold increase in relative risk of developing invasive breast cancer compared with women without proliferative disease. For patients diagnosed with lesions having the next stage of severity, hyperplasias with nuclear atypia, the relative risk of future invasive disease rises to ~5-fold and increases to 10-fold if there is also positive family history (45, 46). These numbers show that, although most patients will not develop invasive disease, a fraction will. With medical advances enabling detection of breast lesions at earlier stages, it will be crucial to develop methods that distinguish between nascent disease and normal biology because current methods relying on

morphologic criteria are insufficient. Improved understanding of molecular signatures within breast lesions holds the promise of identifying those at high risk so they receive appropriate treatment while also identifying the majority who are not at risk so their medical concerns are dispelled (47). The findings presented in this report identify the loss of *Slit* expression as a marker of early lesions that have the potential to progress to invasive disease due to up-regulation of metastasis markers SDF1/CXCR4. We propose that these molecular alterations define a specific subclass of breast lesions whose early detection could lead to treatment strategies that prevent development of invasive disease.

Disclosure of Potential Conflicts of Interest

No potential conflicts of interest were disclosed.

Acknowledgments

Received 4/16/2008; revised 6/30/2008; accepted 7/25/2008.

Grant support: American Cancer Society grant RSG0218001MGO, California Breast Cancer Research Program grant 10PB-0188, and National Cancer Institute grant R01CA128902 (L. Hinck) and Congressionally Directed Medical Research Program grant BC043200 and National Cancer Institute grant U01 CA105490 (R.D. Cardiff).

The costs of publication of this article were defrayed in part by the payment of page charges. This article must therefore be hereby marked advertisement in accordance with 18 U.S.C. Section 1734 solely to indicate this fact.

Santa Cruz Biotechnology generously provided antibodies and siRNA reagents. Other generous gifts were the following: anti-Dutt1 (Dr. Rabbitts, University College, London, United Kingdom), anti-HA (Dr. Doug Kellogg), MCF7 and MDA-MB-231 cell lines (Dr. Bissell, Lawrence Labs, Berkeley, CA), pGL-CXCR4(−375) (Dr. Avraham, Harvard Medical School, Boston, MA), pCRII-SDF1 (Dr. Goffinet, University of Louvain Medical School, Brussels, Belgium), pRL-TK (Dr. Haussler, University of California, Santa Cruz, CA), pSecTagB-*hSlit3*-C-myc (Dr. Roy Bicknell), *Slit3*$^{-/-}$ mice (Dr. Ornitz, Washington University, St. Louis, MO), and *Slit2*$^{-/-}$ mice and *Robo1*$^{-/-}$ (Dr. Tessier-Lavigne, Genentech, Inc., South San Francisco, CA).

References

1. Salvucci O, Bouchard A, Baccarelli A, et al. The role of CXCR4 receptor expression in breast cancer: a large tissue microarray study. Breast Cancer Res Treat 2006;97:275–83.
2. Holm NT, Byrnes K, Li BD, et al. Elevated levels of chemokine receptor CXCR4 in HER-2 negative breast cancer specimens predict recurrence. J Surg Res 2007; 141:53–9.
3. Muller A, Homey B, Soto H, et al. Involvement of chemokine receptors in breast cancer metastasis. Nature 2001;410:50–6.
4. Schmid BC, Rudas M, Rezniczek GA, Leodolter S, Zeillinger R. CXCR4 is expressed in ductal carcinoma *in situ* of the breast and in atypical ductal hyperplasia. Breast Cancer Res Treat 2004;84:247–50.
5. Tait LR, Pauley RJ, Santner SJ, et al. Dynamic stromal-epithelial interactions during progression of MCF10DCIS.com xenografts. Int J Cancer 2007;120: 2127–34.
6. Orimo A, Gupta PB, Sgroi DC, et al. Stromal fibroblasts present in invasive human breast carcinomas promote tumor growth and angiogenesis through elevated SDF-1/CXCL12 secretion. Cell 2005;121:335–48.
7. Allinen M, Beroukhim R, Cai L, et al. Molecular characterization of the tumor microenvironment in breast cancer. Cancer Cell 2004;6:17–32.
8. Lapteva N, Yang AG, Sanders DE, Strube RW, Chen SY. CXCR4 knockdown by small interfering RNA abrogates breast tumor growth *in vivo*. Cancer Gene Ther 2005;12:84–9.
9. Smith MC, Luker KE, Garbow JR, et al. CXCR4 regulates growth of both primary and metastatic breast cancer. Cancer Res 2004;64:8604–12.
10. Helbig G, Christopherson KW, Bhat-Nakshatri P, et al. NF-κB promotes breast cancer cell migration and metastasis by inducing the expression of the chemokine receptor CXCR4. J Biol Chem 2003;278:21631–8.
11. Staller P, Sulitkova J, Lisztwan J, Moch H, Oakeley EJ, Krek W. Chemokine receptor CXCR4 downregulated by von Hippel-Lindau tumour suppressor pVHL. Nature 2003;425:307–11.
12. Lee BC, Lee TH, Zagozdzon R, Avraham S, Usheva A, Avraham HK. Carboxyl-terminal Src kinase homologous kinase negatively regulates the chemokine receptor CXCR4 through YY1 and impairs CXCR4/CXCL12 (SDF-1α)-mediated breast cancer cell migration. Cancer Res 2005;65:2840–5.
13. Li YM, Pan Y, Wei Y, et al. Upregulation of CXCR4 is essential for HER2-mediated tumor metastasis. Cancer Cell 2004;6:459–69.
14. Hinck L. The versatile roles of "axon guidance" cues in tissue morphogenesis. Dev Cell 2004;7:783–93.
15. Dallol A, Dickinson RE, Latif F. Epigenetic disruption of the SLIT-ROBO interactions in human cancer. In: Ablin RJ, Jiang WG, Esteller M, editors. DNA methylation, epigenetic and metastasis: New York: Springer Netherlands; 2005. p. 191–214.
16. Narayan G, Goparaju C, Arias-Pulido H, et al. Promoter hypermethylation-mediated inactivation of multiple Slit-Robo pathway genes in cervical cancer progression. Mol Cancer 2006;5:16.
17. Schmid BC, Rezniczek GA, Fabjani G, Yoneda T, Leodolter S, Zeillinger R. The neuronal guidance cue Slit2 induces targeted migration and may play a role in brain metastasis of breast cancer cells. Breast Cancer Res Treat 2007;106:333–42.
18. Latil A, Chene L, Cochant-Priollet B, et al. Quantification of expression of netrins, slits and their receptors in human prostate tumors. Int J Cancer 2003;103:306–15.
19. Sharma G, Mirza S, Prasad CP, Srivastava A, Gupta SD, Ralhan R. Promoter hypermethylation of p16INK4A, p14ARF, CyclinD2 and Slit2 in serum and tumor DNA from breast cancer patients. Life Sci 2007;80:1873–81.
20. Wu JY, Feng L, Park HT, et al. The neuronal repellent Slit inhibits leukocyte chemotaxis induced by chemotactic factors. Nature 2001;410:948–52.
21. Prasad A, Fernandis AZ, Rao Y, Ganju RK. Slit protein-mediated inhibition of CXCR4-induced chemotactic and chemoinvasive signaling pathways in breast cancer cells. J Biol Chem 2004;279:9115–24.
22. Chalasani SH, Sabelko KA, Sunshine MJ, Littman DR, Raper JA. A chemokine, SDF-1, reduces the effectiveness of multiple axonal repellents and is required for normal axon pathfinding. J Neurosci 2003;23:1360–71.
23. Strickland P, Shin GC, Plump A, Tessier-Lavigne M, Hinck L. Slit2 and netrin 1 act synergistically as adhesive cues to generate tubular bi-layers during ductal morphogenesis. Development 2006;133:823–32.
24. Robinson GW, Accili D, Hennighausen L. Rescue of mammary epithelium of early lethal phenotypes by embryonic mammary gland transplantation as exemplified with insulin receptor null mice. New York: Kluwer Academic/Plenum Press; 2000. p. 307–16.
25. Srinivasan K, Strickland P, Valdes A, Shin GC, Hinck L. Netrin-1/neogenin interaction stabilizes multipotent progenitor cap cells during mammary gland morphogenesis. Dev Cell 2003;4:371–82.
26. Silberstein GB, Daniel CW. Investigation of mouse mammary ductal growth regulation using slow-release plastic implants. J Dairy Sci 1987;70:1981–90.
27. Tissir F, Wang CE, Goffinet AM. Expression of the chemokine receptor Cxcr4 mRNA during mouse brain development. Brain Res Dev Brain Res 2004;149:63–71.
28. Lee GY, Kenny PA, Lee EH, Bissell MJ. Three-dimensional culture models of normal and malignant breast epithelial cells. Nat Methods 2007;4:359–65.
29. Bartoe JL, McKenna WL, Quan TK, et al. Protein interacting with C-kinase 1/protein kinase Cα-mediated endocytosis converts netrin-1-mediated repulsion to attraction. J Neurosci 2006;26:3192–205.
30. Wu X, Chen H, Parker B, et al. HOXB7, a homeodomain protein, is overexpressed in breast cancer and confers epithelial-mesenchymal transition. Cancer Res 2006;66:9527–34.
31. Dallol A, Da Silva NF, Viacava P, et al. SLIT2, a human homologue of the *Drosophila Slit2* gene, has tumor suppressor activity and is frequently inactivated in lung and breast cancers. Cancer Res 2002;62:5874–80.
32. Richardson AL, Wang ZC, De Nicolo A, et al. X chromosomal abnormalities in basal-like human breast cancer. Cancer Cell 2006;9:121–32.
33. Holland JD, Kochetkova M, Akekawatchai C, Dottore M, Lopez A, McColl SR. Differential functional activation of chemokine receptor CXCR4 is mediated by G proteins in breast cancer cells. Cancer Res 2006;66:4117–24.
34. Lin EY, Li JF, Gnatovskiy L, et al. Macrophages regulate the angiogenic switch in a mouse model of breast cancer. Cancer Res 2006;66:11238–46.
35. Orimo A, Weinberg RA. Stromal fibroblasts in cancer: a novel tumor-promoting cell type. Cell Cycle 2006;5: 1597–601.
36. Kang H, Watkins G, Parr C, Douglas-Jones A, Mansel RE, Jiang WG. Stromal cell derived factor-1: its influence on invasiveness and migration of breast cancer cells *in vitro*, and its association with prognosis and survival in human breast cancer. Breast Cancer Res 2005;7:R402–10.
37. Rubin JB, Kung AL, Klein RS, et al. A small-molecule antagonist of CXCR4 inhibits intracranial growth of primary brain tumors. Proc Natl Acad Sci U S A 2003; 100:13513–8.
38. De Falco V, Guarino V, Avilla E, et al. Biological role and potential therapeutic targeting of the chemokine receptor CXCR4 in undifferentiated thyroid cancer. Cancer Res 2007;67:11821–9.
39. Kang H, Mansel RE, Jiang WG. Genetic manipulation of stromal cell-derived factor-1 attests the pivotal role of the autocrine SDF-1-CXCR4 pathway in the aggressiveness of breast cancer cells. Int J Oncol 2005;26:1429–34.
40. Luker KE, Luker GD. Functions of CXCL12 and CXCR4 in breast cancer. Cancer Lett 2006;238:30–41.
41. Zagzag D, Krishnamachary B, Yee H, et al. Stromal cell-derived factor-1α and CXCR4 expression in hemangioblastoma and clear cell-renal cell carcinoma: von Hippel-Lindau loss-of-function induces expression of a ligand and its receptor. Cancer Res 2005;65:6178–88.
42. Zhong H, De Marzo AM, Laughner E, et al. Overexpression of hypoxia-inducible factor 1α in common human cancers and their metastases. Cancer Res 1999; 59:5830–5.
43. Dang DT, Chen F, Gardner LB, et al. Hypoxia-inducible factor-1α promotes nonhypoxia-mediated proliferation in colon cancer cells and xenografts. Cancer Res 2006;66:1684–936.
44. Miller LD, Smeds J, George J, et al. An expression signature for p53 status in human breast cancer predicts mutation status, transcriptional effects, and patient survival. Proc Natl Acad Sci U S A 2005;102:13550–5.
45. Hartmann LC, Sellers TA, Frost MH, et al. Benign breast disease and the risk of breast cancer. N Engl J Med 2005;353:229–37.
46. Fitzgibbons PL, Henson DE, Hutter RV. Benign breast changes and the risk for subsequent breast cancer: an update of the 1985 consensus statement. Cancer Committee of the College of American Pathologists. Arch Pathol Lab Med 1998;122:1053–5.
47. Jeffrey SS, Pollack JR. The diagnosis and management of pre-invasive breast disease: promise of new technologies in understanding pre-invasive breast lesions. Breast Cancer Res 2003;5:320–8.